THE MICRODOSIMETRY OF PLUTONIUM-239 IN BONE USING ELECTROCHEMICAL ETCHING AND POLYCARBONATE FOILS

A THESIS

Presented to

The Faculty of the Division of Graduate Studies

By

Gary Bouldin Stillwagon

In Partial Fulfillment

of the Requirements for the Degree

Doctor of Philosophy

in the

School of Nuclear Engineering

Georgia Institute of Technology

September, 1978

THE MICRODOSIMETRY OF PLUTONIUM -239 ON BONE USING

ELECTROCHEMICAL ETCHING AND POLYCARBONATE FOILS

Approved:

Karl Z. Morgan, Chairman

Geoffrey G. Eichholz

Robert H. Fetner

Patton H. McGinley

John W. Poston

Date approved by Chairman: Sept. 20, 1978

ACKNOWLEDGMENTS

I would like to thank the large number of individuals who collectively enabled this work to proceed smoothly and reach the final results and conclusions in the form presented herein. First of all, it is with the greatest of pleasure that I acknowledge the seemingly inestimable contributions of my distinguished thesis and academic adviser, Dr. Karl Z. Morgan, Neely Professor of the School of Nuclear Engineering in the Georgia Institute of Technology. He provided not only excellent technical advice and review throughout the entire course of this work but also maintained a moral and spiritual standard in his work that I will carry with me throughout my life and practice in my own work. No matter what formal titles I will hold in life, I will always be proud to be called a health physicist. I wish to also thank him for his painstaking review and critique of this dissertation.

I would also like to express my appreciation to the other members of my thesis committee, Drs. William F. Bale, Geoffrey G. Eichholz, Robert F. Fetner, Patton H. McGinley and John W. Poston, for their deep interest in my work and comments on this dissertation. Dr. Eichholz's comments and suggestions were always timely and helpful in shaping this dissertation into its final form. I would also like to add a special word of thanks to Dr. Fetner for his unselfish aid and assistance in providing sorely needed equipment and quick answers to questions from a non-biologist to one who is a biologist in the most real sense. Many bumps

were smoothed by Dr. Fetner when he let me borrow equipment I would have otherwise found difficult to obtain. I would also like to thank Dr. Bale for his early interest in this work and comments throughout and Dr. Poston for his advice in the early stages in the design of the vacuum-sealed alpha calibrator. Additionally I would like to thank Dr. Lynn E. Weaver, Director of the School of Nuclear Engineering, for his interest and the School of Nuclear Engineering for financial assistance during arbitration of our DOE contract.

Many other persons provided various forms of assistance to this work. My deepest appreciation is given to Dr. W. S. S. Jee, Acting Director of the Radiobiology Laboratory at the University of Utah, for all his absolutely invaluable assistance to me. He provided many beagle dog bone samples, technical advice, use of his facilities, access to his personnel and kind treatment during my 10 day visit to his laboratory. I received many rewarding experiences during that visit as well as excellent advice and technical data from Dr. Jee after the visit. A number of the staff members at the Radiobiology Laboratory helped me during my visit, Becky Dell and her staff at the Bone Laboratory, Dr. F. W. Bruenger and Mr. D. R. Atherton in the Chemistry Group and Dr. R. D. Lloyd in the Laboratory itself. A special note of thanks is extended to Dr. J. M. Smith at the Radiobiology Laboratory who provided warm hospitality, knowledgeable conversation and the loan of the calibration sources that became so vital to this work. Dr. B. D. Breitenstein, associated with the Transuranium Registry at Hanford, Wash., added extra depth to these studies when he gave us several human bone samples from workers at the Hanford facility that had been exposed to bone-seeking alpha emitters. I would also like to thank

Dr. Naomi H. Harley at the New York University Medical Center for her enlightening conversations and for providing the energy absorption data from ^{239}Pu alpha particles that were important in the conversion of these results to rads/year. Also, Dr. John T. Godwin, Director of the Pathology Department at St. Joseph's Hospital, Atlanta, graciously provided the expertise and facilities to prepare the human bone samples.

Many other persons at Georgia Tech added to this research also. Dr. Edward L. Fincher, School of Applied Biology, helped with the early microscope work by providing materials and Dr. Richard W. Fink loaned his 2.0 uCi ^{239}Pu source throughout the duration of this work. I would also like to thank Mr. B. D. Statham for his technical assistance concerning the electronics associated with this work and his enjoyable conversations. Mr. W. B. Jeter performed many of the machining tasks on the vacuum-sealed alpha calibrator and other pieces of equipment as well as some of the photography work. Mr. R. M. Boyd provided the ^{239}Pu solution used in the early phase of this work and maintained some of the health physics aspects associated with our lab. I would also like to especially thank all my many personal friends in the School of Nuclear Engineering who brightened the days and gave me their warm friendship, Messrs. Adel Alapour, Shian-Jang Su, Mehdi Sohrabi, Michael T. Ryan, John Massey, Holger St. John, Bruce Byrne and others. I know I will never forget the fellowship of these friends. A note of thanks is also extended to our secretarial staff and especially Mrs. Ruth Salley and Mrs. Phyllis Frost who helped me with administrative problems.

I also give my personal thanks to Mrs. Lydia S. Geeslin and Mrs. Lydia F. Sweatt for their professional treatment concerning the typing of

this dissertation. It was a pleasure to work with them both.

Special thanks are also extended to Mr. Robert L. Butenhoff in the Division of Biomedical and Environmental Research, Department of Energy, for his support and financial assistance under DOE Contract No. EY-76-S-05-4814. This work would certainly have been altered from its present form without this assistance. I would also like to thank my girlfriend, Ms. Leta Fern Miller, for her patience and understanding for the times missed during the writing of this dissertation.

Most importantly I give my deepest thanks and appreciation to my family, my father, my mother and brother, who have always been solidly behind me in all my endeavors and in such a loving manner. They have always taken a great interest in my work, followed it until completion and continually been an inspiration and driving force behind me. It is such a comfort to me to have an interested and close family to share any small accomplishments that I may make.

TABLE OF CONTENTS

TABLE OF CONTENTS (Concluded)

LIST OF TABLES

LIST OF ILLUSTRATIONS

LIST OF ILLUSTRATIONS (Continued)

LIST OF ILLUSTRATIONS (Concluded)

SUMMARY

The dosimetry of internally deposited alpha emitters such as ^{239}Pu has been of interest for many years as a means to determine directly such quantities as maximum permissible body burden (MPBB) instead of the present practice of setting these values based upon comparison with ^{226}Ra. A new technique that will yield this dosimetry information directly by experimental measurement is a desirable task to perform and would provide data sorely needed by health physicists.

A procedure involving the electrochemical etching of polycarbonate foils to amplify the damage tracks produced by the alpha particles emitted by ^{239}Pu deposited in the skeletons of dogs and man was investigated to examine its feasibility for this application. This electrochemical etching technique was used to provide dose measurements and has been shown to be feasible for bone dosimetry applications of internally deposited alpha emitters. The technique delineated is general in nature and could be used for the dosimetry of other internally deposited alpha emitters, even in tissues other than osseous tissue.

During examination of the feasibility of the electrochemical etching system, several parameters were examined prior to the bone dosimetry application since the dosimetry system had not been calibrated for alpha particle dosimetry prior to this time. Several foil reading techniques were examined such as the transparency projector and microfiche reader. The compound microscope operated in the phase contrast mode was used for bone dosimetry. Background reduction studies resulted in a background of

2.0 tracks/cm^2 of foil surface, routinely achievable. Optimization of the electrochemical etching of polycarbonate foils considering background and sensitivity indicated 800 V, 2 kHz, 45% KOH etchant solution and four hours etching time provided low background and reasonable sensitivity. Sensitivity as a function of etching time and waiting time (time between irradiation and etching) were also examined. Efficiency of alpha particle track production as a function of energy was determined. A Bragg curve was achievable and the efficiency obtained at the peak of the Bragg curve was obtained when the energy of the monoenergetic alpha particle was lowered by the injection of 27-28 μm of polycarbonate absorber between the source and detector giving an efficiency of 1.0×10^{-3}%. A device called the vacuum-sealed alpha calibrator was designed for this purpose and housed a 2.0 μCi ^{239}Pu source as well as either polycarbonate foils or a surface power detector. Track diameter as a function of etching studies resulted in the discovery of two categories of track diameters appearing on foils irradiated by alpha particles and etched electrochemically. This effect was quantified as a function of incident alpha energy and a proposal offered to explain the effect. Reproducibility studies yielded an error of ± 15% in the dosimetry studies. These studies included foils etched weeks apart with different 45% KOH etchant solutions and different energies of alpha particles incident on the foils.

The bone dosimetry studies utilized undecalcified sections of beagle dog bones and decalcified human bone sections. The procedure used was as follows: (1) Polycarbonate foils were pressed tightly against the bone samples plus infinitely thick calibration sources and then etched electrochemically after appropriate exposure times. (2) Counting was performed

by randomly scanning the foils and counting tracks in a square 120 μm on each side. (3) Dose in rads/year was presented in two sets, one included the scans resulting in zero scans, D_o, the other did not, D_w. Efficiencies obtained from the infinitely thick calibration sources ranged from 2.22×10^{-3}% to 0.38%. Doses ranged from 16.7 rads/yr to 39580 rads/yr for D_o and 440 rads/yr to 317900 rads/yr for D_w. A factor was found that could be multiplied by the experimentally determined dose to make it equal to the ICRP permissible limit of 0.3 rad/yr (15 rem/yr). This value was then multiplied by the known skeletal burden to find an experimental maximum permissible skeletal burden for each bone section taking into account the mass difference of the dog and human skeleton. **The average of these experimental maximum permissible skeletal burdens was one half the present ICRP value of 0.036 μCi, the maximum and minimum values were four times greater and 700 times less than the ICRP standard, respectively.**

CHAPTER I

INTRODUCTION

Alpha particles are emitted in natural radioactive decay by numerous elements. Physically the alpha particle is a helium nucleus, $^{4}_{2}He^{++}$, and as such is considered to be densely ionizing as it passes through an absorbing medium. The ionization produced by an alpha particle is confined to a region very close to the track of the particle (Vaughan et al.).[1] In fact, ninety percent of the ionization is contained in a cylinder of radius 0.01 μm whose axis lies along the track. This dense ionization can cause dramatic effects in tissue; therefore, health physicists are very concerned with the dosimetry of internally deposited alpha emitters. There are several methods available to measure the local dose deposited in bone. These include a number of autoradiographic techniques whereby photographic film, e.g. NTA emulsions, is placed over the bone for various exposure periods and developed. The tracks are then counted visually (Rowland and Marshall),[2] (Jee et al.),[3] (Wronski et al.),[4] (Smith et al.),[5] or the track density determined densitometrically (Twente and Jee)[6] to obtain an estimate of the relative dose deposited on the bone surface. Another technique (James and Kember)[7] uses a thin "stripping film" about 3 μm thick so the emulsion can be removed from the backing, and after exposure the film is viewed with an eyepiece marked with 5 μm circles. Counting tracks in the circles will yield the particle fluence and then the dose. The effects produced in tissue after irradiation by

alpha particles can be quite severe indeed, even at a fairly low, macroscopically calculated dose. Carcinoma involving epithelial cells of the sinus cavity and the surrounding bone, pulmonary neoplasia fibrosis, necrosis, spontaneous bone fractures, tooth and tooth socket effects, osteomyelitis, osteoporosis, osteosarcoma, hemorrhage, edema and even leukemia are all possible results of alpha irradiation in vivo. It has been reported that death can be caused by an average skeletal dose of only 60 rads (Mays and Lloyd)[8] in beagles when injected with ^{239}Pu citrate intraveneously, a dose of 90 rads in humans injected with ^{224}Ra solution (Spiess and Mays),[9] or by an average skeletal dose of 1200 rads in humans ingesting ^{226}Ra (Evans et al.).[10] Our primary concern here will be plutonium-239. Its toxicity has been shown to be quite great in a number of studies at the University of Utah (Twente and Jee),[6] (Mays and Lloyd),[8] (Jee),[11,15,16] (Arnold and Jee),[17] (Stover and Jee),[12] (Mays et al.),[14] (Stover et al.),[13] at the University of California (and in conjunction with the Metallurgical Lab)(Durbin and co-workers),[18-22] (Hamilton and co-workers),[23-25] in France (Lafuma and co-workers),[26-30] and at Hanford (Bair, Thompson, Clarke and co-workers).[31-46] A good summation is given in Bustad et al.[47] This toxicity can be attributed to a large extent to the chemistry of plutonium-239 (aside from its radioactivity) which distinguishes plutonium from other actinides (Taylor).[48] Not unlike the other actinides, plutonium is a bone seeker, but unlike most of the other actinides (except thorium) plutonium is preferentially deposited on the bone surfaces (Jee),[11] (Arnold and Jee).[17] This action brings the radiosensitive proliferative cells under heavy alpha irradiation by plutonium. The amount of ^{239}Pu which is deposited on the bone

surfaces depends on such factors as mode of administration, species of animal, state of health, age of patient, chemical form of the plutonium and chemical state.

Due to the possibility of widespread use of plutonium for power and military purposes it behooves our society to ensure the safe containment of this highly toxic substance as well as to be aware of the effects of ^{239}Pu in man at various concentrations in vivo. Of course this tacitly requires the availability of adequate and accurate dosimetry of ^{239}Pu in bone (the present critical organ for ^{239}Pu).

To assist in this task, the dosimetry of ^{239}Pu in bone was the goal of the work described here. To accomplish this by the track-etch method chosen, several parameters were needed in the new dosimetry system selected for this research. This system is the electrochemical etching system (Sohrabi).[49] Results obtained from work on the etching system itself are also presented.

1.1 The Alpha Radiation Hazard

1.1.1 Characteristics of Alpha Particles

Alpha radiation was first characterized as such by Rutherford in 1899 by noticing the absorption of this radiation in relation to other radiations which he denoted as beta radiation (Rutherford et al.).[50-54] It was during that same year when Rutherford and F. Soddy identified "alpha" radiation as an inert gas. We now know this inert gas was created when the alpha particle, a $^{4}He^{++}$ nucleus, captured two electrons after emission during the radioactive decay of another nucleus and subsequent slowing down in an absorbing medium. Normally alpha particles

are emitted in a monoenergetic fashion but can occur in discrete energy groupings if the product nucleus is left in various states of excitation. These excited states will be subsequently transformed to the ground state by gamma emission. Known alpha particle energies in radioactive decay range from about 1.5 MeV (^{142}Ce) to about 11.7 MeV (^{212m}Po). This relatively small range in energies is contrasted with an enormous range in half-lives of the various alpha emitting nuclei. These half-lives range from less than 10^{-6} second to more than 10^{10} years for the various alpha emitting radionuclides, a variation by a factor of 10^{27}.

As alpha particles traverse a medium, they lose energy by the processes of ionization and electron excitation with some contribution from inelastic scatter reactions with low Z absorber atoms. Upon traversal of air or tissue an alpha particle will lose, on the average, about 34 eV of energy for every ion pair it creates. This value is about twice the ionization potential of the medium because excitation of the atoms and molecules diverts part of the available energy away from the ionization process to the excitation process and recombination. Possession of a high electrical charge and relatively low velocity, due to its large mass, causes the specific ionization of an alpha particle to be very high compared with photons and beta particles, on the order of tens of thousands of ion pairs per centimeter in air (Cember),[55] compared to ten to a hundred ion pairs per centimeter for a beta particle.

Because of this high rate of energy loss, alpha particles are extremely limited in their ability to penetrate matter. The dead outer layer of skin of the adult is sufficiently thick to absorb all alpha

particles emanating from external alpha sources. As a consequence, alpha radiation is not considered to be a serious external hazard. The effects of an internal deposition of alpha emitting nuclides, though, are quite different and serious in their consequences as will be discussed later. In air, even the most energetic alpha particles from alpha emitting nuclides travel only several centimeters, while in tissue the range is of the order of a few tens of microns. For a given alpha particle energy, Bragg has shown that (Price)[56]

$$\frac{R\rho}{\sqrt{A}} \cong \text{a constant} \tag{1.1}$$

where

R = alpha range in a particular absorbing material

ρ = density of this same absorbing material

A = atomic weight of the material

This relation allows calculation of the approximate range of a particular alpha particle in any uniform medium if the range of this alpha particle is known in another medium and the density and atomic weight of both media are known. The alpha particle has the characteristic that the rate of energy loss in an absorbing medium is approximately a constant for most of the trajectory of the alpha until the end of the path is approached, see Figure 1. The sharp rise in ionization at the end of the range is caused by the increase in the interaction cross section of the electrons of the absorbing medium with respect to the alpha particle. This increase can be attributed to the larger impulse (Ft) received by the orbital electrons when the alpha particle is moving at a slower

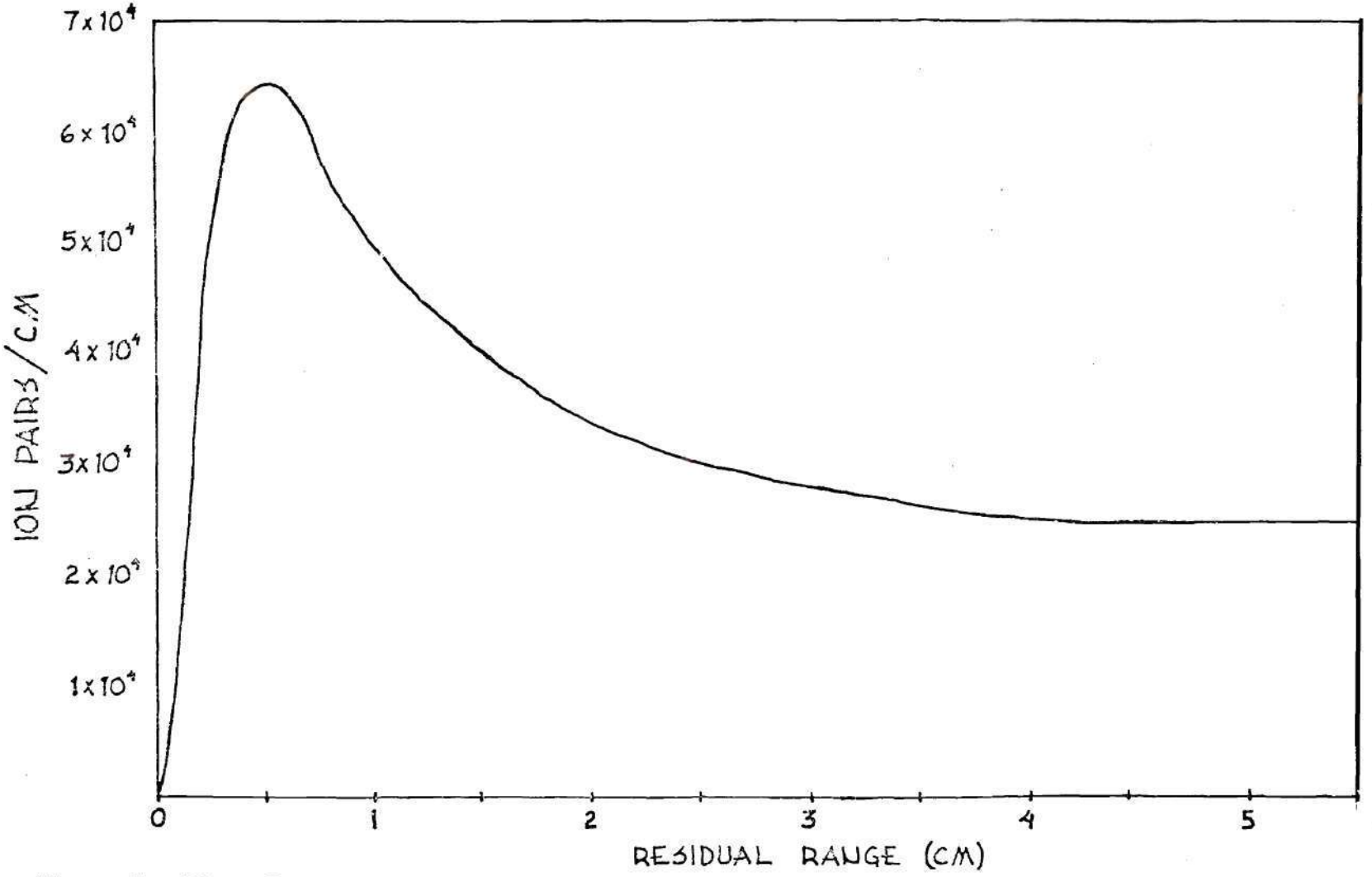

Figure 1. Plot of Specific Ionization versus Alpha Particle Energy (Bragg Curve). (Here residual range is used as a measure of the particle energy, the greater the residual range the greater the alpha particle energy.)

velocity (at the end of its range) than when it is moving at a more rapid velocity (at the beginning of its range). The larger impulse results from the longer time elapsing while the alpha particle is close enough to the electron to cause interaction at the slower velocity than at the faster one. In fact, at the end of the path of the alpha particle, its velocity is approximately equal to the velocity of the orbital electron allowing maximum possible interaction between the two.

1.1.2 Effects of Alpha Particle Energy Deposition in Tissue

The effects of alpha particle irradiation *in vivo* tend to be localized in the volume surrounding the alpha tracks and to a short distance from the point of deposition of the alpha emitter due to the short range in tissue of these particles. This is somewhat different from the effects of electromagnetic radiations which can cause widespread effects throughout the body, such as erythema, anemia, necrosis and temporary sterility at high doses, and cataracts, leukemia and other tumorigenic effects at low doses (Morgan and Turner)[57] and (Warren).[58]

Warren[58] notes three problems found in the final determination of the late effects of photon irradiation. These problems are also worth considering for alpha particles induce tumorigenic effects. The first is a special susceptibility believed to be present in some individuals. The evidence supporting this theory is found in his multiple malignancy studies. Here an individual with one malignancy was shown to have a probability significantly greater than the population average of contracting other malignancies. Presumably this could be interpreted as a genetic influence. The second problem involves confusing the tumorigenic effects

attributable to radiation alone. As the age of an individual increases so does the probability of observing a malignancy in this individual. It is known that radiation can increase the aging process (Morgan and Turner).[57] Therefore it could be difficult to determine unambiguously whether the tumorigenic effect observed was caused by the radiation itself or the effective increased age of the individual and his resultant higher probability of incurring a malignancy. The third problem is the wide variation observed in individual radiosensitivity to various biological effects such as tumorigenic effects and white blood cell count. Warren found variations by as much as a factor of fifty or more in the doses needed to induce certain malignancies in various strains of mice. He also noted wide variations in the response of white blood cells among four men receiving approximately 60 rads from a cyclotron beam in the same radiation accident.

Other effects also should be considered when considering long term effects of radiation. One phenomenon is the latency period. Latency is the time elapsing between the induction of the tumorigenic change to the clinical presentation of the tumor. The latency period varies widely among the different types of tumors of course but varies among individuals as well for the same type of tumor. This latter variation could be due to differences in individual immune systems. An example of this variation is the latency period for osteosarcoma in humans, three to six years (Marshall and Groer).[59] This variation in latency period also needs to be included in calculations of overall dose-effect relationships for tumorigenic change.

Although some of the above effects are observed after the administration of alpha emitters such as ^{239}Pu (Stover and Jee),[12] (Bair et al.),[34,35,36] (Thompson et al.),[41,43] effects such as anemia, necrosis and sterility are not observed until toxic doses are reached. On the contrary, effects due to internally deposited alpha emitters tend to be more subtle and require a longer latency period before manifestation of the effect. These effects include osteosarcoma (Vaughan et al.),[1] (Stover and Jee),[12] (Jee),[11] (Mays and Lloyd),[8] (Evans et al.),[10] (Hasterlik et al.),[60] pulmonary neoplasia and other lung and lymph node effects (Bair and co-workers),[31,32,34,37,38] (Thompson and co-workers),[41,42,44] (Bustad et al.),[47] tooth effects (Evans et al.)[10] (Hasterlik et al.)[60] and liver effects (Durbin),[19-21] spontaneous fractures, other non-fatal bone effects (Stover and Jee),[12] (Evans et al.),[10] (Vaughan et al.),[1] (Hasterlik et al.),[60] and altered osseous circulation (Jee et al.).[3]

In general for cells in tissue cultures, the mechanism of radiation from alpha radiation seems to be characterized as a "one-hit" process with no repair at LET's above about 25 keV/μm (Vaughan et al.)[1] as supported by James and Kember.[7] It does appear that the sensitive portion of the cell is the nucleus (Lea)[61] and (Vaughan).[1] Due to the high ionization density, there is a very high probability, approaching one, that an alpha particle passing through the cell nucleus will render the cell incapable of division "reproductive death" (Lea),[61] (Casarett)[62] and (Vaughan).[1] However, Marquart[63] has shown the mitochondrion to be the most susceptible cellular component to radiation damage from alpha particles in his study using mice injected with ^{224}Ra salt solution. But damage to a mitochondrion may not be as debilitating as damage to the

chromosomes of the cell nucleus.

Even though the last statement concerning the cell's nucleus is generally true, it cannot be assumed that the same effect will be produced in any type of cell for a given dose. In fact some cell types in human tissue show an extraordinary resistance to radiation damage from deposited ^{239}Pu, even when the cell contains enough ^{239}Pu to make irradiation of the cell nucleus inevitable. Macrophages in the lung and peritoneal cavity are capable of containing hundreds of $^{239}PuO_2$ particles of the order of one micron in size and still function (Bair).[37] They tend to lose reproductive capability, however, and are therefore incapable of malignant transformation; these cells do retain phagocytic activity for as long as seven days while in this condition. It appears, in fact, that the lifetime of a macrophage in this particulate-filled condition is at least a factor of one hundred greater than the time required to replace a damaged macrophage because a damaged macrophage is not seen under microscopic examination (Vaughan).[1] Macrophages could be considered among the most radioresistant cells in terms of cell function, whereas some cells such as epithelial and stem cells (Lea)[61] and (Evans)[64] are very sensitive to ionizing radiation. What then are the criteria which determine a cell's sensitivity to ionizing radiation? These criteria were examined by Bergonie and Tribondeau and stated in what has now become known as the "Law of Bergonie and Tribondeau" (Bergonie and Tribondeau)[65] which states that cells are more radiosensitive if: (1) they have a high mitotic rate, (2) they have a long mitotic future and (3) they are of primitive type (stem cells). Thus we can see why certain cells exhibit more radiosensitivity than others. One notable exception to this "law"

is the lens of the eye. Lenses are high radiosensitive, yet the cells present do not have a high mitotic rate. Possibly for high LET radiations, such as fast neutrons, little or no repair occurs allowing damage to accumulate.

Bone cells possessing the most primitive character are the pre-osteoblasts, also called osteoprogenitor cells. These normally reside on the surface of the bone and out to a distance of about 10 microns removed from the surface of the bone (Vaughan).[66,1] Since this subject will be discussed again in the section concerning plutonium toxicity, let it suffice to say that, if an alpha emitting nuclide is positioned such that these cells receive the majority of the alpha irradiation, maximum damage will be inflicted upon the bone possibly resulting in a malignancy.

When mentioning a leukemic transformation, or any malignant change, one is referring to the change in a cell causing it to lose the prior function it had and to be removed from the controlling influence of the body. This change does not indicate an increase in mitotic rate. In fact, the leukemic white blood cells divide only one third as rapidly as normal white cells. The reason an accumulation of leukemic cells occurs and normal white cells remain constant (or decreases) is leukemic cells do not travel to the spleen to be destroyed after 120 days, upon a signal from the body, as do the normal cells. Tumor cells cannot undergo repair as is common among normal cells. This latter property is the biological basis for treating malignant tumors with radiation therapy. Although healthy tissue is irradiated with the cancerous tissue, the healthy tissue will attempt to repair itself whereas damage to cancerous tissue is cumulative. The other malignancy we have discussed, the osteosarcoma, seems

to be caused by a two hit mechanism by alpha particle irradiation (Marshall and Groer).[59] The osteosarcoma is one cancer in a group collectively named bone tumors. Bone tumors have a maximum natural incidence during adolescence with a rate of about three per 100,000 (Rubin).[67] About 28 percent of these bone tumors, the most common, is the osteosarcoma. This tumor is of osteoblastic origin and is more radioresistant than some of the other bone tumors. When considering combination treatments of osteosarcoma utilizing chemotherapy, radiotherapy and surgery, the five year survival is between five and twenty percent, the second lowest of the nine bone tumors considered by Rubin.[67] Marshall and Groer[59] envision this tumor to be induced by two separate hits on two targets. Then a promotion period follows after which the tumor is clinically presented. The two hits could occur along the path of one alpha particle or by two separate alpha particles. The calculated areas of each of the two targets are about the size of 100 pairs of nucleotides along the DNA double helix. These nucleotides could be the ones controlling the biologic switch which in turn controls mitosis. Competing with this two-hit mechanism is cell killing and cell replacement, occurring about 10^5 more times than progression down each step in the chain to malignancy. They found an initiation probability of 4×10^{-8}/rad for osteosarcoma in man based on the radium cases and the probability of cell killing to be 10^{-2}/rad. In this theory only the initiation and killing probabilities are controlled by radiation, cell replacement and promotion proceed at the same rate regardless of the radiation. This two-hit mechanism of damage by alpha particles does not conflict with the one-hit previously mentioned since the latter one was concerned only with single cells in cultures and the

two-hit mechanism is concerned with an entire man.

The macroscopic effects of internal deposition of alpha emitting radionuclides were discussed above but the question arises as to what is occurring on the microscopic, cellular, level which could cause these observed gross effects. There are of course many effects observed in the cell after irradiation depending upon the amount of absorbed dose, as well as other factors (Casarett).[62] The one effect which seems to be most sensitive to radiation, especially at the low dose end, is the frequency of chromosome aberrations (Muller),[68] (Lyons et al.).[69] This observation can be used to quantify the various types of radiation according to a dose response relationship (Lea).[61] When this is done, it becomes apparent LET is one of the most important factors in determining the degree of increase in frequency of chromosome aberrations (Lea).[61] Another crucial effect on the cell after irradiation is inactivation or reproductive death.

In an effort to explain inactivation of cells as a result of ionizing radiation, the Target Theory was developed by Lea.[61] According to this theory, inactivation of a cell will result when a hit (or hits) occurs within a specific sensitive region (or regions). The hitting of this one particular region will result in inactivation of the cell. Hits in other locations can possibly occur without causing inactivation of the cell but can result in some of the indirect radiation effects to be discussed later. The sizes of targets vary from about 4-40 nanometers.

There are many changes which can occur in a cell that has been irradiated by ionizing radiation. Some of the immediate changes encountered can be summarized as follows (Bacq and Alexander)[70]:

(1) Delay in the onset of mitosis followed by normal mitoses. The first cell division after irradiation may show some temporary disturbance in the chromosome separating mechanism (called chromosome stickiness), which does not usually persist and as far as can be seen histologically does not produce ordinarily permanent injury unless it does persist. In humans chromosome stickiness can result in Down's syndrome, accounting for one eighth of all mentally defective infants.

(2) Complete inhibition of mitosis. The cell continues to live, i.e. to metabolize, but has permanently lost its capacity to divide and is said to have suffered reproductive death.

(3) Death of cells following one or more divisions after irradiation.

(4) Death of the cell occurs many hours after irradiation but without any intervening division. This effect is known as interphase death.

(5) Instant death under the beam following very high doses (~ 100 krads), called "beam death." This quantity of radiation will coagulate many proteins causing "instant" death.

(6) Chromosome aberrations and breakage.

(7) Interference with the functions of the cell. This may be temporary or permanent and the dose needed to achieve it varies widely.

(8) Other effects such as damage to cell blood supply, formation of radicals in the water surrounding the cell, etc.

Not only is the number of effects seen in the cell upon irradiation large but also the sensitivity of cells and components of cells varies widely. The dose that will kill all but 37 percent of the cells present in an experimental setup, called the D_o dose, ranges from 100-200 rads for mammalian cells to millions of rads in enzymes (Casarett).[62] To complicate the situation even further, the radiosensitivity of cells and cellular components is subject to considerable variation within identical groups. This sensitivity will change by a factor of two or three depending on the conditions existing before, during and after irradiation within a group of identical cells (Elkind and Whitmore).[71] Some of the conditions during irradiation that affect radiosensitivity are temperature, water content, oxygen and the presence or absence of certain substances. The various post-irradiation treatments commonly studied include heat, exposure to NO, presence or absence of oxygen, etc. The presence of water is important in determining the effect of ionizing radiation in tissue (Casarett).[62] The radiochemistry of water is quite complex and tends to amplify the effect of the incident radiation. Water causes this amplification by the formation of free radicals, which we might mention parenthetically is the operational basis for chemical dosimeters such as the ferrous-ferric ion dosimeter. The role of these free radicals in determining the damage inflicted on tissue containing radicals depends on such factors as presence of oxygen and magnitude of the deposited dose (Okada).[72] These radicals can cause damage in cells which have not even suffered a direct hit by the radiation. This could be accomplished by a number of mechanisms (Okada).[72] First the free radical is formed, say the peroxyl radical HO_2°, in a location removed from the chromosomes of

the cell nucleus. This radical could then migrate to the chromosomes and interact with one of them causing a large radical to be formed by abstraction of a hydrogen ion from the chromosome. This is now quite a different molecule from the original chromosome and will therefore interact with its surrounding medium in a different manner. The chromosome could become disabled in this manner even though it was not directly hit by ionizing radiation. This effect is called an indirect effect of ionizing radiation and has the capability to alter significantly the final effect caused by ionizing radiation (Casarett).[62]

To move from the effects realized at the cellular level to the more macroscopic effects mentioned earlier, the various tissues in the body need to be discussed. In the human body there are four major tissues (Villee and Dethier)[73]; these are epithelial, connective, muscular and nerve tissues, each containing cells of varying functional and morphological characteristics. The collective connecting tissues are vascular tissues (blood, lymph), connective tissue proper (white fibrous, yellow fibrous, reticular, adipose and areolar), cartilage and bone. The major functions of the connective tissues are the support of body structures and the binding of its parts together. Tissue histologically is referred to as the assemblage of similar cells with a specific function. The differing characteristics and functions of the cells in tissue cause them to exhibit varying degrees of radiosensitivity. When looking at the risk of tumor formation from internal alpha emitting nuclides in bone, the risk is found to be associated with the following factors (Jee)[11]:

(1) The volume of cells at risk from alpha irradiations, i.e. related to the alpha particle range in tissue

(2) The intensity of the alpha radiation impinging on the bone surface

(3) The proliferative potential of the cell.

The effects of alpha emitters retained in vivo have been examined by a host of researchers at many different locations throughout the world: at the University of Utah by Jee, Mays and co-workers[6,8,9,11,12]; at the University of California by Durbin,[18-22] Hamilton and co-workers[23-25]; at Hanford, at Washington by Bair, Thompson, Clarke and co-workers[31-46]; in England by Vaughan and Bleaney[1]; and in France by Lafuma and co-workers.[26-30] Evans[10,64] and Hasterlik et al.[60] have extensively studied what is certainly the largest body of human data concerning internally deposited alpha emitters, human exposure to radium. Data on radium deposition in man are derived primarily from three sources (Evans).[64] The first category includes radium dial painters, who ingested a radium containing self-luminous compound when they used their lips to point the fine brushes used to paint numerals on watches, clocks and instruments. This mouth tipping was ordered discontinued in the United States around 1926 following identification of "radium jaw" in 1924 by Theodore Blum, a New York dentist (Evans).[64] In this country there were about fifty dial painting "studios" and the total number of employees at risk during the high exposure period was of the order of at least 2000. The median age of the survivors of this group in 1966 was about 60 years (Evans).[64] The second category includes radium chemists who were employed in about 23 refineries and radium laboratories. The total number of chemists and technicians so employed seems to be difficult to determine but appears to be between 500 and several thousand (Evans).[64] The median age of

those surviving until 1966 in this group was 75 years. The third and also the largest category comprises iatrogenic cases, i.e. those individuals to whom radium was administered by a physician internally by ingestion or injection for medical reasons. The internal use of radium was removed from the "American Medical Association New and Nonofficial Remedies" about 1932. Prior to that time and for some years thereafter it is known there were more than 53 physicians or clinics administering radium internally to patients. The total number treated was estimated by Evans[10,64] to be several thousand. One clinic alone, during a five year period around 1920, gave more than 14,000 intravenous injections of radium (usually 10 μCi each) and more than 22,000 oral administrations of radium. Aside from these iatrogenic cases several patent medicines containing radium were available. One of the most popular was Radithor which was a mixture of one μCi of radium and one μCi of mesothorium in one-half ounce of water. It was sold in cartons of 30 vials, to be taken at the rate of three per day after meals. Some 22,000 vials of Radithor were sold in 1925 alone and between 1926 and 1930 the records indicate that 406 mg of radium and 471 mg-equivalents of mesothorium, or enough for between 400,000 - 500,000 treatments, were sold. The median age of the survivors of this large group of iatrogenic and nostrum (patent medicine) cases was 74 years in 1966. Evans found that, for residual skeletal burdens greater than about 0.5 μCi ^{226}Ra, the occurrence of osteoporosis, dense bone necrosis, trabecular coarsening and spontaneous fractures increased with increasing residual skeletal burden. For residual skeletal burdens falling in the range 0.5 - 60 μCi ^{226}Ra, the fractional incidence of osteo-

genic sarcoma and carcinoma of the paranasal sinuses or of the mastoids was about 40 percent and seemed to be independent of the residual body burden within this range. There was a difference however in the tumor appearance time or induction-plus-latent period. It tended to increase substantially as the residual body burden decreased until finally the tumor appearance time could be considered to be greater than the life span of man for sufficiently small residual body burdens. The body burden fulfilling this latter criterion is referred to by Evans as the "practical threshold" and in support he points out he observed no clinically significant symptoms below a residual body burden of 0.5 μCi. The initial burden tended to exceed the final skeletal burden by a factor of about 20. Therefore, Evans believed these two facts give a degree of confidence in the current value of the maximum permissible body burden (MPBB) in bone equal to 0.1 μCi for ^{226}Ra.

It could be agreed that the degree of confidence placed in the 0.1 μCi value by the above is actually less than the confidence level expressed when the value was originally established in 1941 by the NCRP.[74] It was stated at that time (1941) that the value of the MPBB for bone was established at 0.1 μCi because no serious injury to radium dial workers was known to have occurred with a burden ten times this value (Morgan and Turner).[57] At the present time, however, that MPBB value for ^{226}Ra has been opened to question. Hasterlik has found a tumor in a person whose residual body burden was 0.1 μCi. Gofman and Tamplin[75] have challenged Evans' hypothesis of the "practical threshold," where the burden of ^{226}Ra is so low that the latency period for the tumor is beyond the remaining life span of the individual. They point out the vast in-

crease in population size needed to observe an effect occurring with decreasing frequency as dose decreases. In fact, their calculations indicate one would not expect to observe cancer at the lower dose ranges considered by Evans and Hasterlik for the population sizes they were forced to use. But, as Gofman and Tamplin[75] point out, no real conclusion can be drawn to support or disprove a linear hypothesis from Evans' and Hasterlik's data[60,64] and certainly a practical threshold is not supported in an irrefutable manner. Therefore, we cannot be absolutely comfortable with the 0.1 μCi burden of ^{226}Ra in a man as an acceptable burden in the occupational radiation worker.

Another study of thirty persons exposed to radium by the mechanisms mentioned above was performed by Aub et al.[76] They divided the examined cases into four groups as shown in Table 1.

Table 1. Dose-response Relationship for Ingested Radium in Man

Group	Radium Body Burden (μg-eq)	Number of Tumors	Size of Group	Tumor Incidence (%)	Average Latency Period (yr)
I	> 8	2	8	25	19.5
II	2-8	3	9	33	24.6
III	0.7-2	3	9	33	23.6
IV	< 0.7	0	4	0	--

The four patients placed in Group IV had less than 0.7 microgram equivalent of radium in their bodies, the greatest being about 0.5 microgram equivalent of radium. The results of their study proved to be quite inconclusive from the viewpoint of establishing a dose-response realtion-

ship for radium. No clinical symptoms were observed at a body burden below 0.5 microgram equivalent of radium. No conclusions could be drawn other than for the small number of cases considered, the tumor incidence and induction time showed little variation with different degrees of radioactivity.

Twenty-two radium patients were studied by Hasterlik et al.[60] They reported fifteen cases of osteosarcoma and eleven other tumors of the cranial sinuses which were not osteosarcomas. In no patient with a body burden less than 0.6 μCi ^{226}Ra could a tumor be found at the time of measurement. The range of radium burden was 0.6 - 10 μCi, 30-40 years after exposure. Again, this result could be construed to be somewhat reassuring since the current MPOB in bone for ^{226}Ra is 0.1 μCi and these are burdens measured 30-40 years after exposure; the initial burdens would have been much greater. But before any conclusions can be drawn from these data, the Gofman discussion concerning population size would need to be examined once more and applied accordingly. In addition, Morgan[77] has shown there is a tendency toward malignancy even for these data down to a body burden of 0.1 μCi.

There is another category supplying information as to the effects of internally deposited alpha particle emitters. This category includes the men working in the Schneeberg cobalt mines of Saxony and at the Joachimsthal pitchblende mines of Bohemia who inhaled particulates and radon daughters (Bair),[32] (Morgan and Turner).[57] The high incidence of lung disease which occurred in these miners was noted as early as the 1500's but was not systematically examined until the end of the nineteenth

century. The incidence of lung cancer was very high among these miners and was actually approaching 40 percent between 1875-1912 (Bair).[32] From 1922-1939 the lung cancer incidence was even higher, averaging 50 percent with a peak around 83 percent; this was believed to be caused by the startup of radium and uranium mining (Bair).[32] These data from miners are not considered as the direct or inclusive evidence for the effects of alpha irradiation in man as would first be thought. This unfortunate situation is due to the many different contributing factors which were present and also known to be carcinogenic. Therefore it appears radiation may have been only one of several factors involved. These mines were not very clean mines compared to today's standards. The miners inhaled large quantities of dust containing silica, arsenic, cobalt, etc. as well as the alpha particle emitters (Bair).[32] Another factor to be considered is the large percentage of miners who smoke cigarettes. Lung cancer among the smoking miners in the Colorado plateau uranium mines occurred at an incidence equal to 700 cancers/10^5 miners whereas the incidence among miners who did not smoke was only 4 cancers/10^5 miners (Bair).[32] Thus there appeared to be a synergistic effect when smoking was combined with working the Colorado plateau uranium mines. Martell[78] believes the ^{210}Po present in the cigarette smoker's lung is the cause of lung cancer and other effects associated with cigarette smoking.

There have been studies of human exposure to other alpha emitters such as the Looney[79] studies of patients ingesting Thoratrast ($^{232}ThO_2$ in suspension) which produced hepatic tumors primarily, described briefly in Morgan and Turner[57] and in greater detail in Looney,[79] to which the reader is referred. Before ending this discussion of the human data available

concerning the internal deposition of alpha emitters, we can examine one nuclide, ^{224}Ra, for which human data exist and have close bearing to ^{239}Pu, the nuclide of main concern in this paper. The reasons for interest in this nuclide in relation to the effects of ^{239}Pu in man are threefold: (1) when first administered, bone seeking nuclides tend to concentrate on bone surfaces before moving into the bone, (2) the time required for the nuclide to move into the skeleton is long enough so that about half the skeletal deposit of ^{224}Ra (half-life 3.62d) will decay on the surface of bone and finally (3) the data are human data which are of value since no adequate human data exist for the effects of ^{239}Pu in man (Spiess and Mays).[9,80] This study is a quantitative examination of a group of patients in Germany who were injected with large amounts of ^{224}Ra from 1944-1951 as treatment for tuberculosis, ankylosing spondylitis (similar to rheumatoid arthritis) and various other diseases. The injections involved large amounts of essentially pure ^{224}Ra with its daughters removed. Activities ranged between 329 μCi injected over a twelve month period administered to a girl just over fourteen years old, up to 4116 μCi over a fourteen month period administered to a boy almost seventeen years old.

The total number of patients studied here was 854: 212 juveniles and 642 adults (Spiess and Mays).[9,80] To calculate the doses to bone received by these patients certain data concerning the behavior of ^{224}Ra were needed. After a comparison with existing radium, ^{45}Ca and ^{90}Sr data, it was decided that 50 percent of the injected dose appears in the excreta, primarily feces, 10 percent decays in the gut and 40 percent decays in either bone or soft tissue. Of this 40 percent there is about an equal

amount deposited in bone and soft tissue and about half the 20 percent in bone decays on the bone surface (10 percent of the injected dose) (Spiess and Mays).[9,80] It was found by this technique that the dose calculated to have been deposited on endosteal tissues out to a distance of 10 microns from the bone surface was nine times greater than the dose calculated for the same amount of ^{224}Ra assuming it was homogeneously distributed throughout the bone, i.e. the average dose multiplied by nine gave the endosteal dose for ^{224}Ra. In an analogous manner, they found the endosteal dose for ^{226}Ra was the average dose multiplied by 0.63. It was concluded that an average (whole bone) dose of 90 rads deposited by ^{224}Ra was the lowest dose observed to have caused an osteosarcoma (Spiess and Mays).[80] For ^{226}Ra, Evans[10,64] had found that 1200 rads was the estimated lowest dose to cause the induction of an osteosarcoma in man. These numbers compare favorably if appropriate factors are used to observe only endosteal surface dose. Calculating this dose for ^{224}Ra, 90 rads x 9 = 810 rads and for ^{226}Ra, 1200 rads x 0.63 = 760 rads, using the weighting factors described above. So it seems an endosteal surface dose equal to about 800 rads is sufficient to cause the induction of an osteosarcoma (Spiess and Mays).[80] The average whole bone doses calculated to cause induction of osteosarcoma in dogs is 60 rads for beagles injected with ^{239}Pu citrate and 130 rads for beagles injected with ^{228}Th citrate (Mays and Lloyd).[8] The value of 90 rads (whole skeleton) for osteosarcoma induction in man is between these latter two values for the surface seekers ^{239}Pu and ^{228}Th when considering osteosarcoma induction in beagle dogs but quite different from the 1200 rads required to induce osteosarcoma

in man using ^{226}Ra. Therefore ^{224}Ra is better compared with a surface seeker than a volume seeker when describing its ability to induce osteosarcoma.

1.2 Objectives of This Research

Because it is difficult to determine actual plutonium concentrations in the surfaces of bone, it was felt that it would be useful to develop a new approach that would lend itself to a more direct determination of alpha particle dose to trabecular bone surfaces.

The main objectives of this research, therefore, were:

1. To find the best dosimeter that can be adapted to the determination of the average dose to the endosteal surface of bone out to a distance of 10 μm.

2. To examine the parameters of this system with regard to reading methods, background reduction, bulk etching rate and reproducibility.

3. Since the dosimetry system selected, the electrochemical etching of thick polycarbonate foils, had not been applied to alpha particle dosimetry before, the characteristics of polycarbonate foils after alpha particle irradiation required better definition. These included track production efficiency and track diameter as a function of etching time and sensitivity as a function of etching time and waiting time.

4. The determination of the average dose to the 10 μm layer removed from the endosteal surface of various bone sections as a function of total body burden of ^{239}Pu.

CHAPTER II

BONE SEEKING RADIONUCLIDES

2.1 Osseous and Concomitant Tissues

Bone is a highly specialized form of connective tissue. There are certain characteristics that differentiate it from other forms of connective tissue, the most striking difference being that much of the tissue is extremely hard due to the deposition within a soft organic matrix of a complex mineral substance largely composed of calcium phosphate, carbonate and citrate (ICRP).[81] Bone can be regarded as a two component system comprising (1) a mineralized part, which consists of crystals of a calcium salt embedded in a matrix of collagen fibrils and a ground substance, occupying the intercellular spaces in bone. It has an effective atomic number, $Z \cong 14$, determined by the summation $a_i Z_i$, where a_i is the fraction of element i in bone and Z_i is the atomic number of element i, and bone has a density $\cong 1.9$ g/cm^3. Bone is also composed of (2) soft tissues which include cells within the mineralized part and adjacent to its surfaces (Spiers).[82] The nonliving part of the hard bone consists mainly of cortex (compact bone) and trabeculae (spongy bone), Figure 2 (Thomas).[83] The surfaces of bone are covered with non-mineralized layers of connective tissue called periosteum on the external surface, endosteum on the surfaces lining the marrow cavities and the Haversian canals throughout the mineralized bone in which run blood vessels. Also within the mineralized bone are much smaller spaces, lacunae, containing single

bone cells called osteocytes, connected with one another throughout the matrix by extremely finc processes running in the bone canaliculae, Figure 3 (ICRP).[81]

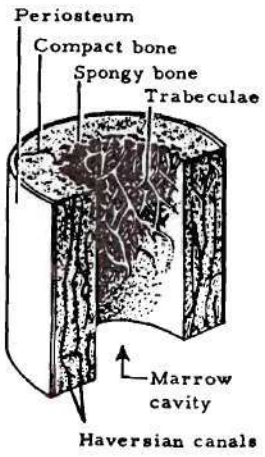

Figure 2. Cutaway of the Shaft Portion of Bone

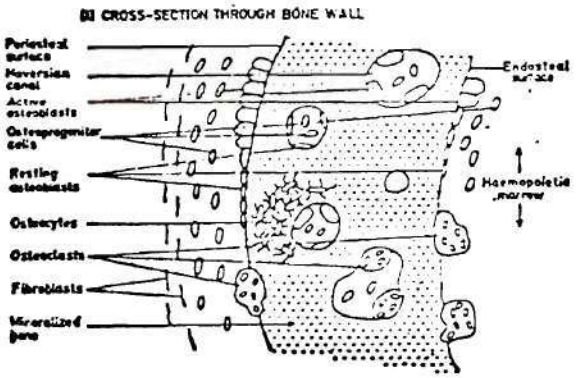

Figure 3. Diagrammatic Representation of the Relation of Osteogenic Cells to Bone Surfaces (not to scale)

In bone, the radiosensitive cells appear to be located

(1) among the osteogenic cells of the bone surfaces;

(2) in hematopoetic marrow;

(3) in certain epithelial cells close to bone surfaces.

The cells of bone are organized in a manner analogous to that in most tissues. A proliferating cell population (often referred to as stem cells) exists which differentiates into the nondividing functional cells of bone. These latter cells are the osteoblasts, the cells responsible for cell formation and the osteoclasts, the cells responsible for bone removal.

Cells on the periosteal surface of growing bone are arranged in well defined layers. Adjacent to the bone surface are the osteoblasts. Further away from the bone surface are the precursors of the osteoblasts called preosteoblasts or osteoprogenitor cells which are the main region of cell division. Beyond these is a region of fibroblasts, Figure 3 (ICRP).[81]

It is likely that the same cellular organization exists on endosteal surfaces and within Haversian canals though it is more difficult to distinguish the different cellular layers in these regions. To identify cell density, cell nuclear size, cell nuclear distance from bone surface and the cell DNA synthetic activity, Jee and Kimmel[84] have examined the thoracic vertebral body #2 from an adult beagle. Using a Merz grid they examined fine sections at 1000 X and identified four cell types. These were flat cells, osteoprogenitor cells, osteoblasts and osteoclasts. Flat cells possessed a nucleus about 8 μm by 1 μm and little visible cytoplasm. The 8 μm length of the nucleus was arranged parallel to the

trabecular bone surface. There were about 3×10^3 of these flat cells per mm^2 of trabecular surface, about one percent of which were synthesizing DNA. They tended to adhere quite tightly to the bone surface, 91 percent were within 2 μm of the bone surface, but a few were found as far as 8 μm away. The distances refer to the distance between the bone surface and the nucleus of the respective cell considered. About 600-1000 osteoprogenitor cells were found per mm^2 of trabecular surface, one to two percent of which were synthesizing DNA. Each cell nucleus was about 11 μm by 6 μm arranged in a variable manner with respect to the bone surface. They found 48 percent of the osteoprogenitor cells within 2 μm of the bone surface, 27 percent within 2-4 μm 15 percent between 4-6 μm and a few as far away as 10 μm from the trabecular bone surface. Osteoprogenitor cells also tended to have little visible cytoplasm. This work indicated about 500 osteoblasts per mm^2 trabecular surface, of which approximately five-tenths percent were synthesizing DNA. These cells had round nuclei containing one or two nucleoli with abundant cytoplasm and golgi apparatus. They were usually found in groups within 3 μm of bone surfaces. The final cell type, osteoclasts, were seen to occur in a frequency 200 osteoclasts per mm^2, none of which were synthesizing DNA. Osteoclasts contained many nuclei (usually two, three or four) and vacuolated cytoplasm. They were also found quite close to the bone surface. The work of (Arnold and Jee)[17] implicates the osteoclast in bone resorption (removal). This work will be discussed in greater detail in the section on plutonium but here we will just mention the steps proposed to occur during osteoclastic resorption of a bone surface. First the osteoclast acts in some manner to fragment the bone surface.

The osteoclasts then ingest the bone fragments and finally digest them. Kimmel and Jee[84] were somewhat surprised to find DNA synthesis in one percent of the flat cells on quiescent trabecular surfaces. The osteoblastic activity and osteoprogenitor cell synthetic activity were not surprising, since the latter is the stem cell and found mainly in areas of bone formation. Cells in the narrow spaces between trabeculae of growing metaphyseal bone (between diaphysis (shaft) and epiphysis, Figure 4 (Thomas)[83]), similar in character to the preosteoblast of the periosteal surface have been described as reticulum, spindle and mesenchymal cells, Figures 3 and 5 (ICRP).[81] The active osteoblasts on the surface may lay down sufficient matrix to surround themselves and thereby become osteocytes, laying in bone lacunae.

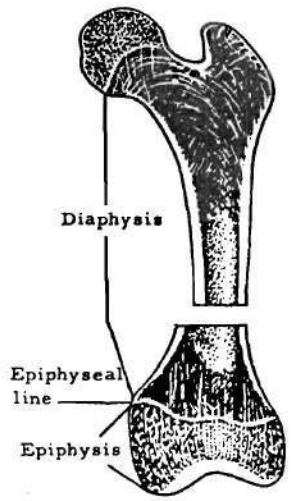

Figure 4. Macro-Components of Bone

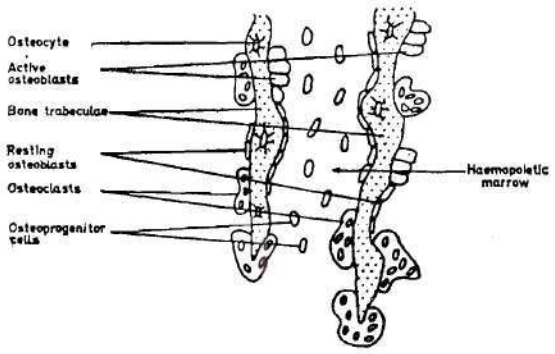

Figure 5. View Looking in from the Side of Figure 3

The layers of cells on the bone surfaces, often spoken of as the osteogenic layers, varies in thickness and in proliferative potential, depending on the age of the animal and the particular region of the skeleton. Recalling from Chapter I, radiation damage is most rapidly expressed in cells which are going to divide, the cell most likely to be at risk is the cell with greatest proliferative potential; in bone this is the preosteoblast or osteoprogenitor cell. However, it is possible that in abnormal circumstances other cells may be stimulated to divide as in the case of a fracture, osteoblasts and fibroblasts (ICRP).[81]

The area of bone covered by the periosteum is very much less than the area of bone covered by the endosteum since the latter covers the surface of all trabeculae. Until recently, numerical estimates have only been available for certain trabecular and periosteal surfaces. In man the trabecular surface area in a vertebral body of approximately 40 cm^3 is ~ 1000 cm^2 whereas the periosteal surface area is only 80 cm^2 (ICRP).[81] Spiers[85] has just added the six human long bones to the list of bones

which have been measured with respect to cortical and trabecular surface area. Of course, in all bones there are variations, depending particularly on age, in trabecular surface area but these variations do not alter significantly the relative proportions of endosteal and periosteal surfaces. Due to greater surface area, except in young animals, the processes of resorption and apposition (burying and building, respectively) are much more active on trabecular surfaces than they are on periosteal surfaces and within Haversian systems. These two factors, namely the greater number of cells at risk and the greater activity of these cells, probably account for the fact that the endosteal osteogenic cells, particularly those associated with marrow spaces, appear to be at greater risk than the periosteal osteogenic cells (ICRP).[81]

Now let us turn our attention to the hematopoietic cells. Hematopoietic stem cells, whether multipotent to form all cell lines of the peripheral blood or unipotent and differentiated to one line, originate in the bone marrow. There is evidence that stem cells may pass into the general circulation (ICRP).[81] Nothing conclusive is known about the number and precise location of such stem cells in man. It can be assumed, until better evidence is available, that in children the stem cells are randomly distributed in young active hematopoietic marrow throughout bone and in adults in active hematopoietic marrow within trabecular bone (Morgan and Turner).[57]

Whether or not only the most differentiated ancestral cell is at risk in marrow is not known. The blast cell mentioned above which shows some differentiation may again divide without further differentiation. It can be argued that cells as differentiated as the myelocyte (the large

cell in active bone marrow from which leukocytes are derived) can constitute a self-sustaining pool. Furthermore, in granulocytic leukemia (leukemia involving granulocytes, a granular leukocyte) the pH' chromosome appears to be not only in the leukemic population of myelocytes but in erythroblasts (red corpuscles) and megakayocytes (marrow cells with large or multiple nuclei) as well (ICRP).[81] This suggests that the final stage of the leukemic transformation occurs in the largely self-sustaining pool of myelocytes If both blast cells and myelocytes are capable of active proliferative activity the number of cells at risk may be considerable. Lymphocytic cells (lymph cells or white blood cells without cytoplasmic granules) are also found in blood marrow, but it is not yet clear what the relation of these cells to hematopoietic stem cells might be (ICRP).[81] Next, let us examine the epithelial cells surrounding bone. On general radiological principles it would be expected that the cells at risk for tumor induction in the epithelium close to bone surfaces would be the stem cell with greatest proliferative potential when irradiated by alpha and beta particles originating in bone. This has been shown to be the case in rabbits developing squamous cell carcinoma (involving flat epithelial cells) of the external ear (Vaughan).[86]

In human skulls carcinomas arise in the mastoid air cells and the paranasal sinuses. Anatomically these are among the few areas in the human skeleton where the epithelium is directly adjacent to bone. The total thickness of the epithelium and connective tissue in man in the paranasal sinuses and the mastoid air cells (spaces in temporal bone) is reported to be 50-100 μm causing those proliferating cells to lie

within the range of high energy alpha particles emerging from the underlying bone.

It can now be realized from the foregoing discussion that radiation dose to certain identifiable tissues within or associated with bone is likely to be the important parameter in determining maximum permissible levels rather than dose to "bone" considered as a single uniform entity. The geometry of the microstructure and the location of a particular nuclide in relation to the radiosensitive portions of the bone microstructure would then become important. This microstructure will also determine the type of biological abnormality observed. There are observations on man (Evans)[64] that suggest that if the endosteal osteogenic cells or epithelium close to bone surfaces are selectively irradiated, osteogenic sarcoma or carcinoma will result but that if hematopoietic tissue is equally at risk, as with x-rays or neutrons during whole body irradiation, leukemia is the more likely hazard.

Now we can perceive a clearer picture of the complexity of the situation when concerned with deposition of a radionuclide in bone. Depending on its location in the bone different components of the bone of varying radiosensitivity come under irradiation by the deposited nuclide. Also of importance in determining the effect a particular radionuclide will produce at a position on the bone surface is the activity occurring at the site. In other words which of the three states of bone are present, the resting, resorbing or forming state. Specific tissues could then be considered the critical "organ" depending on the nuclide of concern and its type of emitted radiation. Also the dose to these critical organs would necessarily need to be determined in setting maximum permissible

limits, just as with any critical organ, even though these critical organs are a part of the bone microstructure, e.g. osteogenic cells of trabecular bone. It is toward this end that this study is directed.

2.2 Categories of Bone Seekers

All the actinide elements and alkaline earth metals (Ca, Sr, Ra, etc.) are placed into a category called "bone seekers" due to their preferential deposition in the bone. After deposition into the bone, though, all these elements are not found at the same location in the osseous tissue. Some elements, such as radium, strontium, calcium, phosphorus and carbon are distributed more or less in a reasonably even fashion throughout the entire bone volume including cortical, trabecular and periosteal bone although radium may have a component in hot spots of the bone. Other elements like plutonium, americium and probably other transuranics are found preferentially on the endosteal and periosteal surfaces as well as the linings of the Haversian systems. The former group is referred to as "volume seekers" due to the characteristics of the distribution pattern, whereas the latter group is referred to as "surface seekers" due to their specific distribution pattern.

Due to variations among the constituents of the two classifications of bone seekers, a further division into four groups can be fashioned (ICRP)[81]:

(1) the alkaline earths

(2) plutonium and thorium

(3) americium and probably a large group of rare earths and transuranic elements the distribution of which has not yet been studied in detail

(4) phosphorus and carbon.

The alkaline earths (1) (calcium, strontium, radium, etc.) tend to be associated with the mineral portion of bone (ICRP),[81] (*Momeni et al.*),[87,88] (Lloyd et al.),[89] (Lloyd).[90] The distribution of these alkaline earths tends to be somewhat uneven but governed mainly by the presence of the processes of apposition and resorption. This uneven distribution tends to smooth into a more even distribution if the alkaline earth is administered in a continuous fashion. On the other hand, plutonium and thorium (2) tend to collect mainly on the endosteal, Haversian canal and periosteal surfaces, decreasing in concentration in that order (Jee et al.).[91] The ratio of plutonium on the endosteal face to that on the periosteal face of bone is about 1 to 3.6 in Beagles (Jee).[11] Americium (3) is taken up on all bone surfaces but does not seem to be concentrated on the endosteal surface to the extent that plutonium is (ICRP),[81] (Taylor).[92] In dogs the ratio of periosteal to endosteal Americium concentration is 1 to 2.0 (Jee),[11] about half that of plutonium. Other elements with probably the same distribution as americium are actinium, curium, cerium, berkelium, californium, einsteinium, etc. Phosphorus and carbon (4) become incorporated into the bone mineral not unlike the alkaline earths but in addition are incorporated into the nucleoprotein fraction of all cells (ICRP).[81] In particular this refers to the proteins of the lymph nodes, spleen and bone marrow. Carbon and phosphorus are both taken up in the DNA contained in the cell nucleus (ICRP).[81] Of particular interest to the discussion here is the characteristic of plutonium to become preferentially concentrated on the bone surfaces, especially the endosteal face, as mentioned several times before.

This point is raised again to give added stress because it appears to hold the key to the explanation of the profound toxicity of plutonium.

2.3 Desirable Characteristics for a New In-Situ Osteogenic Cell Microdosimeter

The determination of the average dose to the endosteal surface of bone from ^{239}Pu alpha particles is a highly specialized task indeed. There are many characteristics we would consider desirable for a dosimeter to possess to perform the given task. Some of the dosimetry systems which have been tried before have possessed some of these characteristics but the system chosen here is believed to be the most readily adaptable. We would like the dosimeter to

1. be of a geometry allowing the desired spatial resolution (micron range) to yield a meaningful dose distribution
2. be sensitive down to the low doses expected to be encountered with body burden levels of the radionuclide
3. resist fading so that rechecking of results at various intervals and over various time spans would be possible
4. operate without the use of any residual or induced activity to avoid the radiation hazards therein
5. be economical to use
6. operate without an excessively complex procedure to obtain data, thereby expediting reproducibility
7. have a small background correction
8. be adaptable to large scale usage to obtain as many data points as possible at one time.

2.4 Previous Bone Dosimetry Techniques

In general, methods of detecting alpha particles, including alpha spectrometry, tend to be more numerous than methods of determining absorbed dose due to alpha particle energy deposition. Physical characteristics of alpha particles can be determined by analysis of the pulse height distribution in proportional counters, pulse ionization chambers or scintillator spectrometer arrangements (Kiefer and Maushart)[93] and information on the spatial distribution of alpha emitters from solid state detectors (Becker and Johnson),[94] (Hamilton),[95] (Simmons et al.),[96,98] (Schlenker and Oltman).[97]

In the past there have been several techniques used to obtain indirectly an estimate of the dose delivered to localized areas of bone. Before describing the method used in this research to obtain a more direct dose reading we will first discuss some of the basic principles underlying these past methods then discuss the methods themselves.

One device that will be considered as a possible selection for this research is the scintillation counter. The scintillator counter consists of several components including the photomultiplier tube, scintillator material and a photocathode (Morgan and Turner).[57] A configuration which can be used in a scintillator type detector is shown in Figure 6[57] and a schematic configuration in Figure 7.[56] Light photons produced by the scintillator material impinge upon the photocathode located inside the photomultiplier tube, so that the electrons produced will be traversing a vacuum. The electrons produced by the photocathode are directed to the first dynode of the photomultiplier tube by a potential difference applied between the first dynode and the photocathode. Another potential difference exists between the second and first dynode of the photomultiplier

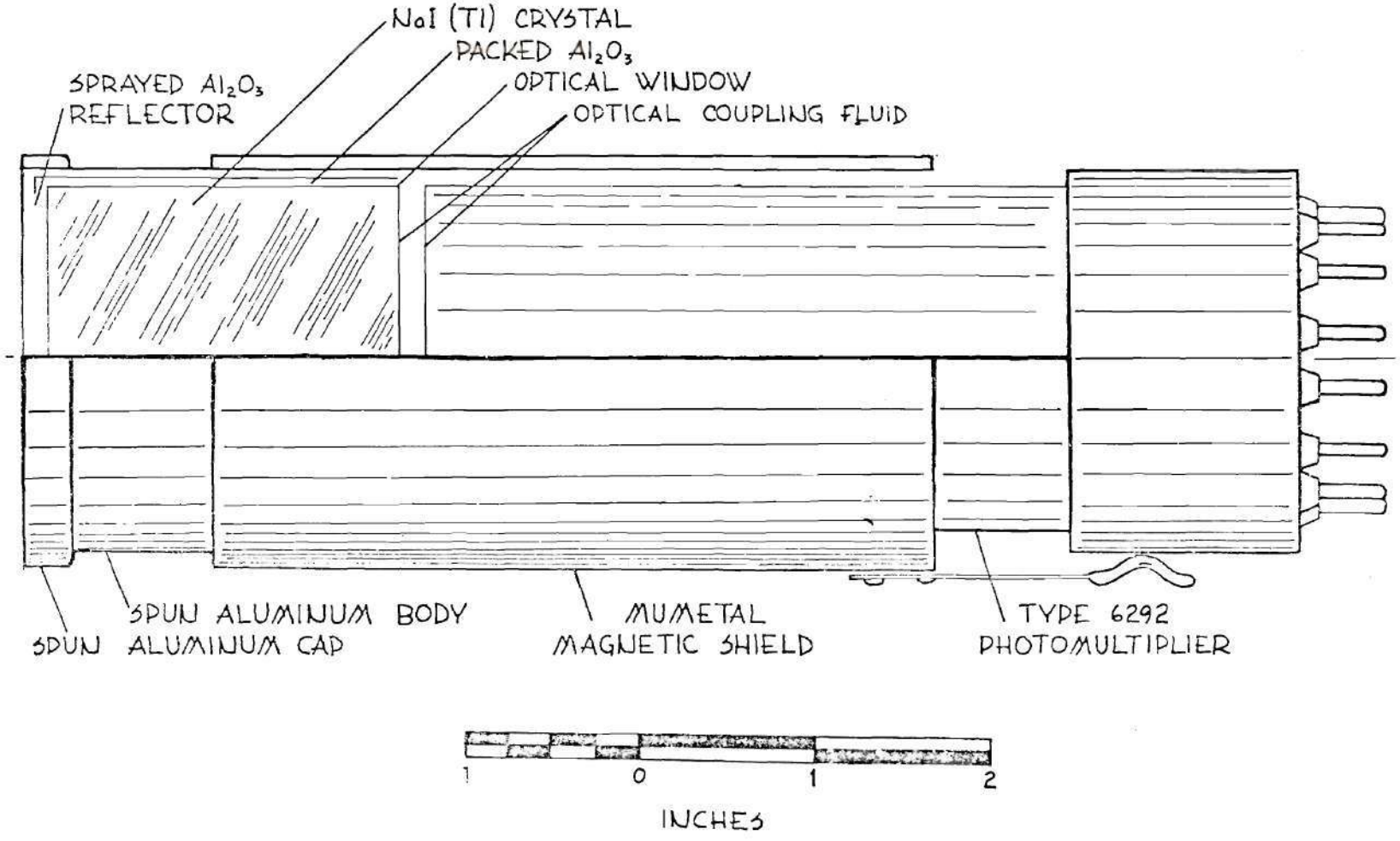

Figure 6. Scintillation Counter Assembly

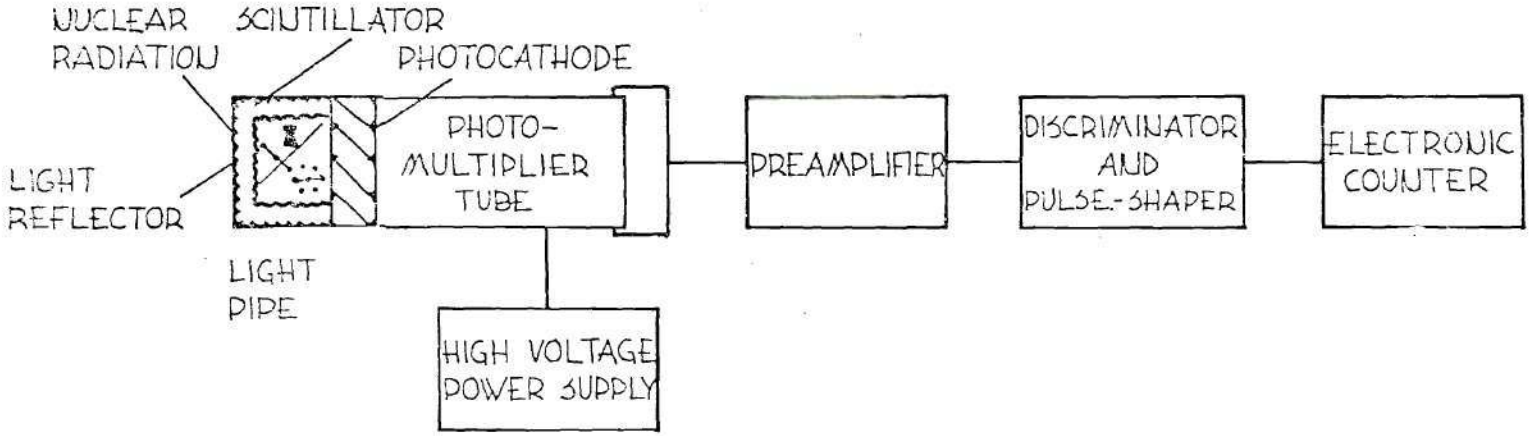

Figure 7. Schematic Diagram of a Scintillation Detector

tube which drives the incident electron plus several more electrons (multiplication has occurred) to the second dynode. This process is continued through the third, fourth, etc. dynodes until the anode is reached. At this point a multiplication of about 10^6 (assuming 10 dynodes and four additional electrons released at each dynode per each incident electron) will have been effected. The number of electrons arriving at the anode is proportional to the number of electrons released by the photocathode, which is proportional to the number of light photons created by the scintillator which, in turn, is propoportional to the energy released within the scintillator volume. So the scintillator is usable as a spectrometer. Several desirable characteristics for the detector to possess are: (1) the scintillator should be transparent to its own light photons, (2) the photocathode should have a high probability of producing electrons at the energy of the photons created by the scintillator and (3) the scintillator should have a high photon production efficiency for the desired incident radiation.

Inorganic scintillators are normally used to detect alphas (Price).[56] These scintillators combine several desirable features for this application including large light output, high stopping power which allows a relatively small volume to be used and reasonably fast decay times. The most common phosphor for alpha counting is silver-activated zinc sulfide phosphor. This phosphor has a very high efficiency for conversion from particle kinetic energy to photons, but its transparency is low. However, by preparing the zinc sulfide scintillator in a layer of thickness comparable to the range of alpha particles, the loss due to low transparency is minimized. Around 5 to 10 mg/cm^2 is the optimum thickness

for detecting most alpha particles emitted in radioactive decay. Although other types of radiation such as gamma photons may be present and will also produce scintillations in the zinc sulfide, these can be discriminated against because of the relatively small amount of energy they convert to light in the medium. Zinc sulfide scintillators can be coated directly on the glass envelope of the photomultiplier tube or coated on a transparent material such as lucite. For these latter cases, the transparent backing for the zinc sulfide is optically coupled to the photocathode.

Certain semiconductor detectors are useful for the detection of alpha particles (Morgan and Turner)[57] and will be examined as a possible choice for this research. Detectors such as the surface barrier detector are useful for measurements of the energies of particles of high specific ionization and in particular for alpha particle energy analysis. These semiconductor detectors can be used for detecting heavy particles such as alpha particles, protons and fission fragments in the presence of other radiations.

The properties possessed by semiconductor detectors which make them so useful in this area include linearity of pulse height versus energy, rapid response time, high energy resolution, thin entrance windows into the sensitive volume, variable sensitivity with respect to particle energy and relative insensitivity to gammas and neutrons (Price).[56] On the other hand, there are also certain drawbacks with respect to various other detector types. These include small output signal, variations of operating conditions with ambient conditions such as temperature and radiation damage.

In recent years, the availability of semiconductor detectors has revolutionized the spectrometry of charged particles. As compared with proportional counters, the semiconductor detector has the advantages of better resolution, better stability, essentially windowless operation and the ability to discriminate between particles of different ranges by simply varying the applied voltage. Inasmuch as the semiconductor spectrometers are essentially windowless, they can be used to detect fission products. It might also be mentioned, though, when large surface areas are to be counted for alpha contamination, the proportional counter is the instrument of choice.

As mentioned above, surface barrier detectors are generally the semiconductor detectors used for alpha spectrometry (Kiefer and Maushart).[93] If a surface barrier detector of one cm^2 area is used, a full width at half peak maximum (FWHM) of 17 keV is obtainable when spectrometry is performed in vacuo. Of course air in the detecting system and the use of any casing over the sensitive face of the detector or appreciable thickness of the source reduces energy resolution.

Another technique which can be used for both dosimetric and detection applications is the photographic emulsion. Due to the high specific ionization of the alpha particle, a great number of latent images will be created and in fact essentially every silver halide crystal along the alpha particle path will be affected (Rogers).[99] Therefore, the track of an alpha particle in a nuclear emulsion will be very dense and quite straight apart from the chance of deviation as the end of the alpha particle range is approached, i.e. if it suffers a collision with a heavy

atomic nucleus in the emulsion after it has already been slowed down (elastic scatter). The alpha particle track will also be relatively short; in Ilford G5 emulsion, all alphas of initial energies between 4 and 8 MeV will have ranges between 15 and 40 μm in the emulsion. The delta rays created along the alpha particle track give the track an irregular, fringed appearance when viewed at high magnification. An emulsion of low sensitivity will be sufficient to record the tracks of alpha particles in the presence of a gamma field and mild development will make the alpha particle track visible and discriminate against the much fainter gamma produced tracks. The tracks tend to be quite characteristic and easy to record and count, but the quantitative procedures involved requiring observation through a microscope, although simple and reliable, are tedious to perform. It is also possible to extrapolate the tracks back to their point of origin to accurately determine the source location within a few microns (Barkas).[100]

Certain nuclear emulsions such as Eastman Fine Grain Alpha have an extremely low sensitivity to both visible and ultraviolet light and can be exposed by placing a polished alpha emitting surface in direct contact with the emulsion (Yagoda).[101] The developed image is a measure of the alpha particle activity on the surface and the immediate thin layer above the surface of the alpha emitting solid defined by the range of the alpha particles in the solid. Emulsions have been used to determine the distribution and relative activities of long-lived alpha emitters (Till).[102] Fading in emulsions is not too severe if they are maintained at low temperature and placed in a desicator (Yagoda)[101] but it is difficult to

know quantitatively the amount of fading.

These autoradiographic techniques can be used also to obtain estimates of doses deposited in small volumes of bone. Rowland and Marshall[2] described a technique used to determine doses to bone sections taken from persons exposed to radium by various modes. In this case, three autoradiographs were made to illustrate, in three different fashions, the deposition of radium in bone. The first autoradiograph was made with a sensitive emulsion (Eastman Kodak Autoradiographic No-Screen) which yielded a visual picture of the diffuse distribution of activity. The second autoradiograph recorded the alpha particle tracks utilizing Eastman Kodak NTA, 25 μm emulsion. It was from this second autoradiograph that the actual number of alpha particle tracks produced were counted, to be used in subsequent calculations to obtain activity and then dose rate. The third autoradiograph was obtained by covering the bone section with a thin stripping film emulsion (Eastman Kodak permeable-base stripping film) which was developed and fixed in contact with the bone section. By microscopic examination of this third emulsion in conjunction with the bone section beneath, the locations of the sources of the various alpha particles were determined. From the data obtained by counting the alpha tracks appearing on the second autoradiograph the activity was calculated. This was accomplished by using the alpha particle range in bone which is 6.3 mg/cm^2 for radium alpha particles, the efficiency of creating a track, here one-fourth of the emitted alpha particles within one alpha particle range into the bone section was estimated to produce a track. Also they determined 2.53 alpha particles would be released per disintegration of

a radium nucleus, one from radium, and three immediately from radon daughters and one emitted following the longer lived ^{210}Pb (21 year half-life). Assuming a 40 percent retention factor for radon daughters would yield $1 + 0.4(3 + 0.82) = 2.53$ alpha particles per disintegration after thirty years. The number of radium disintegrations per unit time per unit mass would then be

$$\frac{4 \times \text{no. of tracks}}{A \times R} \times \frac{1}{2.53 \text{ alpha particles per Ra disintegration}} \times \frac{1}{t} \quad (2.1)$$

where

A = exposed area

R = alpha particle range

t = time of exposure

Exposure time is determined by the activity of the sample. The dose rate could then be calculated from the Spiers[103] relation Eqn. (2.2) or a slightly modified form of this equation derived by Kononenko.[104] Spiers' equation for a planar surface of bone containing a uniform concentration of radium has the form

$$\text{Dose rate} = \frac{N\sigma R_T}{2\rho'} \times F \text{ ergs}/\mu m^3/\text{day} \quad (2.2)$$

where

N = the number of alpha particles emitted per cubic micron per day

σ = the average energy loss of the alpha particles in soft tissue (Spiers used 0.21×10^{-6} erg/μm)

R_T = the alpha particle range in soft tissue (Spiers' value, 44 μm)

ρ' = the ratio of alpha particle ranges in soft tissue and in bone (Spiers' value, 1.36; range in bone = 32 μm)

F = a tabulated geometry coefficient, dependent on cavity size.

For a 0.8 μCi terminal burden Rowland and Marshall[2] determined the dose (terminal dose rate x number days carried) was 460 rads for diffuse concentration of radium taken from selected areas of bone; it was found to be relatively constant throughout the bone.

Another method using densitometric techniques to determine the activity that created the various alpha track patterns on autoradiographs has been used to determine dose deposited in a localized section of bone (Twente and Jee).[6] In this study ^{239}Pu was the nuclide of interest. They used a 70 μm opening in the densitometer used for the activity determinations. This figure was decided upon by the following argument. The range of the ^{239}Pu alpha particle in bone is 24.1 μm and in the substance used to embed bone samples, Scotch Cast Resin no. 2, it is 29.5 μm. Then the widest imaginable diameter needed would be for an alpha emitter located at the bone-resin interface corresponding to a diameter of 53.6 μm. It was then decided to use 70 μm as a conservative choice. The densitometer was calibrated using a ^{239}Pu standard and various samples were then analyzed. It was found that the values obtained for activity by this technique were about 76 percent of the values obtained for the same samples radiochemically. The average dose rate distributed throughout a volume having radius equal to one alpha particle range was calculated by the following equation:

$$\text{average dose rate} = \frac{Q'E}{2R\rho} \qquad (2.3)$$

where

Q' = the disintegration rate per unit area of the source

E = the energy of the emitted alpha particle

R = alpha particle range in the medium considered

ρ = the density of this medium.

For a dog injected with about 30 μCi ^{239}Pu citrate and sacrificed thirty days later, the dose rate to bone tissue at time of death (average) determined by the above equation for the endosteal bone surface was found to be 41 rads/day. It can be inferred from these two range equations that the dose rate is not very dependent on range since in one case range is in the numerator and in the other it is in the denominator.

There is another method which can be used to determine the local dose once the fluence of alpha particle tracks has been determined by scanning of the autoradiograph through a microscope (James and Kember).[7] The eyepiece of the microscope is equipped with an array of 5 μm diameter circles with a straight line placed in front of the first row of circles which is set on the bone surface when measurements are being recorded, see Figure 8. The circles are placed at distances of 5, 12.5 and 20 microns removed from the bone surface. The technique involves first counting the number of tracks within the various circles and then converting to particle fluence (number of particles crossing unit area perpendicular to the directions of the incident particles). Approximation of a spherical volume is obtained by using a cylinder of similar height

and diameter where the thickness of the film, 3 μm, is the height of the cylinder and the 5 μm circle is the diameter.

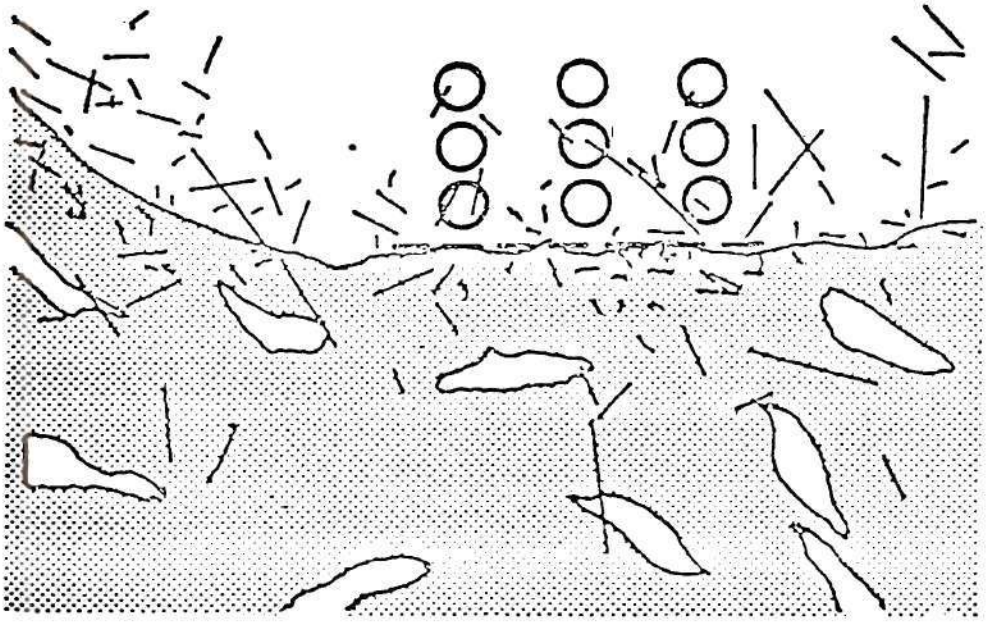

Figure 8. Diagram Showing the Positions of the Array of Circles Marked on the Microscope Eyepiece and Projected onto the Section under Examination (The line is shown placed over the bone surface and the 5 μm diameter circles are at 5, 12.5 and 20 μm distance removed from the bone surface.)

These two quantities, average cross-sectional area of the cylinder and number of tracks within the various cylinders, yield fluence. Once fluence is found, dose is given by $D = \phi \times LET/\rho$, where ϕ is fluence, LET is linear energy transfer and ρ is density. Problems encountered from this method include the error introduced by reading the fluence from an altitude 1.5 μm from the bone surface rather than on the bone surface, differing absorptions in the emulsion and tissue (differing ranges) and LET variations which tend to give different values for the microdose for different loca-

tions of the circles. They used this technique to determine the incidence of one-hit events to cell nuclei, i.e. the number of cell nuclei receiving one alpha particle hit as opposed to none or two or more. They found the number of cells receiving two or more hits increased as time progressed after ^{239}Pu deposition.

Another method, used by the Utah group, involves the technique of NIAR which stands for Neutron Induced Autoradiography (Stover),[13,105] (Kimmel et al.),[106] (Smith et al.)[5] and (Wronski et al.).[4] First 300 μm thick bone sections were cut from a bone sample and sandwiched between two foils of Lexan polycarbonate. This assembly was then irradiated in a thermal neutron column to a fluence of approximately $10^{16} n/cm^2$. Next the foils were counted on a microscope stage at a power of 100X to determine the lineal track density, F tracks/cm. This value could then be converted into activity, or concentration, $\nu (pCi\ ^{239}Pu/cm^2)$ by the equation (Smith et al.),[5] (Wronski et al.)[4]:

$$\nu = \frac{2c}{\sigma \emptyset R \eta} F \qquad (2.4)$$

where

σ = thermal neutron fission cross section for ^{239}Pu, 742b

$\emptyset$ = thermal neutron fluence

R = fission fragment range, 18 μm

η = fission fragment detection efficiency, empirically determined, 0.488

c = a units conversion factor

The concentration would then be converted to dose in rads by one of the

previous formulations. Problems were encountered in this conversion due to the assumptions required, i.e. planar source of alphas and use of the peak energy of the alpha particle which does not allow alpha particles to originate below the bone surface.

Sometimes it is desirable to determine the whole body burden of a nuclide such as ^{239}Pu, especially during the course of animal studies. A procedure has been used by Bair[37] which utilizes four arrays of NaI(Tl) crystals, thirteen crystals to an array (fifty-two total), connected in parallel to detect the L X-rays from ^{235}U (after the alpha decay of ^{239}Pu) and 60 keV γ-rays from ^{241}Am (after the beta minus decay of ^{241}Pu) being emitted from dogs after inhalation experiments involving various forms of ^{239}Pu. About four percent of the ^{239}Pu disintegrations result in X-rays from ^{235}U which occur in three energy groups, 13.6, 17.0 and 20.2 keV. If the beta emitter impurity ^{241}Pu is present, then in about 35.9 percent of its disintegrations a 60 keV γ-ray is emitted from the daughter ^{241}Am nuclide. But the ^{241}Am (halflife = 458. yr) builds up slowly from the ^{241}Pu (halflife = 13.2 yr). In fact ten years after the deposition of 1.0 μCi pure ^{241}Pu only 0.012 μCi ^{241}Am have formed. There are also other low energy radiations present but of only minor significance, these include 100 keV gammas from ^{241}Am (0.04 percent) and 52 keV gammas from ^{239}Pu (0.02 percent). These gammas occur in such a low yield, they would not be expected to give meaningful counts using the levels of ^{241}Am encountered. The 60 keV γ-ray would be ideal to use unless the samples is so highly purified ^{239}Pu that the ^{241}Pu activity is so weak as to become lost in the detector noise. To use this method of <u>in vivo</u> whole

body counting several factors need to be considered. The irradiation history and knowledge of the use of chemical processing of the plutonium prior to release are important because if significant amounts of ^{241}Pu are present, the X-ray activity will actually increase with time due to the buildup of ^{241}Am (the half-life of ^{241}Pu is 13 yr whereas the half-life of ^{239}Pu is 24,390 yr). In addition, the apparent activity will be a function of time even for a constant body burden due to the different attenuations possessed by the various tissues, the HVL at 17 keV for bone is 0.03 cm whereas for lung it is 1.3 cm, and translocation. Another problem is encountered due to the different metabolic pathways followed by americium and plutonium. The differences are slight in the two pathways but do become noticeable when plutonium is administered in the form of the nitrate. Since americium tends to concentrate to a lesser degree at the endosteal surfaces than plutonium (about half as much), a shift of radioactive material from the endosteal to the periosteal surfaces and Haversian canals would result (americium is also a surface seeker). At a window setting of 13.6-25.6 keV, which includes the 17 keV X-ray, Dr. Bair found for the plutonium he was using a detection limit of 8 nCi, and a limit of 7 nCi for a window setting of 13.6-66.3 keV, which includes the 60 keV γ-ray.

When a bone sample is being examined after sacrifice of the experimental animal or after the bone sample has been removed during surgery, it is desirable to determine the alpha activity contained within this sample. If uniform distribution of the alpha activity is assumed, the dose to this bone sample could be calculated, but no information as to

the spatial distribution of this deposited dose could be elicited using this method. This task can be accomplished easily by the method outlined by McDowell and Weiss.[107] Here the bone sample whose deposited activity is to be determined is dissolved and then placed in a liquid scintillator material and counted using a beta sensitive liquid scintillation counter. To prepare the sample, the bone is placed in solution with concentrated nitric acid and some small quantities of 30 percent hydrogen peroxide. This solution is heated over a gentle heat, to prevent bumping, until a clear solution is obtained. If an aqueous-phase-accepting scintillator, such as dioxane, is used, about one ml of this highly salted aqueous phase solution (just prepared from the nitric dissolution process) can be added directly to the scintillator. This method seems to work best at high activity levels, about 200 counts per minute or more and when the contribution to the background from other beta or gamma emitters in the sample is sufficiently low. Again due to the nature of the sample preparation, no information is obtained concerning the spatial distribution of the dose received by the various parts of the bone.

There has been much effort placed on theoretical calculations of dose to a small volume since many of the experimental techniques employ emulsions to display the alpha-produced tracks. Then by some method, e.g. visual counting, densitometric or the volume counting technique one finds the activity present and converts it to dose using one of these derived equations (Spiers),[82,103] (Kononenko) [104] and (Charlton and Cormack).[108] The equations of Spiers, eqn. 2.2, and Kononenko were mentioned earlier. In some of the first calculations, the dose near a planar interface between bone and soft tissue was determined on the

basis of simplifying assumptions regarding alpha particle ranges (Spiers).[82,103] This method has also been applied to the mean dose in cylinders and the dose at any point in a spherical cavity irradiated by alpha particles arising in the surrounding medium.

Numerical integrations have also been made to derive the dose near a planar interface and within cylindrical cavities both for external irradiation by x-rays and internal irradiation by alpha particles (Charlton and Cormack).[108] In each case, allowance was made for variation of energy deposition along the track of the ionizing particle on the basis of the range-energy relationship:

$$R = AE^m \qquad (2.5)$$

where

R = the range of an alpha particle

E = alpha particle energy

A = an empirical constant

m = 1.75 for secondary electrons released by photons of less than 200 keV and m = 1.5 for alphas

This equation is valid for initial alpha particle energies from 1 to 10 MeV.

Thorne[109,110] has performed Monte Carlo type computer calculations using modified forms of the Bragg equation similar to Harley and Pasternak[111] to calculate the endosteal and bone marrow dose rates for various activities of ^{239}Pu and ^{226}Ra. He assumed the endosteal surface was a

planar source over the range of the alpha particle. Thorne's calculations indicated ^{239}Pu was unlikely to be more than fifteen times as toxic as ^{226}Ra. This result is interesting since we employ a factor of only 5 in our dose-equivalent calculations for ^{239}Pu.

In summary, we have examined six ways to experimentally determine dose deposited in man resulting from the internal deposition of an alpha emitting nuclide such as ^{239}Pu. One involved using a whole body scintillation counter to look at the X-rays emitted from ^{235}U and γ-rays from ^{241}Am to determine an estimate of the body burden of the nuclide, e.g. ^{239}Pu. From the activity and literature knowledge concerning the distribution of the nuclide in the body, an estimate of the dose can be obtained. A second method involved the liquid scintillation counting of a dissolved bone sample containing the ^{239}Pu. From the mass of the sample counted and the activity determined to be in that sample, concentration, e.g. $\mu Ci/g$ could be determined. Next, many other samples could be counted and the concentration of the nuclide determined for each. Then with these various concentrations in $\mu Ci/g$ the following procedures would be used to calculate dose to the skeleton. Dose received by each bone could be calculated in the usual manner from concentration in for the bone in question. Then all the doses could be summed to give total dose received by the skeleton. If there were not enough samples taken to use this procedure, an average value could be calculated from the available concentrations and an average dose calculated from this quantity or the high and low values could be used to bracket the dose received by the skeleton. None of these methods yield any information

concerning the areas receiving this deposited dose because all of these techniques require that the nuclide be homogeneously distributed throughout the bone. This is not a good assumption for certain bone seeking nuclides, especially ^{239}Pu. Some degree of spatial resolution can be obtained however with the four other methods discussed. All the autoradiographic procedures employed found the activity in small volumes along the exposed bone surface and then used one of the theoretically derived relations to convert activity to local dose. Several shortcomings can be noted in this general procedure. These techniques determine dose only indirectly via some sort of calculation; in reality activity, not dose, is the experimentally determined quantity. The conversion to dose in tissue is not as clear as would first be guessed because the emulsions used are subject to inherent problems such as fading and the NIAR technique is observing fission fragments, not alpha particles which irradiate tissue in vivo. Therefore a need still exists for a dosimeter to determine more accurately the average localized dose to the endosteal surface of bone in fulfilling the requests of ICRP concerning bone seeking radionuclides. Better techniques of bone dosimetry have been requested by many different sectors (Mole),[112] (Jee et al.),[3] (Natural Science Group),[113] (Stover),[105] (Stover et al.),[13] (ICRP),[114] (Cross).[115] If such a dosimeter existed and a procedure could be found to apply it to local dose measurements on critical osseous tissues, significant knowledge could be obtained concerning the actual doses received to these critical tissues from deposition in vivo of such nuclides as ^{239}Pu. We believe we now have this dosimeter and have the procedure to provide the requested information.

CHAPTER III

PLUTONIUM IN VIVO

3.1 ^{239}Pu Characteristics and Special Problems Incurred Upon Uptake

There is probably no single element in the periodic table with a comparable saga of discovery, development, manufacture and use covering a span of only one generation (Stannard).[116] Uranium and its isotopes along with its daughter products such as radium and radon have been on the scene for decades. Uranium was known in nature and used in industry long before its possession of radioactivity was known or became of interest and importance. Plutonium, on the other hand, did not exist on earth in measurable quantities, due to its short half-life relative to the age of the earth until Seaborg and his colleagues[117] isolated a tracer quantity of element ^{238}94 on the night of February 23, 1941, and 0.5 microgram of ^{239}94 on March 28 of the same year. (The name "plutonium" was not assigned until the following year.) The ability of this element to undergo thermal neutron fission was found essentially simultaneously with its discovery and thus began the tremendous effort to produce it in quantity for military purposes. The details of the remainder of this chronology are familiar so nothing further need be added except to point out that kilogram quantities were available by the summer of 1946 and now thousands of kilograms are available and being produced in our nuclear

reactors. To insure maximum safety for the general public it behooves those associated with the nuclear industry to know as precisely as possible the conceivable pathways and points of deposition in the human body. It would also be desirable to know the biological effects produced by this deposited plutonium. These considerations imply the necessity of obtaining accurate dosimetry of plutonium in osseous tissue since, as was shown in the previous chapter, it is a bone-seeker. Even if the widespread use of plutonium envisioned by the LMFBR program is never realized the need to have this information on plutonium still exists, since many radiation workers handle plutonium routinely in connection with the weapons program and continuous exposure to the general public is occurring due to atmospheric weapons tests. The amount of ^{239}Pu estimated to have been released to the atmoshpere from weapons tests is about 300 kCi, distributed globally, mainly by tests in the megaton range that injected debris into the stratosphere (Eisenbud).[118] Plutonium tends to be tightly bound to soil and is present in biota only in minute amounts. The estimated soil and air contaminations resulting from this source was 1.4 mCi/km^2 and 0.15×10^{-3} pCi/m^3, respectively (Eisenbud).[118] Due to the small fraction of ^{239}Pu in the usual chemical form that is absorbed from the GI tract to the blood (covered below) the inhalation of the small amount of ^{239}Pu in the air ordinarily causes the greatest absorbed dose following human intake. The absorbed dose expected to be incurred by the average person in fifty years due to the inhalation of the ^{239}Pu environmental contamination is 4.5 mrem to the whole lung and 1000 mrem to the pulmonary lymph nodes (Eisenbud).[118] The dose received from ^{238}Pu inha-

lation is less than 10 percent of these values, even after 17 kCi of ^{238}Pu was released by an aborted space vehicle in 1964. All plutonium nuclides are chemically toxic since the chemistry of nuclides occurs at the atomic level. The radioactive toxicity of alpha emitters depends on specific activity, alpha energy and location of the alpha emitter with respect to critical tissues. The specific activity of ^{239}Pu is less than some alpha emitting nuclides such as ^{241}Am and would lead one to believe the toxicity is also less. This may not be true, however, since ^{241}Am does not tend to concentrate on the critical endosteal tissues as dramatically as ^{239}Pu (Jee).[11] The effects of alpha emitters internally deposited also depend on critical organ and half life. All of these factors taken together yield the clinical end result of the deposition of any given alpha emitter deposited in vivo. The difference between the distribution of ^{239}Pu in osseous tissue and most other bone seekers could override specific activity considerations in determining clinical effects.

Plutonium-239 is the isotope of plutonium existing in the greatest quantity on a gram basis in a ^{235}U-^{238}U nuclear reactor. The production of ^{239}Pu is initiated by the capture of a neutron by ^{238}U which then decays to ^{239}Pu by way of two beta-minus decays. The decay scheme can be written as

$$^{238}_{92}U \xrightarrow[(n,\gamma)]{} {}^{239}_{92}U \xrightarrow[(23.5m)]{\beta^-} {}^{239}_{93}Np \xrightarrow[(2.35d)]{\beta^-} {}^{239}_{94}Pu \xrightarrow[(24,400y)]{\alpha} {}^{235}_{92}U$$

At this time bone is still considered to be the critical organ for ^{239}Pu (ICRP)[120] but there is some feeling that the critical organ may be lung when the inhalation mode of administration is considered (Bair)[36,37]

and for low level, chronic exposure to ^{239}Pu, soluble form, the liver may be the critical organ (Durbin).[20] The dynamic distribution proceeds in the following manner (Durbin).[20,21] Plutonium will be cleared from the soft tissues other than liver and redistributed to the bone and liver. Plutonium deposited in the skeleton is slowly removed a portion of which is redeposited in the skeleton and most of the rest deposited in liver with a small amount excreted. Plutonium deposited in the liver is changed from a soluble form in hepatic cells to insoluble hemosiderin deposits and sequestered in reticuloendothelial cells. Therefore loss from the liver could be occurring at least as slowly as loss from the bone where in past ICRP calculations a biological half life of 200 years has been assumed.

Monomeric plutonium solutions such as citrate deposit primarily in the bone (Stover and Jee)[12] and polymeric plutonium deposits primarily in the liver and bone marrow (Lindenbaum et al.),[121] (Rosenthal et al.),[122] (Markley et al.).[123]

The retention of plutonium in the body has been examined in different animals including man. A review of Langham's original human data is given by Durbin.[20,21] Beagle dog retention data have been studied by Stover[105] and Stover et al.[13]

The distribution of plutonium varies among the different bones in animals as well as within a particular bone. A whole lumbar vertebrae initially takes up about five times as much ^{239}Pu as a whole ulna (Kimmel et al.).[106] The initial surface concentration of the lumbar vertebral body in the beagle indicated a large variation with regard to surface

concentration. Ninety percent of the endosteal-trabecular surface showed a concentration sixty times that found on the remaining ten percent of this bone surface. This is quite different from the distribution found in the ulna. Here seventy percent of the trabecular-endosteal-periosteal surface was found to have a concentration twenty times that found on the remaining surface composed of the Haversian canal system (Kimmel et al.).[106] Additionally, it was possible to relate incidence of osteosarcoma to some of the same factors as in the other studies described below. Only two percent of the observed osteosarcomas originated in the ulna which has (1) low initial ^{239}Pu uptake; (2) a moderate amount of trabecular surface relative to the other bone surfaces, 50 percent; (3) no loss of ^{239}Pu from the whole bone and (4) a slow loss of ^{239}Pu from trabecular surfaces due to processes such as turnover. On the other hand, sixteen percent of the observed osteosarcomas originated in the lumbar vertebral body. The characteristics of this bone possibly yielding the observed clinical result were (1) high initial uptake of ^{239}Pu; (2) large amount of trabecular surface relative to other bone surfaces, 90 percent; (3) rapid loss of ^{239}Pu from the whole bone and (4) a very rapid loss of ^{239}Pu from trabecular surfaces by such processes as turnover (Kimmel et al.).[106] The results presented are in agreement with the Spiers[85] and Wronski et al.[4] studies but do not consider the portions of bone individually, i.e. proximal, distal and mid, as did Spiers[85] and Wronski et al.[4] This, of course, does not lessen the importance of the Kimmel et al.[106] work; it just indicates a different level of approach. Now we will examine the Spiers[85] and Wronski et al.[4] studies mentioned above.

Spiers[85] has tried to correlate occurrence of osteosarcoma with the various surface areas of bone surfaces. Spiers[85] measured human long bone surface areas and examined which portion of the long bones seems to be most susceptible to osteosarcoma production. He found excellent agreement between the magnitude of the trabecular surface area and number of human radium induced bone tumors. He found quite poor agreement between the cortical surface area and bone tumor induction. He was then able to show which portions of the long bones (proximal, distal or mid) were most susceptible quantitatively. For example, the proximal tibia with a trabecular surface area of 0.342 m^2 was the site of four tumors; the distal tibia, surface area 0.126 m^2, was the site of two tumors and the mid tibia, surface area 0.036 m^2, was the site of one tumor. The cortical surface areas for this bone were 0.151 m^2, 0.097 m^2 and 0.116 m^2, respectively. We can see the agreement found with the trabecular surface areas here (Spiers).[85] Similar results were obtained with the other five long bones, namely, the ulna, radius, humerus, fibula and the femur.

The data of Spiers[85] above were in agreement with the most recent findings at the University of Utah (Wronski et al.).[4] Wronski et al.[4] noted the bones and location on these bones where all the observed osteosarcomas have been observed in the Utah dogs to date. The order of highest to lowest incidence of osteosarcoma as a function of position on the bones for the Utah dogs agreed with the human data in Spiers.[85] Wronski et al.[4] used a somewhat different approach to explain this sequence. They examined bone turnover rate and concentration of ^{239}Pu on the bone surface. Bone turnover rate was determined by labeling the bone surfaces

with tetracycline in a 7-5-7-5 regime. Here the attraction of tetracycline to surfaces involved with active turnover is used. The treatment plan was seven days of tetracycline injections, five days rest, seven days tetracycline injections, five days rest, then sacrifice, called the 7-5-7-5 regime. Two labels meant active turnover throughout the treatment time in these beagle dogs and one label indicated turnover was only proceeding in one portion of the regime. No label, of course, indicated lack of turnover during this time span. Beagle dogs used in this study were young adults injected with ~ 0.016 μCi/kg of ^{239}Pu(IV) in the citrate form, then serially sacrificed. Twenty-four days prior to sacrifice, tetracycline injections were initiated. Areas of tetracycline uptake glowed under ultraviolet light, expediting counting of these areas. They found both bone turnover rate and plutonium concentration were dramatically higher in the portions of bone where the greatest number of osteosarcomas have been observed. This study is still in progress as this manuscript is being written, but the results thus far are conclusive enough to be included in their present form in the discussion here. One point to be considered is time of irradiation of these endosteal tissues versus total dose to the endosteal tissues. Although the concentration of plutonium on the endosteal surfaces was higher at the time of sacrifice of the animals (7-56 days post injection thus far) for the areas of highest incidence of osteosarcoma, this concentration could actually drop below the level realized in portions of bone of lowest incidence of osteosarcome due to the vast differences in bone turnover rate between the two. Therefore one could imagine the total dose, t = 0 to infinity, could be greater

for the bone with longest turnover rate. Since highest osteosarcoma incidence occurs in bones with the shortest turnover rate, where the dose could drop below those bones with longest turnover rate, it is conceivable there is a critical time span, immediately after injection (or exposure in an industrial accident involving humans) when the dose deposited is much more effective with respect to tumor induction. Another explanation is that any malignant change would be manifested more rapidly in an area of high mitotic activity such as is the case in the lumbar vertebrae, pelvis and proximal humerus trabecular surfaces than in the distal humerus and proximal ulna trabecular surfaces, areas of depressed mitotic activity.

Regarding the production of the osteosarcoma, the endosteal surface of bone has been shown to be the most likely location of the induction of this tumor (ICRP),[81] (Spiers).[85] Mole[112] has proposed the interesting hypothesis that the endosteum, considered as a whole organ, has the same sensitivity to the induction of bone tumors in every species. This can be interpreted two ways (Mole).[112] Either every species has the same number of cells at risk, regardless of the size of the skeleton, or the cells at risk in the larger animals are somehow less sensitive to turnover induction than the cells of smaller animals. This latter interpretation could be indicative of some means of suppressing neoplasia in the larger animals. The data supporting this view best are the simple relations obtained in the dose-response relationship of beta particles in bone. In the dog and mouse the probability of tumor induction per day followed the simple relations, a constant multiplied by the square of the number of beta particles released during the tumor induction time (time from injec-

tion of beta emitter to death less the time from tumor appearance to death). The constant was remarkably similar in these two dissimilar species, for dog, 0.9×10^{-31} day^{-1} and for mouse, $2\text{-}3 \times 10^{-31}$ day^{-1}. The square of the dose is suggestive of the two-hit mechanism of chromosome damage by beta particles. For high LET radiation, like alpha particles, Mole[112] believed a one-hit mechanism more applicable but could not find a relation for alpha particles as seemed to be possible for beta particles.

When considering plutonium deposition in bone, one quickly finds there is quite an array of parameters determining the degree and rate with which ^{239}Pu reaches the bone. These are the species of animal (Vaughan et al.),[1] age of animal (Vaughan et al.),[1] (Jee),[11] (Durbin),[18] mode of entry (Thompson),[41] (Bair),[37] (Jee),[11] (Vaughan et al.),[1] chemical form (Bair),[36,37] (Durbin),[18,20] (Vaughan et al.),[1] chemical state (Durbin),[19] (Scott et al.),[24] particle size (if insoluble) (Bair),[36,37] (Thompson)[41] and the physiological state of the animal (Durbin).[18,20,21] There has also been discussion on the use of therapy to remove plutonium (Lafuma),[26,27,29] (Markley et al.).[123]

Translocation describes the movement of ^{239}Pu from one location in vivo, possibly the point of deposition, to another location. Of primary interest here is the translocation to bone but it could be mentioned that translocation to other parts of the body is also important (Durbin).[20] For a wide range of animals with ^{239}Pu administered in soluble form (either nitrate or citrate) the following modes of administration proved to provide translocation to the bone, ranked from the greatest

degree of translocation to the least (Jee)[11]: intravenous ≅ intraperitoneal injection > subcutaneous injection > intramuscular injection > intratracheal implantation > inhalation > oral administration > direct application upon unbroken skin. Although many of these routes of entry are very inefficient in delivering plutonium to the skeleton, osteosarcoma has been induced by all the various modes, with the exception of the direct application of the plutonium to unbroken skin.

In order for the ^{239}Pu to be deposited in the skeleton, it must first reach the blood to be transported to the skeleton (Durbin),[18,19,22] (Stover and Jee),[12] (Vaughan et al.),[1] (Taylor).[48] The question then arises as to the form and chemical state in which plutonium exists as it travels in the blood. It appears the chemical state of ^{239}Pu is the same in vivo regardless of the chemical state of the administered soluble plutonium (Scott et al.).[24] This state is the +4 oxidation state (Taylor).[48]

The studies of Arnold and Jee[17] indicate that plutonium tends to be adsorbed on mineralized oseous surfaces. Additionally, they believe the plutonium exists as a colloid which diffuses into the bone, adhering to the first mineralized surface encountered by the process of colloidal adsorption.

Once the plutonium has been deposited on the bone surfaces after injection, bone apposition can occur burying the old, labeled bone with new bone. This new bone appears on autoradiographs as a region of diffuse labeling next to the intensely labeled original bone surface. The concentration of plutonium in the new bone, formed after injection, is dependent upon (1) the level of plutonium in the extracellular fluid, which depends

on time after administration, (2) the chemical affinity of the particular surface for plutonium and (3) the rate of apposition of new bone at osseous surfaces (Arnold and Jee).[17]

In a previous section we mentioned the unusual role of the osteoclasts in plutonium metabolism. Osteoclasts tend to concentrate plutonium as they perform the function of bone resorption. Upon engulfing the freed bone fragments from a resorbing bone surface, the osteoclast dissolves and excretes or metabolizes the bone fragment. However, the plutonium particles cannot be reduced by the mechanisms available to the cell. Therefore the plutonium not only remains as a colloid but grows in size and accumulates, within the cell. The concentration within an osteoclast can be much greater than the concentration of plutonium on the bone surface because plutonium from a reasonably large surface area can be contained in one osteoclast (Arnold and Jee).[17] As time progresses, osteoclasts continually concentrate plutonium which is later transferred to macrophages. Reviewing, once the plutonium has been deposited on the bone surface (it does not tend to diffuse into old bone), it either (1) stays, (2) is removed by osteoclastic resorption, or it is (3) buried by apposition of new bone (indicated by diffuse labeling) (Arnold and Jee),[17] (Jee),[11] (Jee et al.).[3]

Further studies showed ^{239}Pu seemed to be tracing the metabolic pathway followed by iron in the body (Durbin),[22] (Vaughan et al.),[1] (Stover et al.).[124] Since iron is moved throughout the body by the iron-transport protein transferrin, than ^{239}Pu may also be moved by the same mechanism. Three factors that need to be explained in any reasonable

explanation of plutonium distribution in bone are: (1) the long-term low level of free ^{239}Pu in the blood, (2) the deposition of ^{239}Pu on bone surfaces and (3) the initial, early presence of ^{239}Pu single alpha tracks in the marrow that gradually disappear. The transferrin bound plutonium theory accomplishes this in the following manner (Durbin et al.).[22] If ^{239}Pu is administered in a form that can interact readily with plasma proteins, it becomes bound in a manner such that the Pu-TF (TF = transferrin) and Fe-TF bonds are isostructural but the Pu-TF bond is slightly less stable than the Fe-TF bond. It is known that the iron is released in the marrow where it is used in the synthesis of hemoglobin. The release occurs on the surface, or very near the surface of reticulocytes located in red marrow. Thus the marrow possesses a ready made mechanism to release the ^{239}Pu from transferrin. Instead of being transferred to the interior of the reticulocyte, ^{239}Pu follows one of three fates. First, it could be re-bound to transferrin, second, it could diffuse to the nearest bone surface and be bound there, or third, it could be released to the blood and circulate as free plutonium. Thus, this mechanism delineated by Durbin et al.[22] also seems to account for the established facts.

The degree of translocation to bone would then hinge on the ability of the chemical form to interact with the transferrin molecule. The data seem to support this hypothesis (Durbin),[18] (Vaughan et al.),[1] see Table 2 (Durbin).[18] The values in each row of the table do not add up to 100 percent because some of the plutonium was retained in other soft tissues.

Table 2. Distribution of Plutonium in Rats 4-8 Days after Intravenous Injection of Either Soluble Pu Complexes, Hydrolyzable Pu Salts or Prepared Pu Colloids (Durbin)[18]

Pu Preparation	Pu Content (% Injected Dose)			Excreta
	Liver	Spleen	Skeleton	
Soluble Complexes				
^{238}Pu(VI) citrate, 3%[1]	9	0.6	55	27
^{239}Pu(VI) citrate	9	0.5	56	14
^{239}Pu(IV) citrate, 3%[1]	10	0.7	57	12
Hydrolyzable Salt				
^{239}Pu(III) chloride	23	0.7	45	18
^{239}Pu(VI) nitrate	28	0.4	44	8
^{239}Pu(IV) nitrate	40	1.2	29	16
^{239}Pu(III) chloride	40	0.7	36	12
^{239}Pu(IV) nitrate	64	0.8	13	13
Prepared Colloid				
^{239}Pu(IV) citrate, 0.1%, pH 5	78	1.7	13	3
^{239}Pu(IV) carbonate, pH 8	83	---	8	7

[1] Percent by weight of citrate.

Those compounds existing in a complexed form can interact easily with the protein since complexing shields the plutonium ion from hydrolysis. A free plutonium ion generated from a salt, any of the (III), (IV) or (VI) forms, will undergo hydrolysis leading to polymers, e.g. $[Pu(OH)_2^{++}]_n$ (Taylor).[48] The degree of hydrolysis depends on such factors as pH, concentration of plutonium, temperature and the presence of other ions (Taylor).[48] Therefore, salts would be expected to demonstrate a somewhat erratic behavior *in vivo* depending upon the degree of polymerization existing in the injected solution. This is in agreement with the present experimental data. The higher the polymerization, or the presence of colloidal particles, the more effective the filtering action of the liver (Durbin).[18] The chemical state also can cause variations in the degree of translocation from the point of entry to the blood, and consequently, to the skeleton (Thompson),[41] (Durbin).[19] This effect would only be manifested when the route of entry was one other than injection, e.g. by inhalation or a puncture wound. It was shown that the smaller ion diameter, i.e. the greater the positive charge, the larger the percentage of the injected dose that will be deposited in bone and the smaller the percentage deposited in liver (Durbin).[19] The increase in solubility and decrease in basicity resulting from decreasing atomic size was suggested to be causing this effect.

The route of entry is significant not only in determining the degree of plutonium uptake but also it is a controlling factor in the initial di-distribution of the plutonium (Thompson).[41] Factors such as age, presence of acidity, presence of Pu(VI) and presence of complexing agents (citrate)

can greatly alter the pattern. For example, in rats administered plutonium in a soluble form by ingestion, the fraction absorbed from the GI tract to the blood is about 3×10^{-5}. By adding Pu(VI) and high acidity, pH 1, this factor can be increased by a factor of about 630 to 0.019 (Thompson).[41] Also, other effects can cause variation in the fraction absorbed from the GI tract to the blood, f_w. If some damage has been inflicted upon the GI tract such that abrasions exist in the walls of gut, the f_w value tends to increase.

With respect to age differences, the initial distribution of ^{239}Pu from liver to bone is more marked in juvenile animals than in the adult (Vaughan et al.),[1] (Jee).[11] For example, if sheep are injected with ^{239}Pu(IV) citrate intravenously, at age 23 days (lamb) 62.2 percent of the injected dose is retained in the skeleton but only 8.6 percent is found in the liver. But if injection occurs at age 180 days (sheep) 36.0 percent of the injected dose is found in the skeleton and 12.6 percent in the liver, a less drastic distribution between bone and liver (Vaughan et al.).[1] This means for one given dose, the juvenile will possibly receive a greater absorbed dose (rads) to the skeleton than will the adult. Sometimes differences in distribution can be great for one mode of entry even within a particular species (Norwood and Newton).[164]

When considering the inhalation method of exposure, which is so important in the industrial accidental exposure analysis, the number of variables involved makes the determination of translocation and long-term distributions quite difficult. Not only are the chemical form, particle size and shape important here, but in the case of the oxide even the method of particle preparation was shown to be a factor (Bair).[36] Experiments

with beagle dogs using the inhalation mode of entry (Bair et al.),[35] (Bair),[36,37] (Thompson et al.)[38] have shown that a small particle size for the oxide favors translocation to other tissues. The first experiment of the group just mentioned (Bair et al.)[35] used $^{239}PuO_2$ aerosols ranging in size from 0.2 to 7.6 microns mass median diameter (MMD) administered by a single exposure to their dogs. The particles with a MMD of 5-7 microns yielded a greater lower lung deposition than the particles with a MMD of 0.2-2 microns because the latter had a greater tendency to be exhaled. The larger particles tended to be deposited in portions of the respiratory tract where clearance processes were not very effective. The greater deposition observed with the larger particles and greater translocation noted with the smaller particles caused the larger particles to have a longer retention in the lung and therefore become the more hazardous of the two. Bair et al.[35] attributed the greater translocation of the smaller particles to two factors, the increase in the surface to volume ratio as particle size decreases resulting in greater solubility of the smaller particles and the probability that very small particles can be translocated, in tact, in vivo by phagocytosis. The importance of the chemical form in determining the magnitude of translocation and final distribution for the inhalation route of entry has been recognized (Vaughan et al.),[1] (Bair),[36,37] (Thompson et al.),[38] (Thompson).[41] Bair[36,37] has examined the relative results obtained for several different compounds administered to dogs by the inhalation mode of administration. He used $^{239}Pu(NO_4)_4$, $^{239}PuF_4$ and four oxides of the formula $^{239}PuO_2$. The oxides differed by the method each was synthesized. The two methods used to

make these oxides were calcining of the oxalate and oxidation of the delta phase form of the metal. The first method was performed at two temperatures, 1000°C and 350°C and yielded particles of 0.5 micron CMD (2.8 microns MMD) and 0.45 micron CMD (2.8 microns MMD), respectively. The second method was carried out at 450°C and 123°C and yielded particles of 0.50 micron CMD (4.8 microns MMD) and 0.46 micron (1.3 microns MMD), respectively. The nitrate particles were 0.12 micron CMD and the fluoride particles were 0.2 micron CMD. The results for the nitrate at one month were as follows: the lung contained 60-70 percent of the injected dose, bone 20 percent and liver 12 percent and from 75-119 days, the lung contained 30-40 percent, 20-50 percent in the skeleton and 5-10 percent in the liver. Whole body retention had a half-life of 400-1000 days and lung retention was 100-200 days. The fluoride yielded somewhat different results as would be expected. Here 70-80 percent remained in the lung at three months, 20 percent went out in the feces, 2-9 percent in the urine and less than 2 percent in other tissues with the skeleton retaining more than the liver. Whole body retention proceeded with a half-life between 127 and 405 days and lung retention with a half-life of 78-266 days. The oxides all maintained a whole body retention between 1000-3400 days except for the 350°C calcined oxalate particles which had a whole body retention between 300-400 days. All the oxides yielded lung deposit of 90+ percent except the 350°C calcined oxalate particles where the lung deposit was 80-87 percent of the inhaled plutonium. Translocation was greatest for the 350°C calcined oxalate particles and least for the 1000°C calcined oxalate. The long-term retention of the

oxide was clearly demonstrated here as a gradual accumulation in the tracheal-bronchial lymph nodes. The toxicity of the 350°C calcined oxalate particles seemed less than the toxicity of the other oxides due to the higher translocation and excretion rates.

To illustrate the species differences in the distribution of ^{239}Pu in vivo let us examine the distribution occurring in several animals and man, see Table 3 (Vaughan et al.),[1] (Durbin).[21] The dog and mouse data compare quite well but the man data show a more even distribution between the liver and skeleton. For 5-15 months in man, the situation had not changed drastically. Here 47.5 percent remained in bone and the liver concentration had increased slightly to 31.2 percent. (The increase in the liver concentration was offset by a decrease in the soft tissue concentration (Durbin).[21])

Now a more complete picture of the problems associated with the internal deposition can be appreciated. The number of variables is large and each combination can result in a different probability of translocation and distribution within the body. Translocation occurs at a different rate in different animals. But even for the same animal at the same age and general state of health, translocation occurs at a different rate for different chemical compounds of ^{239}Pu, different chemical states of ^{239}Pu and different routes of admission as well as varying tissue distributions once initial deposition has been completed. Polymeric plutonium favors liver deposition whereas monomeric plutonium (transferrin bound) favors skeletal deposition. Injection favors a liver-bone deposition whereas inhalation of ^{239}Pu preferentially deposits mainly in the lung.

Table 3. A Comparison of the Species Variation Seen in ^{239}Pu Distribution When Administered Intravenously in Citrate Form

Animal	Chemical Form of ^{239}Ou	Time After Injection	% of Injected Dose	
			Bone	Liver
Rat	Pu(IV) Citrate	8 days	50	10
Mouse	Pu(IV) Citrate	5 days	65	22
Dog	Pu(IV) Citrate	29 days	62	22
Man	Pu(IV) Citrate (3 cases)	4-6 days	53	27
	Pu(IV) Nitrate (1 case)	4 days	43	--

NOTE: Rat, mouse and dog data from Vaughan et al.[1]; man data from Durbin.[21]

So, some of the greatest problems associated with plutonium are those concerned with establishing the critical organ for ^{239}Pu. At present the bone is considered as the critical organ for all soluble intakes of ^{239}Pu and the lung for insoluble intake by way of inhalation (ICRP).[120] Arguments now exist to set the lung as the critical organ for all inhalation exposures (Bair),[37] the liver for long-term exposure (low level) in man (Durbin)[20,21] and possibly a different, unspecified, critical organ for juveniles (Vaughan).[1] Of course, more accurate microdosimetric techniques would aid in the solution to these problems by providing quantative numbers to support each of the above claims, or reject them. Better dosimetric techniques would also give a more accurate estimate of the toxicity of ^{239}Pu. This toxicity will be discussed in the next section and our microdosimetric technique applied to bone will be discussed in the next chapter.

3.2 Plutonium Toxicity

Plutonium seems to have become a word capable of eliciting remarks such as "the most toxic substance known to man" from certain segments of our society. Whether or not this statement is literally true remains to be shown but surely no one would question the fact that ^{239}Pu is a highly toxic substance. Small amounts of ^{239}Pu that can hardly be detected by means other than measurement of the radioactive decay of the mass present (on the order of micrograms) have been shown to be capable of producing fatal results in experimental animals (Mays and Lloyd),[8] (Jee),[11] (Bair),[36] (Thompson).[41] Plutonium-239 derives its high toxicity from several characteristics, mentioned in previous sections. First, ^{239}Pu is an alpha

particle emitter with a specific activity greater than alpha emitters such as ^{235}U but less than other alpha emitters such as ^{238}Pu and ^{241}Am. Thus ^{239}Pu is capable of dispensing large amounts of energy in a small volume (of radius about 35 microns) due to the emission of this densely ionizing but short-range particle. Second, ^{239}Pu possesses the unfortunate characteristic of concentrating in bone preferentially around the cells which are the most susceptible to undergoing neoplastic change (Jee),[11] (Scott et al.),[24] (Durbin),[22] (Evans),[64] (Vaughan et al.).[1] Finally, once deposited in the bone ^{239}Pu tends to be removed at a very slow rate, with a half-time for removal about 200 years for bone and about 178 years for the whole body in man (ICRP).[120] Durbin[20,21] has found somewhat different values for man. She determined the biological half-times to be 88 years for the skeleton and 204 years for the whole body.

Looking now at the effects of the deposition of ^{239}Pu in man we find that the only work in the field has been derived from animal studies. This is because to date no serious exposures have occurred in man which involved a large enough deposition of ^{239}Pu to cause detectable effects for the population size considered and, therefore, one had to fall back on animals. This fact is presumably due to the extraordinary precautions imposed when plutonium is expected to be present in any activity. The many animal studies mentioned earlier have permitted examination of different parameters concerned with animal exposure to plutonium. The most significant biological effect detected thus far of plutonium as a bone seeker is its ability to induce carcinogenic transformation in the cells

at risk (Vaughan).[1] Although other severe effects have been noted such as severe aplasia of the marrow and dysplasia of the bone (fractures, changes in bone growth, etc.) none of these has been noted at less than the carcinogenic dose. The most sensitive indicator of the presence of ^{239}Pu deposited in bone, i.e. the effect observed at the lowest dose, is the incidence of osteosarcoma (Vaughan),[1] (Stover and Jee).[12] But death occurs in the shortest time due to lung effects induced by the inhalation mode of administration (Bair)[36,37] for beagle dogs and comparable amounts of administered plutonium as in the injection studies. Osteosarcomas can be induced at extremely low absorbed doses. In the rat, only 3.6 rads to the skeleton (averaged over the skeleton) was required to induce an osteosarcoma (Jee).[11]

The animal used throughout the work at the University of Utah was the beagle dog. Plutonium-239 was administered by the intravenous injection of $^{239}Pu(IV)$ in the form of a citrate and maintained at an acidic pH (Stover and Jee).[12] Initially they used many different injected activity levels ranging from 0.016 μCi/kg to 2.9 μCi/kg but were forced to use still lower levels when osteosarcomas appeared at the lowest level (Stover and Stover).[125] Finally levels as low as 0.00064 μCi/kg were used. The 0.016 μCi/kg level corresponds to about 25 times the present MPOB in bone for ^{239}Pu, i.e. 0.04 μCi and 0.00064 μCi/kg corresponds to about one MPBB. The various levels of ^{239}Pu injected in successive runs were as follows in Table 4.

Table 4. Injected Activities of ^{239}Pu(IV) Citrate in University of Utah Dogs (Stover and Stover)[125]

Dose Level Code Number	Injected Activity of ^{239}Pu-citrate ($\mu Ci/kg$)
5	2.9
4	0.91
3	0.30
2	0.095
1.7	0.048
1	0.016
0.7	0.010
0.5	0.005
0.2	0.0019
0.1	0.00064

NOTE: Original dose levels used in the early studies are indicated with an integral "code number."

Four principal effects were observed in the dogs injected with ^{239}Pu(IV) citrate (Stover and Jee)[12]: (1) osteosarcomas were observed over the entire injected range from dose level 1-5, (2) hepatic lesions and/or changes were observed over the range, dose level 1-5, (3) lifeshortening was observed from dose level 1.7 to 5, and (4) hematologic changes were observed from dose level 2-5. Although these data seem quite conclusive concerning osteosarcoma, it must be recalled these exposures were given in an acute manner. Here the incidence of leukemia was such that osteosarcoma was the major cause of death. For a chronic, low-level exposure it seems just the opposite is true, leukemia ordinarily becomes the major carcinogenic hazard (ICRP).[81] Aside from the cancerous effects induced in the University of Utah dogs, other less toxic malignant consequences of the intravenous injection of ^{239}Pu(IV) citrate were noted (Taylor et al.).[126] At the fifth level a significant number of pathological fractures was noted. The earliest occurred approximately 390 days post-injection with an average skeletal dose of 3180 rads. The number of these fractures decreased until a threshold seemed to be reached at around dose level 4 (0.91 μCi/kg) where only one fracture was observed in seven life-span dogs. Most of the fractures developed in the ribs and thoracic vertebrae with very few being produced in the weight-bearing bones. Another effect of ^{239}Pu in these studies was an increased incidence of tooth loss. A detectable increase above the natural incidence was noted down to dose level 1.7 (0.048 μCi/kg). The sites of earliest loss were generally the first incisor and the second premolar in the upper arcade and the first incisor and the third molar in the lower arcade. Although

an increase in soft tissue tumors was noted at about 3-20 percent greater than controls, some doubt was expressed as to whether this increase was actually plutonium-induced. In any event, lymph node hyperplasia was observed in some dogs injected at dose level 1 to 1.7 (0.016 to 0.048 μCi/kg) after relatively long latent periods, but these did not undergo neoplastic change. The difficulty in determining the increase in tumors in soft tissue was due to the bias introduced by the shortened lifespan of the irradiated dogs. Although the level of plutonium in the kidney was ten times the plasma level, no neoplasms were observed throughout the entire injected range. There were some "hot spots" noted in the kidney which seemed to account for much of the kidney burden. The few plutonium-induced lesions observed, always occurred adjacent to these "hot spots" (Taylor et al.).[126]

As a side note, the data for dose levels 0.1 to 0.7 will not be available for some years to come due to the long lifespan of the beagle (Stover and Jee).[12]

The studies of Bair, Thompson and Clarke[31-46] at Hanford have been concerned with administration of plutonium by inhalation. They have examined the change in effects observed with parameters such as chemical form and physical state. These studies are of particular interest because it is felt that the inhalation route of exposure is the one most commonly encountered in human exposure as a result of industrial and military applications of plutonium as well as environmental contamination (Thompson),[41] (Bair).[36,37] Plutonium can cause different effects to occur in the experimental animal depending on the form in which it is inhaled, i.e. chemical form such as nitrate, oxide, fluoride, etc. and particle

size. Soluble plutonium nitrate has a greater chance of causing damage to bone and liver due to its greater capacity to translocate to other areas of the body. In the insoluble oxide form the plutonium does not have as much tendency to translocate, so the effects of this form of plutonium are mainly confined to the lung and tracheal-bronchial lymph nodes (Bair).[37] A summary of the effects seen in lungs due to an exposure to $^{239}PuO_2$ particles 0.1 - 0.6 μm count median diameter (CMD) in dogs at an acute, high activity level are as follows (Bair).[37] Immediately after exposure, the activity was distributed throughout the lung evenly but after seven days conducting and respiratory vessels were devoid of activity. After this time the remaining medium and large particles not removed by ciliary action were located mostly in the walls of the terminal bronchioles and the smaller particles in the lower part of the lung. Except for hyperplasia in some of the alveolar cells and some loss of mature bronchial lymph node cells, no clinical symptoms were visible. Almost all the plutonium particles had been phagocytized by macrophages at this time. At seven days the dose to the lungs was about 150 rads. Between 14 and 30 days hyperplasia had increased and the beginnings of peribronchiolar fibrosis were noted. By 30 days (D = 700-1900 rads) peribronchiolar fibrosis could be seen at many foci, numerous macrophages were present and inflammation could be noted. After 65 days alveolar cell metaplasia could be seen and was especially heavy in the locations of maximum deposit of $^{239}PuO_2$ (D = 4000-13,000 rads). The bronchial lymph nodes were showing necrosis with only small islands of lymphatic tissue remaining. Between 124-384 days metaplasis was severe around the

alveolar cells and could be seen localized around some of the bronchioles. Scars were visible as well as hemorrhage in the lung itself. Fibrosis in the bronchiolar epithelium was quite severe by now as well as in the alveolar cell region. Beginnings of the transformation from metaplasia to neoplasia could be noted in many regions. By 855 days fibrosis was prominent and early bronchopneumonia was detectable in one lobe. Some of the other effects of this alpha irradiation were an increase in respiration rate as death approached, a change in the blood gas level (oxygen content decreased and carbon dioxide content increased), weight loss, and finally a decrease in the immune response. Three modes of death were noted in these dogs by Bair.[36] The first was an acute form of death characterized by severe inflammation, edema and destruction of vital lung tissue occurring only at high exposure levels. Death occurred in about one week at which time the animal simply drowned in its own fluid. The second mode of death occurred after about one to two months post-exposure and was also considered to be an acute death. Here fibrosis had time to form causing interference with normal breathing and contributing to destruction of lung tissue. For this mode, death occurred due to respiratory insufficiency just preceded by a decrease in the oxygen level in the blood, an increase in the carbon dioxide level and increased respiration rate. The third mode was considered to be sub-acute but somewhat similar to the second mode. Here again fibrosis formed but at fewer loci initially. But as time passed, fibrosis slowly involved the entire lung causing death by cardiopulmonary insufficiency in one to five years. In some of Bair's dogs, death occurred after three to six years by pulmonary neoplasia. He

also hypothesized a form of death occurring after many years due to the long-term low-level effects on the lung, bronchial lymph nodes and liver (Bair).[36] His data seemed to indicate that a lung burden greater than 0.1 μCi/g lung would cause death in about one year from pulmonary insufficiency and a burden less than 0.1 μCi/g lung would cause death by formation of a pulmonary neoplasm.

When estimating lung exposures from aerosols in man we employ a lung model. In 1966 a new lung model was proposed by ICRP Committee II (Task Group)[127] superseding the old one (ICRP).[120] This new model divides the lung into three regions, the nasopharyngeal, tracheobronchial and pulmonary regions with pulmonary lymph nodes as a possible fourth region. These regions connect with one another and a cross-flow of material is allowed between them and the blood, the gastrointestinal tract and the lymphatic system. Here, considerations of the physical and chemical nature of the inhaled aerosols are included in estimating deposition and retention. All of the fractions of the inhaled aerosol initially appearing in the various regions are given as a function of particle size, varying exponentially with particle size, with the exception of the fraction passing through the nasopharyngeal region and depositing in the tracheobronchial region. This fractional deposition is given as a constant, equal to 0.08. Since the masses of these regions are difficult to determine and they are structurally complex with many branching pathways, the Task Group did not discuss the problem of estimating the absorbed dose to these tissues. To obtain an idea of the approximate magnitudes of dose, one could refer to the curves in Morgan and Turner[57] generated by W. S. Snyder under the normalized condition of 1 MeV energy/disintegration, a

standard particle size of 1 μm and 1 μCi inhaled.

When dealing with dose to lung tissue Cochran and Tamplin[128] proposed the necessity of considering whether the radionuclide was evenly dispersed or contained in areas of concentrated activity. This was the now famous "Hot Particle Theory" and qualitatively states "when a critical tissue mass is irradiated at a sufficiently high dose, the probability of tumor production is high." The issue seems to be settled now by majority opinion which states that, for an equal amount of activity a diffuse distribution seems more toxic than the same activity contained in many "hot spots." This could be caused by the extensive cell killing occurring near the hot spots which eliminates the cells from any possibility of undergoing the malignant change. Another possibility is that smaller, finely dispersed particles suffer less self absorption and affect a larger lung volume, hence causing a larger dose.

In summary, the most dramatic effects of plutonium observed in the animal studies were the induction of (1) osteosarcoma, (2) leukemia, (3) carcinomas of the epithelial cells surrounding bone, and (4) liver lesions. These consequences were observed in the University of Utah beagle dogs after intravenous injection of ^{239}Pu(IV) citrate. When the mode of administration is inhalation, the most dramatic effects are fibrosis leading to death by respiratory insufficienty at a high level of exposure and pulmonary neoplasia at a low exposure level (less than 0.1 μCi/g lung tissue). These effects are of interest to researchers for the simple reason that they are all fatal to the animal. It is interesting to note that 60 μCi of ^{239}Pu in citrate form, i.e. in soluble form, administered by inhalation to one dog and by intravenous injection to another

dog resulted in the death of the first dog ten times sooner than the second dog.

The toxicity of ^{239}Pu has been studied in animals at the University of Utah (Stover and Jee),[12] (Jee),[11,15,16] (Mays et al.)[14] for deposition in bone and liver by the intravenous injection of ^{239}Pu(IV) citrate compounds and for initial deposition in the lung at Hanford by Bair and Thompson and others.[31,33-38,45,46] The toxicity of ^{239}Pu and its relation to other nuclides can be shown by Table 5, drawn from Mays and Lloyd,[8] which shows percent incidence of osteosarcoma per rad of the nuclide. Mode of administration is by injection for every case except the ^{226} & ^{228}Ra data for man which were ingested radium. This table not only shows the high toxicity of ^{239}Pu but alludes to the similarity between the behavior of ^{224}Ra and ^{239}Pu for the female mice that occurs for the reasons previously mentioned. The University of Utah experiments are utilizing a unique method which they hope will lead to greater knowledge of toxic levels for substances such as ^{239}Pu for which essentially no toxicity data exist directly. This goal can be expressed by the following ratio (Stover and Jee),[12] (Evans)[64]:

$$\frac{\text{Toxicity X (beagles)}}{\text{Toxicity } ^{226}\text{Ra (beagles)}} = \frac{\text{Toxicity X (man)}}{\text{Toxicity } ^{226}\text{Ra (man)}}$$

where X is the nuclide for which the toxicity data are desired. This ratio is making use of the vast information available concerning radium exposure in man. Toxicity here is the activity required of a particular nuclide to cause a given endpoint. The idea is to determine the toxicity

Table 5. The Relative Effectiveness of Causing Osteosarcoma in Three Species of Animals for Several Bone-Seeking Nuclides (compiled from Mays and Lloyd[8])

Animal	Nuclide	Osteosarcoma Incidence % per rad
Beagles	^{226}Ra	0.043
	^{228}Ra	0.13
	^{239}Pu	0.38
Mice (NMRI) Male	^{224}Ra	0.0073
Female		1.3 ± 0.12
Mice (CF1) Female	^{239}Pu	1.1 ± 0.1
	^{226}Ra	1.1 ± 0.043
Man	^{226} & ^{228}Ra	0.0046
Man (adult)	^{224}Ra	0.009
Man (juvenile)		0.015

of nuclide X and ^{226}Ra in beagles by experiments to find the value of the ratio on the left side of the equal sign. This value could then be multiplied by the value of the toxicity of radium in man (e.g. in μCi) to obtain the similar quantity for nuclide X in man. The assumption involved here, of course, that such an equality is in fact valid, is an unproven assumption at present. As a numerical example of the use of the above equation, let us consider that it has been found osteosarcoma can be induced by injected dose levels as low as 0.34 $\mu Ci/kg$ of ^{226}Ra and 0.016 $\mu Ci/kg$ of ^{239}Pu (ICRP).[81] The left side of the above equation would then be about 0.047 or approximately 1/21 for osteosarcoma in beagles.

There has been interest in finding a method to treat ^{239}Pu exposure due to the consequences of intake of even small amounts of this substance (Lafuma and co-workers,[26-30] (Thompson et al.),[38] (Thompson),[41] (Vaughan et al.)[1] and (Markley et al.).[111] Working in France, Lafuma has been particularly interested in this area. Some of the substances used were zirconium citrate, EDTA and DTPA. The one proving to be most effective was DTPA (diethylenetriamine-pentaacetic acid) (Thompson).[41] Lafuma[26] stressed the need to begin treatment immediately after the accident occurred, even before the magnitude of contamination has been determined. When treatment was initiated immediately after exposure in rats administered $^{239}Pu(NO_3)_4$ by intramuscular and inhalation contamination (Lafuma),[30] a reduction in the ^{239}Pu content <u>in vivo</u> by a factor of 4 for the case of intramuscular injection and by a factor of 8 for the lung administration pathway from that present in controls was effected. Lafuma and co-workers stated that DTPA acts in two ways to reduce the contamination by preventing further bone deposition and by acting directly on bone to remove the

contaminant (Nenot et al.).[29] They also recommended a treatment procedure (Lafuma).[26] If the contamination is particulate in nature, DTPA is ineffective and physical removal is the only possible course (e.g. lung lavage). Therapeutic treatment consists of a three step procedure: (1) administer DTPA locally and generally immediately after contamination, (2) if a port of entry is present, remove as much contamination as possible by physical means, such as surgery or lavage, and (3) if contamination persists, begin a chronic treatment, the magnitude and duration determined by the results of radiological examination.

One method of quantitative evaluation of the toxicity is by calculation and comparison of maximum permissible body burdens (MPBB). The maximum permissible organ burden is obtained by determining the fraction, f_2, of the radionuclide in the particular organ to that in the total body and multiplying the MPBB by f_2.

The maximum permissible body burden for a bone seeking radionuclide is set by the relative effect of the radionuclide considered in bone as compared to radium. Radium-226 was chosen as the standard because of the large quantity of existing human data (Morgan and Turner),[57] (Evans)[10,64] and (Hasterlik).[60] For ^{239}Pu the maximum permissible body burden (based on bone as the critical organ) is 0.04 μCi (ICRP).[120] A number similar to this can be calculated by the usual method to determine the maximum permissible organ burden, i.e. one calculates the deposited activity (Ci) which will deliver the maximum permissible dose rate to the critical organ. This will now be calculated for ^{239}Pu. First we need to calculate E (MeV/dis x rem/rad) for ^{239}Pu (Morgan and Turner)[57]:

$$E' = \sum_i \sum_j f_i \; E_i \; F_{ij} \; Q_{ij} \; N_{ij}$$

where

f_i = probability per disintegration of producing radiation type j

F_{ij} = fraction of the energy from j absorbed in organ i

E_i = energy (MeV) absorbed per disintegration

Q_{ij} = quality factor and is a function of radiation LET

N = relative damage factor = 5 for bone-seeking alpha emitters when radium is not the parent nuclide and is 1 otherwise.

Plutonium-239 emits several possible alpha particles in its decay to ^{235}U. Uranium-235 is sufficiently long-lived in comparison to the half-life of ^{239}Pu and the life span of man that its radiations need not be considered. Also, Q = 10, for alpha particles, F_{ij} is 1 and the mass of the skeleton is 7000 g so that

$$E' = (1)(10)(5)[(0.733)(5.157 \text{ MeV}) + (0.151)(5.145 \text{ MeV}) + (0.115)(5.107 \text{ MeV})]$$

$$= 257.2 \text{ MeV/dis} \times \text{rem/rad}.$$

According to the recommended procedure (ICRP),[120] the bone is allowed to receive 30 rem/yr for occupational exposures. This yields finally

$$\frac{30 \text{ rem}}{\text{yr}} = Q \; \mu\text{Ci} \times 3.7 \times 10^4 \text{ dis/sec-}\mu\text{Ci} \times 257.2 \text{ MeV/dis} \times \text{rem/rad} \times 8.64 \times 10^4 \text{ sec/day} \times 365.25 \text{ day/yr} \times 1.6 \times 10^{-6} \text{ erg/MeV} \div 7000 \text{ g} \times 100 \text{ erg/g-rad}$$

where

Q = maximum permissible bone burden = qf_2

$\cong$ 0.04 μCi (ICRP gives this value as 0.036 μCi)

This value for the bone burden of ^{239}Pu has been the center of discussion in recent years. This value was calculated assuming the ^{239}Pu was distributed homogeneously throughout the bone, yet as we know ^{239}Pu is distributed in a highly inhomogeneous fashion. Additionally, ICRP has recently proposed the quality factor for alpha particles be increased to 20 (ICRP).[114] The 0.04 μCi value has remained in use depite the request of the ICRP to refine the MPBB for bone based on the dose delivered from 0 to 10 microns removed from the endosteal face of osseous tissue (ICRP).[114] Should improved methods of microdosimetry become available, such a revision could be envisioned. Whether dosimetry resulting in these measurements would cause the MPBB to be raised, lowered or remain the same is unimportant to this research. The important objectives should be to make certain the MPBB is based on a firm foundation.

Several of the arguments of critics suggesting the lowering of MPBB for bone are quite logical in their approaches. Edsall[129] has suggested we should set the standard of this nuclide in line with those standards our society currently accepts as permissible risks. He points out the 50,000 traffic deaths occurring each year, 100,000 deaths occurring per year due to occupational causes, etc. Edsall[129] then mentions that at one MPBB for lung, approximately one person in eight will develop a lung cancer. If plutonium were a food additive this would certainly be considered an unacceptable risk according to present Food and Drug Administration practices which desire a new additive to cause much less than

two tumors per 1000 individuals. The value for ^{239}Pu at one MPBB lung was one in eight or 125 in 1000. This appears to be a double standard, Edsall concludes (though no one proposes using plutonium as a food additive).

Morgan[130] offers four arguments which lead to a reduction in the MPBB by a factor of 240: (1) according to the Utah dog studies the relative toxicity of ^{239}Pu to ^{226}Ra should be 15 instead of the general value assigned to all non-radium bone-seeking alpha emitters of 5, a factor of 3 correction; (2) the surface to volume ratio for the trabecular bone of the dog is about twice that for man; therefore, the same amount of ^{239}Pu in man would mean the trabecular concentration in man is twice that in the dog, a factor of 2; (3) the rate of apposition in dog bone is about 10 times that in man which would cause any ^{239}Pu existing on the bone surface to be removed about 10 times faster in dogs to the less radiosensitive cortical bone, a correction factor of 10; (4) studies have shown that the baboon is about four times as radiosensitive as dogs when dealing with $^{239}PuO_2$ inhalation. Since man is more similar to the baboon than the dog, a factor of 4 should be introduced. The total reduction would then be $3 \times 2 \times 10 \times 4 = 240$, which corresponds to a change in the MPBB for bone from 0.04 μCi to 0.17 nCi.

Now the need for better dosimetry of ^{239}Pu as it resides in the bone becomes clearer than ever. If the requests of the ICRP to supersede the value of the MPBB for bone by a value not based on the admittedly incorrect homogeneous distribution assumption are to be fulfilled as well as the critics answered by improved quantitative data, a step must be

taken to acquire the desired dosimetric data. As this section points out, the toxicity of this nuclide is great, so a note of urgency should be added to the quest for this microdosimetric determination. Now that the groundwork has been laid and the need for the research contained herein has been established, the system used to determine the average dose to the endosteal surfaces of bone will be described.

CHAPTER IV

THE CURRENT ELECTROCHEMICAL ETCHING SYSTEM

4.1 Principles of Electrochemical Etching

It has been known for many years that tracks will be left in some materials when irradiated by high LET particles and these can be preferentially etched by appropriate chemical etching techniques (Price and Walker).[131] In more recent times, this technique has found use in a large number of areas including geology, space science and nuclear science (Fleischer et al.)[132] and (Iyer and Rao).[133] There have been several attempts (Boyett et al.)[134] to explain the formation of tracks in solids but the one that seems to account for most of the observations in crystals is the "ion explosion spike model" of Fleischer et al.[135] According to this model, the ionizing particle traverses the solid, stripping away electrons from the atoms closest to the path of the ionizing particle. The result is many positively charged atoms very close together. These repel each other and move rapidly away from each other resulting in the track. The boundaries of the affected track region would then be in a state of stress which would explain the characteristic of the tracks being preferentially etched. A different mechanism would be expected in the case of foils composed of polymers such as polycarbonate. Here the high LET ionizing particles simply break the polymer chains as they traverse the foil. The broken ends of the polymer molecules would be left in a chemically reactive state including some radicals. Therefore

the broken polymers may now be more reactive with the etchant solution than the unirradiated volume explaining the preferential etching of the track. The simple etch attack procedure for the development of damaged track regions was modified in the early seventies when a new process was introduced by (Tommasino et al.)[136] expanding the possibilities of etching. The new advances involved placing an alternating voltage across the cellulose nitrate or polycarbonate dosimeter to etch the damaged tracks in a 30% KOH solution; this procedure was called electrochemical etching.

Improvements have been effected in the plastic foils since then and attempts made to better understand the parameters (Sohrabi),[49] (Sohrabi and Morgan),[137-141] (Beach and Becker)[142] and (Somogyi et al.).[143,144] Beach and Becker[142] showed Lexan polycarbonate could resolve tracks from two fine UO_2 microspheres placed 5 μm apart. Somogyi et al.[143] examined the effects of irradiation geometry, particle energy and environmental conditions on such parameters as optical density, etching time and track density for three foils, cellulose nitrate, cellulose acetate and polycarbonate.

In 1975 a workable system was proposed with many of the etching parameters optimized by Sohrabi.[49] This system used a chamber containing two reservoirs of 45% KOH solution separated by the polycarbonate foil to be etched. Best results were obtained when an alternating potential of 800 volts was applied at 2 kHz for four hours.

The system selected for the bone dosimetry application described here is a version of the Sohrabi-Morgan system (Morgan and Sohrabi).[137-141]

The equipment consisted of two plexiglas cylindrical chambers, each 4.8 cm long and 10.2 cm in diameter, see Figure 9. Seven 250 μm thick Transilwrap polycarbonate (Transilwrap Co., Doraville, Georgia) foils can be etched at the same time and are placed between the chamber halves on non-standard sized "O"-rings 1 inch O.D., 5/8 inch I.D. and 3/16 inch thick, constructed from neoprene sheets. The portions of the chamber are then placed together and bolted tight to insure that the chamber is watertight and electrically insulated by the foils themselves. The chamber is then filled with the 45% by weight KOH etchant solution at room temperature, Figure 9. The high voltage is applied across the chamber by means of two stainless steel electrodes located in the far end of each chamber half. The high voltage is generated by an audio generator supplying the input to an amplifier of the push-pull type to maintain the necessary stability in frequency and voltage. A diagram of this circuit appears in Figure 10 (Sohrabi)[49] and a picture of the experimental setup in Figure 11 (Stillwagon et al.).[145,146] The voltage and frequency used throughout much of this study were 800 V at 2 kHz. After the desired etching time has elapsed, the foils are cleaned, removed from the chamber and prepared for counting. The track counting equipment used included a transparency projector, microfiche reader and the light microscope with phase contrast and oil immersion capabilities as well as one equipped with a Filar micrometer for track diameter measurements.

The electrochemical etching technique of polycarbonate foils was selected to be applied to the bone dosimetry application considered herein over all other techniques because it fulfilled more of the desirable

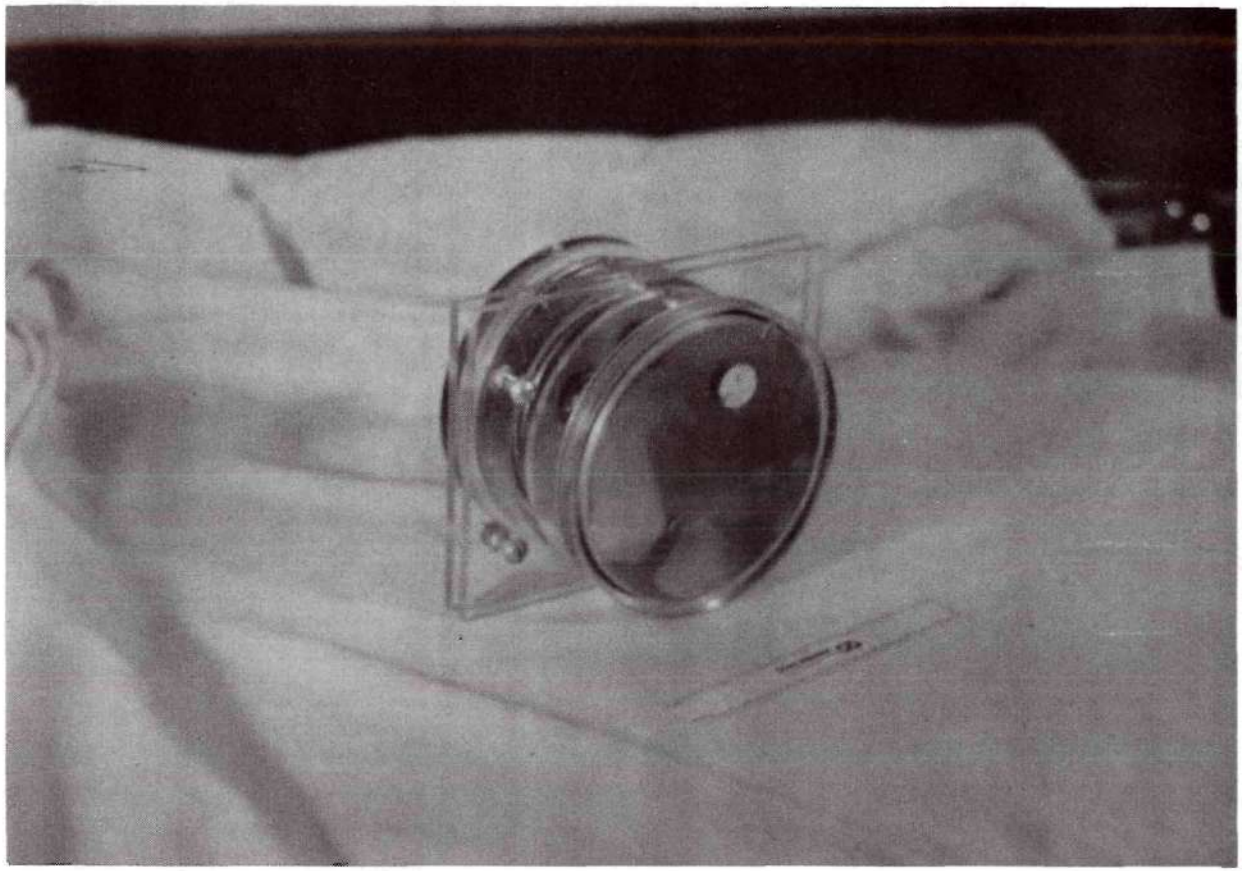

Figure 9. A Plexiglass Etching Chamber

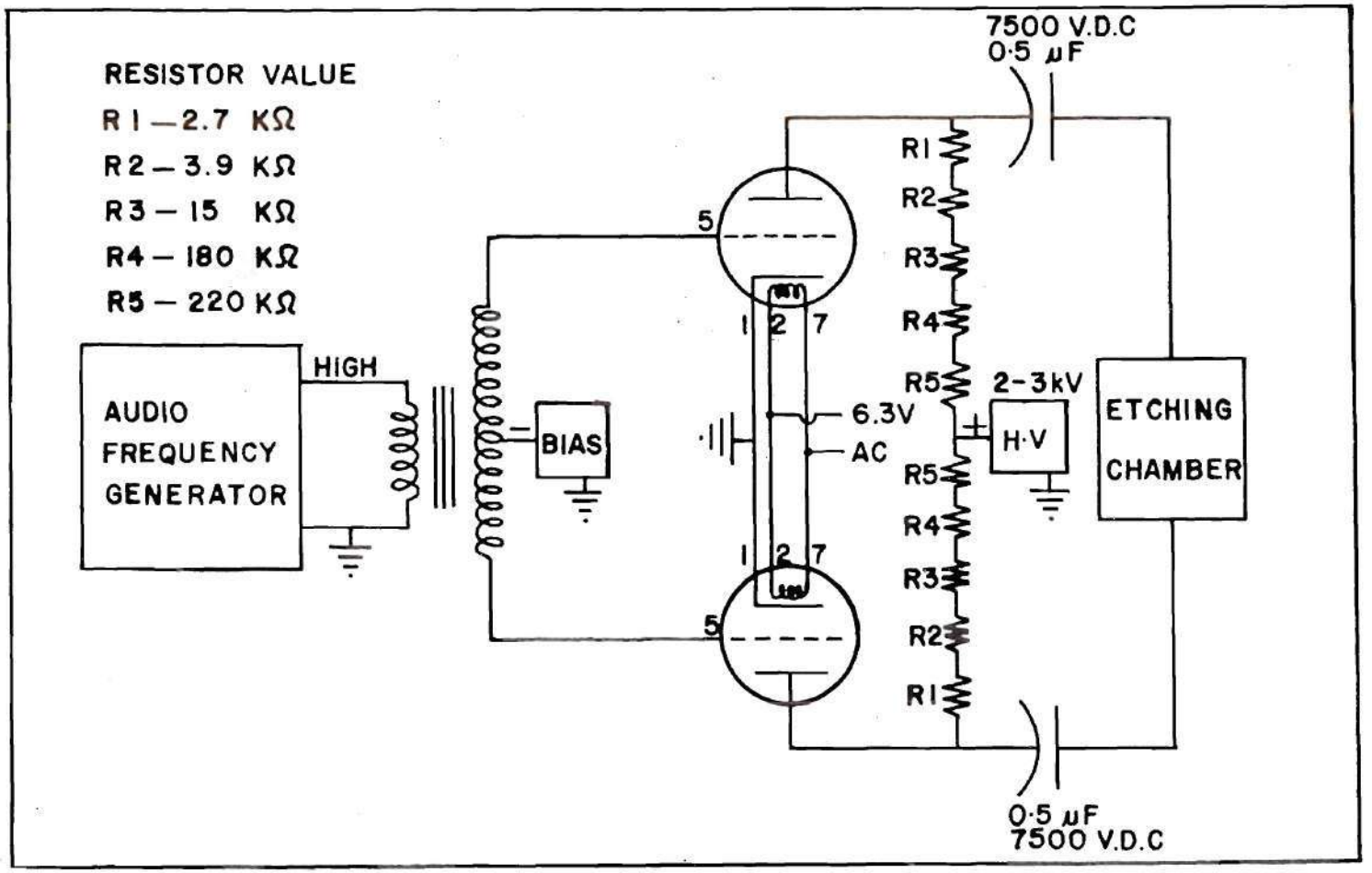

Figure 10. Diagram of Electrochemical Etching System Used in This Study

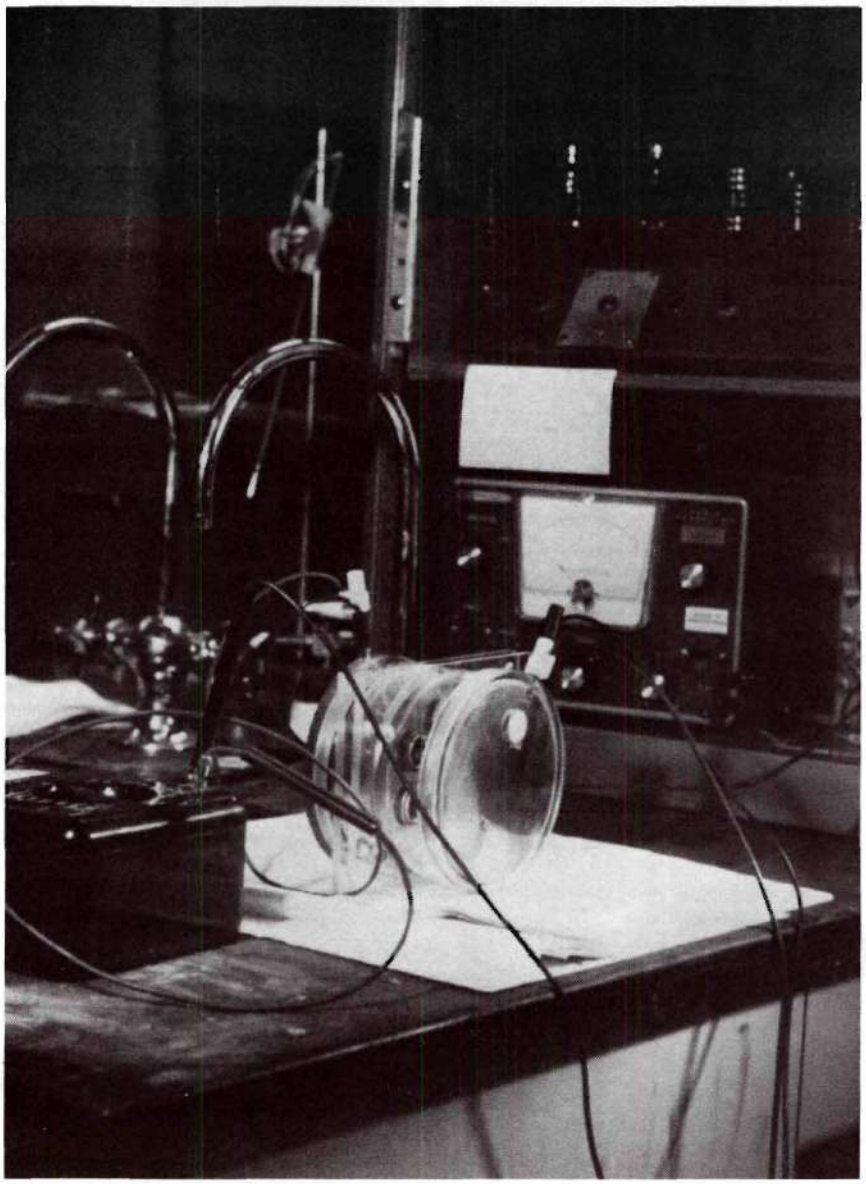

Figure 11. Electrochemical Etching Apparatus Showing Etching Chamber, Audio Oscillator, Amplifier and Volt Meter

characteristics for a bone dosimeter listed on page 37 than any other practical system imaginable. With reference to the criteria listed there, the advantages of this system over others will be analyzed point by point.

1. The geometry of this system is such that the foils can be placed flush against the bone section, thereby allowing tracks from only the areas of bone under consideration to be counted. If a surface barrier detector was placed against the bone sample all alpha particles, regardless of origin on the bone sample, would be counted. In addition, it is virtually impossible to maintain a surface barrier detector coupled with a multichannel analyzer absolutely electrically constant for the long irradiation times required at the activity levels encountered here. Some photographic emulsions allow a similar close geometry. The liquid scintillator suspension technique described above suffers from the lack of spatial resolution since the sample must be taken whole to obtain sufficient activity for the operation of this technique.
2. The sensitivity of these polycarbonate foils is believed by some to be somewhat less than that of emulsions but this prohibitively may not be so. It is certainly greater than that of the liquid scintillator suspension technique.
3. Fading with time after irradiation is essentially nonexistent with polycarbonate foils. In fact, there is evidence that sensitivity may actually increase with time after irradiation

before etching. There is no possible fading at all after the foil has been etched. Emulsions suffer severely on this point. There is fading between irradiation and development, but worse it varies with many parameters and from batch to batch, e.g. storage temperature and length of storage.

4. None of the present techniques involve any residual activity found in the detection system as is common with neutron activation methods.

5. Each polycarbonate sheet used during this work was 24" x 48" cost two dollars and provided approximately 1000 foils per sheet. Possibly as many as 1500 foils were used during this entire project Clearly the cost is almost negligible. Photographic emulsions, on the other hand, would have required quite an investment if, say, 1500 NTA, 25 μm thick nuclear track plates had been used (current price: $12.10/plate, $18,150.00 with the total not including developing costs).

6. The developing procedure for the electrochemical etching system is quite simple and data can be obtained by a novice his first try. It requires only about 5-10 minutes to perform and no time limits are required. The entire process is carried out in daylight at room temperature. Before using photographic emulsions, the developing process must be mastered. This requires not only knowing the procedure involved, using developers, fixers, observation of dose time tolerances and maintaining careful temperature control, but also adeptness in the darkroom

since the process must be performed in darkness. During mounting of the bone samples and during exposure of the emulsions, darkness must be maintained unlike polycarbonate which requires no darkness at any time. Therefore there is no danger of losing a large quantity of data after a long exposure time due to a light leak with our system. Also emulsions must be maintained under refrigeration, especially if long term storage is required as is the case with low level bone dosimetry and controls must be run with each batch.

7. Our studies (Stillwagon et al.),[145] (Su et al.)[147] have indicated a constant background of about 2 tracks/cm^2 on the foil surface when counting both sides of the foil. Since alpha particle irradiation produces tracks on only one side of the foil (the foil is infinitely thick to alpha particles) the background can be divided by two and becomes negligible for many applications. Emulsions, on the other hand, have a background that can be quite appreciable, though sometimes distinguishable, for older emulsions, emulsions improperly stored at a high temperature or emulsions improperly developed. It is evident that background can vary considerably from batch to batch.
8. Both emulsions and polycarbonate can be used in large quantities, however the economics and ease in development favor polycarbonate.

On consideration of these eight points, the electrochemical etching system appeared most attractive. Another point of lesser importance is

the tissue equivalence of polycarbonate. In fast neutron dosimetry this property of polycarbonate was considered quite important. For the bone dosimetry application described in this paper, this property may only serve to allow one to mention that the tracks in the polycarbonate will be of the same shape, structure and length as those formed in tissue. For the purpose of track counting alone, this may not be of great importance and so the non-tissue equivalence of the emulsion could be considered acceptable. Perhaps other, more theoretical uses of polycarbonate would make great use of the similarity of track structure here and in tissue when considering alpha particle irradiations. In fact the tissue equivalence of polycarbonate was used in this study and will be described in the next chapter (in the section concerning the two track sizes appearing on our foils after alpha particle irradiation (Stillwagon and Morgan).[149,150] It is possible the effect noted there would have never been observed using emulsions due to the heavy silver and halide atoms present.

4.2 Further Electrochemical Etching Studies

These studies were performed by the author and, in some cases, in conjunction with Mr. Shian-Jang Su.

4.2.1 Foil Reading Methods

Two new techniques were developed to facilitate counting of the polycarbonate foils. Both techniques employ optical devices almost every laboratory and university possesses in readily obtainable supply, a microfiche reader and an overhead (transparency) projector. These two techniques offer several advantages over the microscope for low count

density and thick foils (Tripier et al.).[151] Spark counting requires very thin foils (Johnson and Becker)[152] and techniques such as densitometry measurements require a large number of counts (high dose). Advantages obtained by utilization of these two observation techniques over our earlier conventional microscope counting are:

1. A larger foil area is actually counted; the overhead projector providing greatest viewing area, microfiche reader second, and microscope third.
2. Image is reviewed on a screen and not through an eyepiece causing less eye strain.
3. Less time is required per foil for counting.
4. No elaborate equipment is required other than these inexpensive pieces of equipment most institutions possess anyway.

To facilitate counting with the transparency projector a grid was constructed on the screen upon which the image was projected, Figure 12. The grid consisted of two concentric circles of radius 4.3 and 7.0 cm on the screen which were cut into sectors with radii drawn every 20^{o} (18 total). These lines yielded 36 small areas which could be counted easily, their sum equaling the total number of counts contained within the enclosed area, 154 cm^2. The counts appear on the screen as black dots on a clear background so the viewer encounters little difficulty in recognizing them.

The procedure adopted to count foils by this technique was as follows. The number of tracks within the 154 cm^2 area was obtained, then the foil was randomly moved such that another portion of the foil was

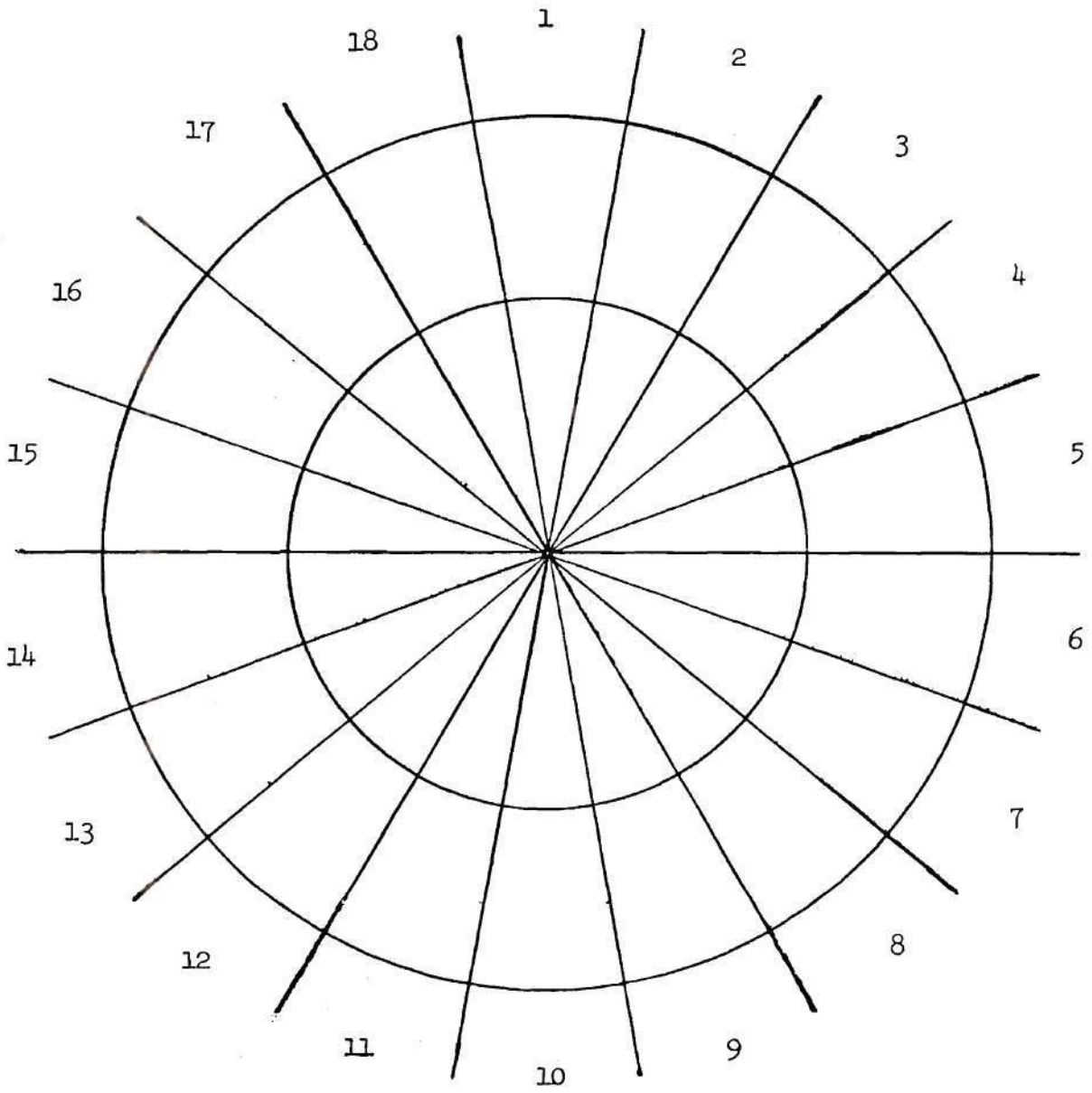

Figure 12. Grid Used in Foil Counting

available for counting. This new section was counted then the numerical average of the two measurements calculated. It was the average of the two countings we called the number of tracks in the 154 cm^2 area. Foil magnification was 14X with a screen to projector distance of 5 m yielding track diameters of 0.6 mm. Of course almost any magnification could be obtained depending upon the distance of separation between the projector and screen. Figure 13 is a typical photograph of the overhead projector screen indicating results obtainable by this technique. The projection shown was found to have 685 counts within the encircled area.

The second technique developed, the microfiche reader, offers other possibilities. The magnification produced by the microfiche reader was 53X, greater than the overhead projector. Track diameters were of the order of 2-4 mm. The procedure followed to count the foils involved placing a set of cross hairs on the microfiche reader screen, dividing the screen into quarters. First one quarter of the screen was counted, then the foil moved such that a different portion of the foil could be counted. This procedure was repeated until four counts were obtained, then a sum was calculated. Figure 14 illustrates the results obtainable by the microfiche reader for a foil determined to have 142 tracks on the entire foil. The actual area of the screen photographed was 17 by 13 cm and the horizontal line is a portion of the crosshair. Since the magnification was 53X with the microfiche reader, the tracks were viewed in greater detail than when viewed with the transparency projector. The star-like outcroppings from individual tracks became visible, similar to the appearance of the tracks seen by the microscope. Also, not unlike

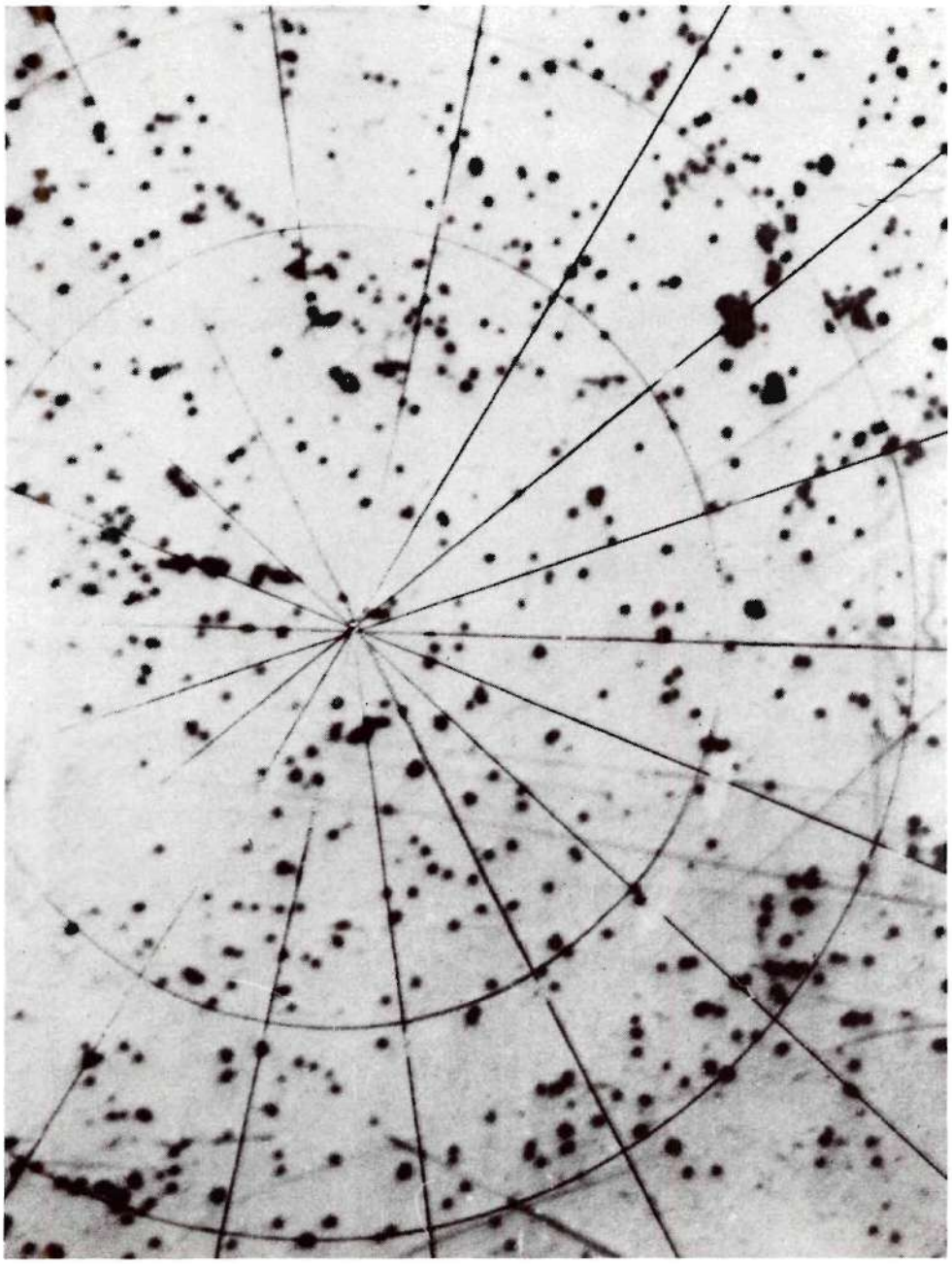

Figure 13. Portion of Transparency Projector Screen Showing High Background Foil

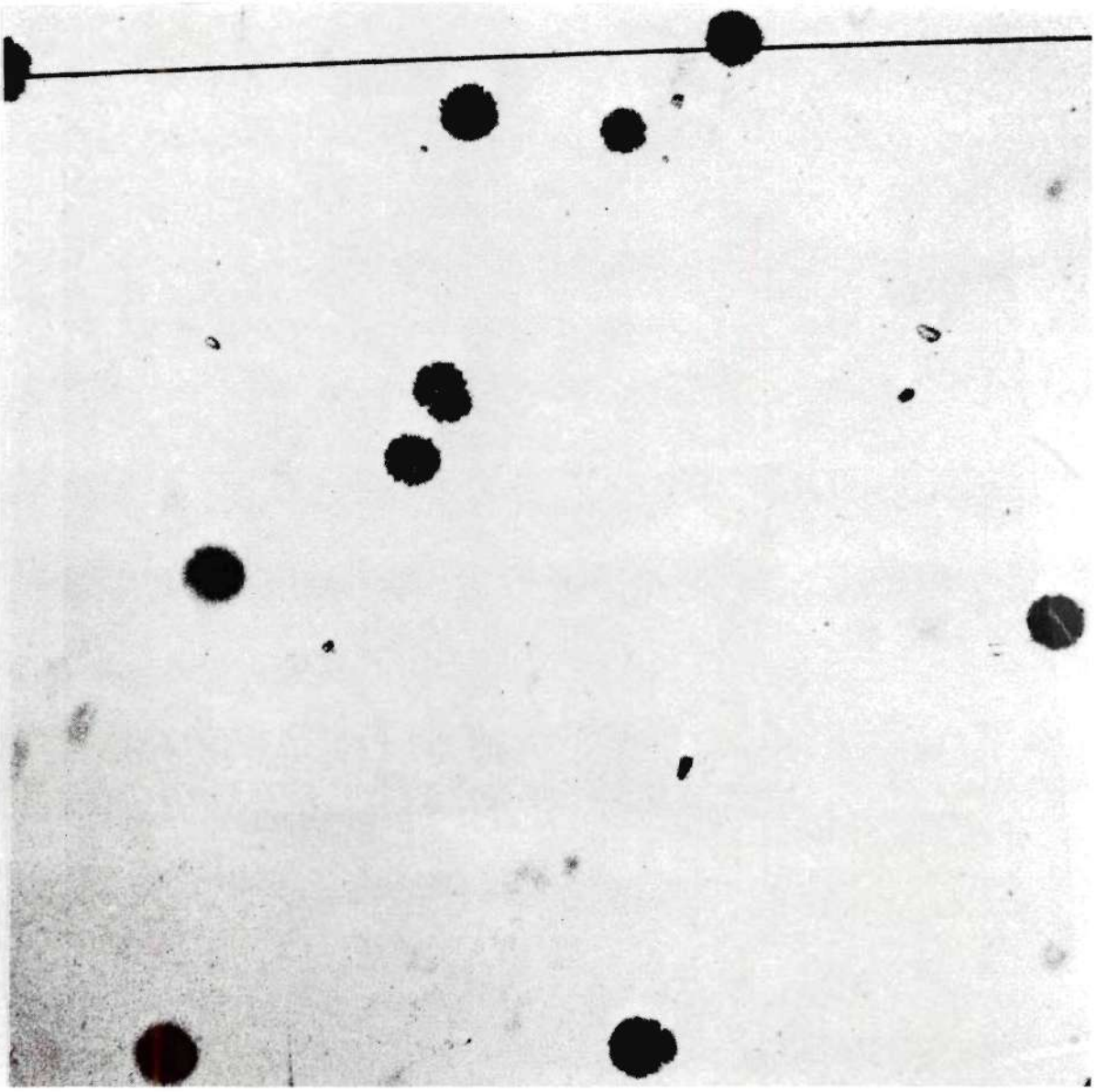

Figure 14. Photograph of Transparency Projector Screen Showing High Background Foil

the case with a microscope, the focus on the microfiche reader can be adjusted so the plane of focus includes only tracks in one plane or on one side of the foil or the other. The tracks on the side opposite the side being viewed appeared as unfocused blurs. This would explain why some tracks were viewed sharply and others were out of focus in Figure 14. A smaller area of the total foil was visible on the microfiche reader than on the transparency projector screen but the tracks were more readily distinguishable from other stray marks on the foil.

It is felt both of these techniques would speed up counting and greatly enhance the efficiency of eliciting data from the Lexan foils when large numbers of foils need to be counted.

For reduction of the bone dosimetry data, however, the microscope was utilized. The higher magnification allows more precise counting of alpha particle tracks than the above methods, since these tracks are smaller than the fast neutron recoil particle tracks considered above. In addition, track diameter measurements were required and can be obtained more accurately with the Filar micrometer attachment on the microscope. Further, very small squares had to be counted on the foils exposed to our bone samples to calculate a statistical average of the counts. This can be easily accomplished by placing a Whipple disk in the eyepiece of the microscope. Our microscope was a Bausch and Lomb WP6360 microscope capable of operating with phase contrast and oil immersion objective (970X).

4.2.2 Background Track Density Reduction

Presence of a high background can sometimes be a problem with

polycarbonate foils. This problem is thought to occur as a result of two factors. Although the duration of a particular irradiation measurement may be fairly short, the foil has been accumulating etchable background from both background radiation (cosmic rays, trace uranium, etc.) and surface abrasions since its production in a factory. Therefore, interest exists to maintain this background as low as possible. We have tried several methods, including annealing, washing with isopropyl alcohol and selection of a foil with an inherently low background.

In our annealing experiments, six groups of foils, seven to a group, were heated to various temperatures for twenty minutes. Then one foil from each group was placed in the seven foil chamber along with a control which had not been annealed. Etching conditions used throughout this study were

1. Etching solution - 30% KOH
2. Voltage - 700 Volts
3. Frequency - 2 kHz
4. Etching time - 4 hours.

It was found that a significant reduction in background and increase in overall track homogeneity resulted in the foils were washed with isopropyl alcohol and rinsed with distilled water prior to annealing. The six temperatures used to anneal the foils were 60^{o}, 105^{o}, 130^{o}, 140^{o}, 155^{o} and 170^{o}C. The foils were counted with the microfiche reader and transparency projector. Finally, the data were arranged so that the counts for each temperature and control could be examined for the seven runs and an average value calculated and plotted, Figure 15. The

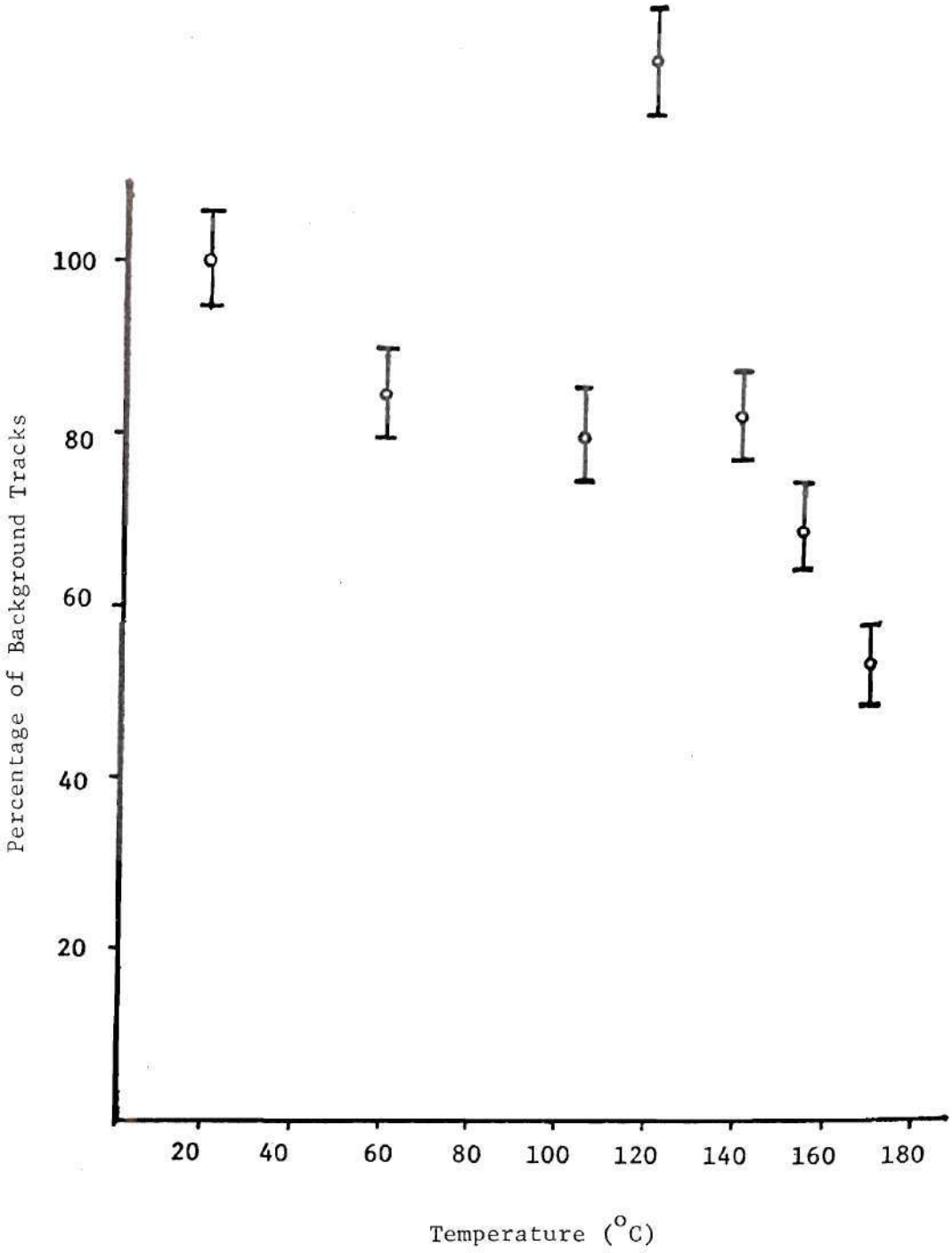

Figure 15. Percentage of Background Tracks After Annealing for 20 Minutes at Different Temperatures Before Etching

background in reference to controls dropped to 69 percent at 155° and decreased rapidly until it was reduced to 54 percent at 170°. The error bars correspond to one sigma. The point at 130° is not considered to be a genuine fluctuation in the overall trend. These background on these foils always exceeded 100 tracks. Other foil types were then used to examine the effect observed on the operational background. The masked foil, 250 μm marketed by Transilwrap, Doraville, Georgia, was utilized in an experiment involving 143 background foils plus controls. These foils were etched at 800 volts for 5 hours in a 45 percent KOH solution. This resulted in a background of 2.2 tracks/cm^2. Therefore it was decided to use this foil exclusively, avoiding any pretreatment of the foils

4.2.3 Optimization Study

Once the type of foil to be used in these studies had been determined, the etching conditions yielding the best results were required. Based upon the data of Sohrabi,[49] a series of foils were etched with controls to systematically examine the effects observed when the various parameters were changed. Different combinations of the following selections were used: etchant, 30 and 45 percent KOH; etching time, 4, 5 or 6 hours; voltage, 700 or 800 volts. The etchings were performed as indicated on Table 6. The optimal set of conditions to be used was a trade-off between several desired effects. It was desired to have the largest track diameter possible, of course, to expedite counting but at the longest etching times two facts became evident. First, at the longest etching time reproducibility suffered because the frequency of premature shutdowns of the etching process increased due to etching through of

Table 6. The Set of Conditions Used During Each Run to Determine the Most Optimal Etching Conditions

Run	Percent KOH	Etching Time Hours	Voltage
1	45	4	700
2	45	5	700
3	45	6	700
4	45	4	800
5	45	5	800
6	45	6	800
7	30	4	700
8	30	5	700
9	30	6	700
10	30	4	800
11	30	5	800
12	30	6	800

the large tracks and etchant leakage. Second, the background increased because deeper layers of the foils were exposed and available for etching at the longest etching time. Therefore, we selected the optimal etching conditions to be 45 percent KOH, 800 volts and 5 hours etching time except when background is less crucial relative to the large track diameter and consequent ease of track counting. In this latter case, 4 hours was chosen to be the best etching time.

4.2.4 Large Scale Etching

One of the problems to be solved in shaping the electrochemical dosimetry system into a practical personnel dosimetry system is increasing the number of foils that can be etched in one batch. Toward this end M. Sohrabi designed a large etching chamber capable of etching several times the number of foils now possible with our laboratory scale chambers. The laboratory scale chambers will etch seven (7) and the large chamber will etch thirty-five (35) foils at one time. This latter chamber (Sohrabi and Morgan)[141] has fixed stainless steel electrodes (24.5 cm in diameter and 75 in thickness and 10 cm total length). The diameter of the chamber is 25.5 cm. There are two holes in the bottom of this chamber connected to two hoses for draining. As pointed out by Sohrabi and Morgan in an earlier report,[141] this chamber did not yield a large degree of reproducibility due to its tendency to allow etchant to leak around the "O" rings, stopping the etching process.

At the beginning of this research, almost half the etching positions leaked severely. During the ensuing period, attempts were made to correct this problem, although this effort was extraneous to the bone

dosimetry project. The first attempt to solve the problem culminated in the construction of a vise-like device to apply pressure directly to the "O" rings at each etching position and thereby reinforce the watertight seal. This succeeded in reducing the leakage from eighteen down to three or four positions, but the upper limit had been reached as to the amount of pressure that could be applied safely to the chamber. The problem seemed to arise from another source. It was determined the recesses where the "O" rings fit into the chamber had small but detectable differences in their machined depth. The "O" rings used were constructed from a reasonably hard material and they were thin (3 mm) so it was concluded that an uneven seal might be created when these rings were pressed together. New "O" rings were ordered to custom specification (not a standard size, as before) which were constructed 4.5 mm thick and with a softer material to facilitate formation of a watertight seal when pressure was applied. This method has been more successful than previous ones but leakage still occurred with a greater frequency than is observed in the small chambers. In order to use routinely this chamber it would probably be advantageous to reconstruct the chamber such that greater pressure can be applied to reinforce the watertight seal with the vice-like device.

4.2.5 Bulk Etching Rate Determination

In order to determine the magnitude of polycarbonate lost during electrochemical etching we found it necessary to evaluate the bulk etching rate of polycarbonate during electrochemical etching (Stillwagon et al.).[148] Since the surface of the foil actually participating in the

electrochemical process and the density of polycarbonate are known, it was decided the bulk etching rate could be determined by the difference in foil mass before and after etching. Groups of non-irradiated 250 μm thick polycarbonate foils were cut and accurately weighed to 0.1 mg. These foils were then etched under the following conditions: 800 V applied at 2 kHz in a 45% KOH solution at room temperature, 25°C. Etching times were stepped in 1 hour increments from 2 hours to 6 hours and then a final etching run performed until breakthrough occurred at 8 hours, 23 minutes. Each foil was reweighed to determine its final mass and Δm was calculated. If we keep in mind that the foil is etched from both sides and let D (cm) represent the etched diameter of the foil, X (μm) the thickness of foil removed by bulk etching from one side of the foil and (g/cm^3) the density of polycarbonate, we have the foil surface removed after each etching period $X = [(2\Delta m 10^4)/(\rho\pi D^2)]\mu m$. If X is divided by the etching time, bulk etching rate results. The data indicated that the bulk etching rate was constant and equal to 0.16 μm ± 0.024 μm/hour from each side of the foil for our etching conditions.

This constant value of bulk etching is in contrast with the track etch rate which increases almost exponentially (Sohrabi),[49] but is compatible with the constant bulk etching rate found in the chemical etching process that also possesses a nonlinear track etching rate (Fleischer et al.).[132] It is difficult to compare bulk etching rates between the electrochemical and chemical etching systems because the etching conditions are so vastly different, but Fleischer et al.[117] have given the chemical bulk etching rate for their material as follows:

4.68×10^{-4} μm/hr, when considering 10.3 μm thick foils etched in 3.1N NaOH at 7.2°C.

This value of the bulk etching rate found for the electrochemical etching process points to the great amplification achievable by this process because the loss of only 0.64 μm of polycarbonate surface from one side of a 250 μm thick foil during a four hour etching period produces a 100 μm diameter recoil particle track on a fast neutron irradiated foil. Incidently, the etching of background tracks in this determination was neglected because the background was so low, 2 tracks/cm^2.

4.3 Applications of Electrochemical Etching

Aside from the present use described here, there are many other conceivable uses for the electrochemical etching of polycarbonate foils for the purpose of dosimetry. This system has been applied to various fast neutron dosimetry applications (Sohrabi),[49,134] (Sohrabi and Becker),[153] (Su)[147] (Stillwagon et al.)[155] involving fast neutron personnel dosimetry and the measurement of the fluence of fast neutrons around high energy accelerators. Polycarbonate is especially suited for the latter task since it is essentially insensitive to photons which allows these foils to be placed directly in the beam to obtain a neutron measurement. Another recent application of this system is in the field of thermal neutron dosimetry (Stillwagon et al.).[156] It is also conceivable these foils can be used in neutron depth dose studies inside heterogeneous phantoms, including alfedo neutron measurement. The electrochemical etching system could be used in many tissue sample dose determinations, such as the present one, when one desires to observe the dose deposited to a small area of tissue surface.

CHAPTER V

ALPHA PARTICLE TRACK PRODUCTION IN POLYCARBONATE

5.1 Efficiency of Alpha Particle Track Production

To date the electrochemical etching system has been used primarily for fast neutron dosimetry applications (Sohrabi),[49] (Su et al.).[147] Up until now the parameters associated with alpha particle track production in polycarbonate amplified by electrochemical etching have not been determined. The four parameters which have been evaluated during the course of our research here are the efficiency of alpha particle etchable track production, the track diameter as a function of etching time (Stillwagon and Morgan)[149,150] sensitivity as a function of waiting time and sensitivity as a function of etching time. Reproducibility will be discussed also. Throughout these two studies, 250 μm thick Transilwrap polycarbonate foils were used. The etching equipment was the same as described and shown on Figures 9 and 11.

In this section we are concerned with the efficiency of alpha particle track production in polycarbonate foils, as amplified by electrochemical etching. The track diameter as a function of etching time, sensitivity as a function of waiting time and etching time and reproducibility will be examined in the next sections. To examine the efficiency of alpha particle track production, a device called the vacuum-sealed alpha-calibrator was designed by this research, Figure 16. It provides a constant source to detector distance; one of the detectors being a

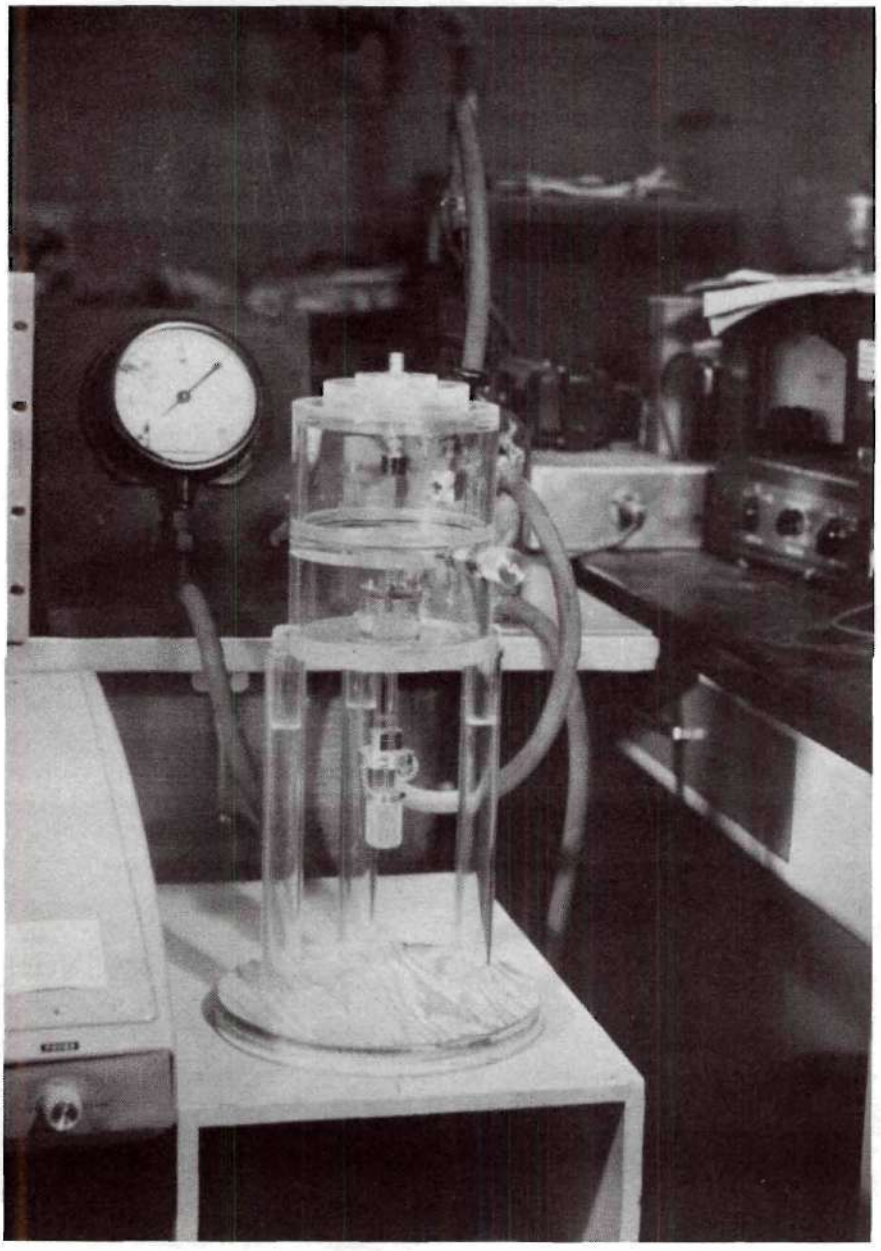

Figure 16. Closeup of the Vacuum-sealed Alpha Calibrator Showing the Vacuum Hookup, Two Compartment Design and the Calibrated Source Stand

surface barrier detector and the other the polycarbonate foil. Different absorber thicknesses can be simulated by varying the air pressure in the chamber. The source used consisted of 2.0 μCi of ^{239}Pu. First various air densities, using the standard temperature and pressure corrections, were used to irradiate an Ortec surface barrier detector which provided input into a Model 8100 Canberra multichannel analyzer. The total number of alpha particles and peak energies were noted. Then the top made to hold polycarbonate foils was employed and, to insure similar geometry and irradiation conditions, ceramic rings were obtained from the Ortec Company identical to the rings employed in the construction of their surface barrier detectors. These were placed on the foil at the position formerly occupied by the surface barrier detector. After irradiation at the same air densities, the foils were etched under standard conditions (for four hours in 28% KOH utilizing an applied potential of 800 V at 2 KHz and 24^{o}C).

The results obtained from the study to determine the efficiency of alpha track production (number of tracks recorded) as a function of polycarbonate foil thickness are shown in Figure 17, where equivalent polycarbonate foil thickness was calculated from the various density thicknesses of air. Each point on the curve represents the average of more than one foil, usually two or three foils, and the error bars correspond to one sigma. No correction for attenuation in the small gold layer on the face of the surface barrier detector was employed in plotting Figure 17 since the surface barrier detector was not in place during the polycarbonate foil irradiations. The shape of the curve in Figure 17 is

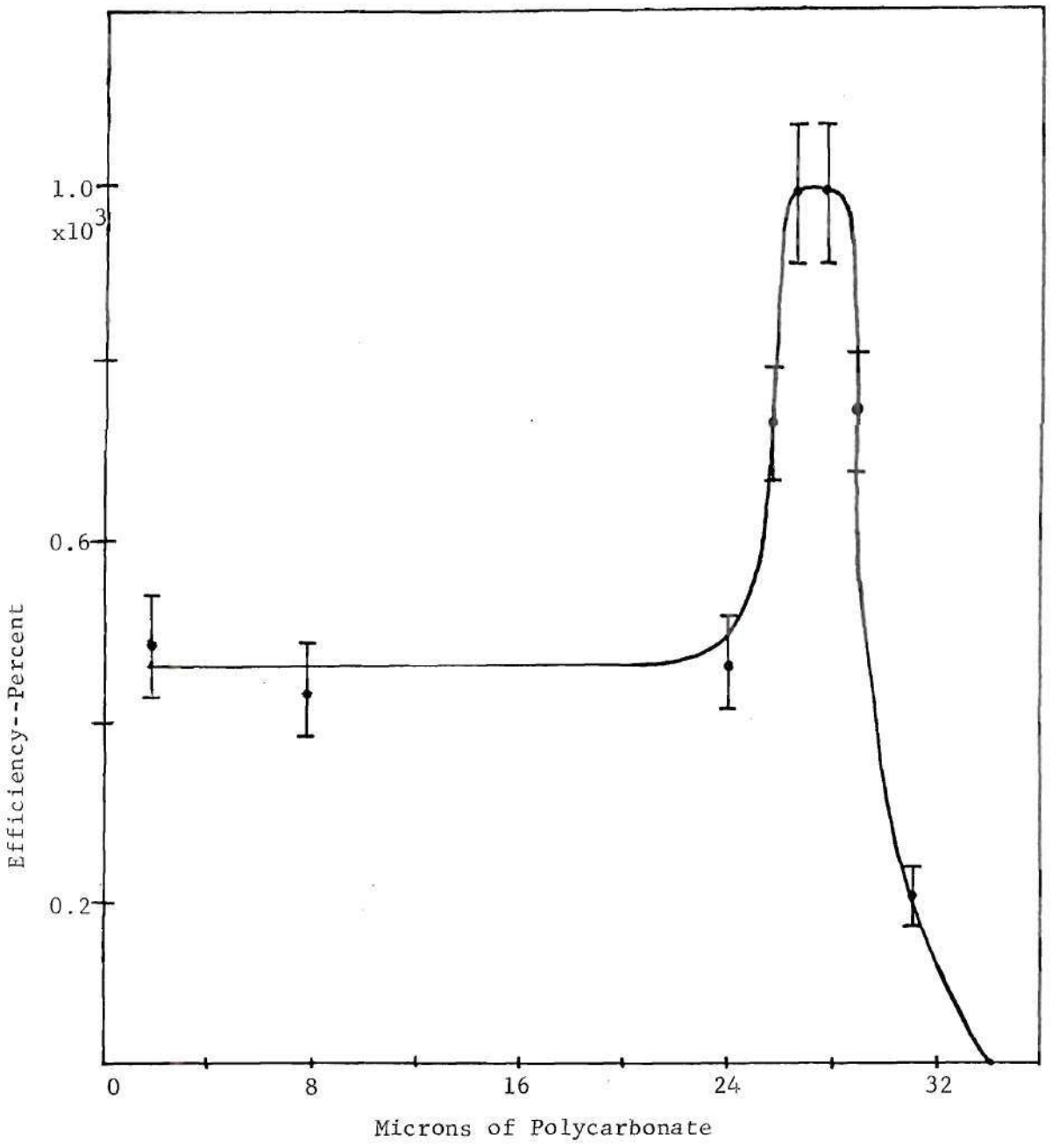

Figure 17. Efficiency of Track Production as a Function of Absorber Thickness. Polycarbonate Absorber Thickness was Calculated From g/cm^2 of Air. Count Rate was 1.6516×10^7/24 hours

quite clearly the familiar Bragg-type curve, peaking at 27.5 μm of polycarbonate. The peak of the curve was slightly more than twice the flat portion. Also, the peak fell off sharply down to zero at 34 μm of polycarbonate, corresponding to the range of the ^{239}Pu alpha particle in polycarbonate, and again toward the flat portion of the curve on the left side of the peak. The total number of counts used in the efficiency determination was 1.6516×10^7 counts. This value was the average of two separate 24 hour irradiations and was recorded on the Canberra multi-channel analyzer system described above.

5.2 Sensitivity as a Function of Etching Time

To perform the sensitivity as a function of etching time determination, we used the vacuum-sealed alpha-calibrator, Figure 16. The same source to detector distance used in all other determinations, 3.51 cm, was used here. The top of the vacuum-sealed alpha-calibrator (VSAC) that holds polycarbonate foils was utilized throughout this experiment. The experiment proceeded as follows. Transilwrap 250 μm thick polycarbonate foils were placed, one at a time, in the VSAC with the foil masking removed from the side of the foil facing our 2.0 μCi ^{239}Pu source. Then the ceramic rings obtained from the Ortec Company, mentioned above, were placed over the foil to insure identical geometry and irradiation conditions during the experiment. A series of foils were exposed to the plutonium source for 24 hours each at an air density selected to simulate a 27 μm thick polycarbonate absorber. Next the foils were etched in 45% KOH with an alternating potential of 800 V applied at 2 kHz for etching times between 2 hours and 4 hours. About six days elapsed between

irradiation and etching. The results appear on Figure 18. This plot of sensitivity (tracks/alpha particle) versus etching time indicates the decrease in sensitivity with decreasing etching time to fall off approximately exponentially. The error bars correspond to one sigma and the total number of alpha particles impinging on each foil was 1.6516×10^7, determined as above. The results of this experiment were used to conclude that a four hour etching time would be necessary during the bone dosimetry experiment since high sensitivity was a requirement for the low activities of ^{239}Pu encountered.

5.3 Sensitivity as a Function of Waiting Time

An experiment very similar to the one described in section 5.2 was designed to examine the sensitivity of our polycarbonate dosimetry system for alpha particle etchable track formation as a function of the time lapse from irradiation to electrochemical etching (waiting time). We used the vacuum-sealed alpha-calibrator once again with the top designed to hold our 250 μm thick polycarbonate foils. Exposure time to our 2.0 μCi ^{239}Pu source was 24 hours for each foil mounted 3.51 cm above the source. Air density was controlled to simulate a 27 μm thick polycarbonate absorber between the source and target foil to change the energy of the alpha particles. We selected 27 μm because we found a maximum in etchable track formation created by alpha particles at an alpha energy corresponding to the 27 μm thick absorber, section 5.1 and (Stillwagon and Morgan).[149] After each irradiation period of 24 hours, various waiting times were allowed to elapse before beginning the etching process. Our waiting times varied from 9 minutes to 15 days.

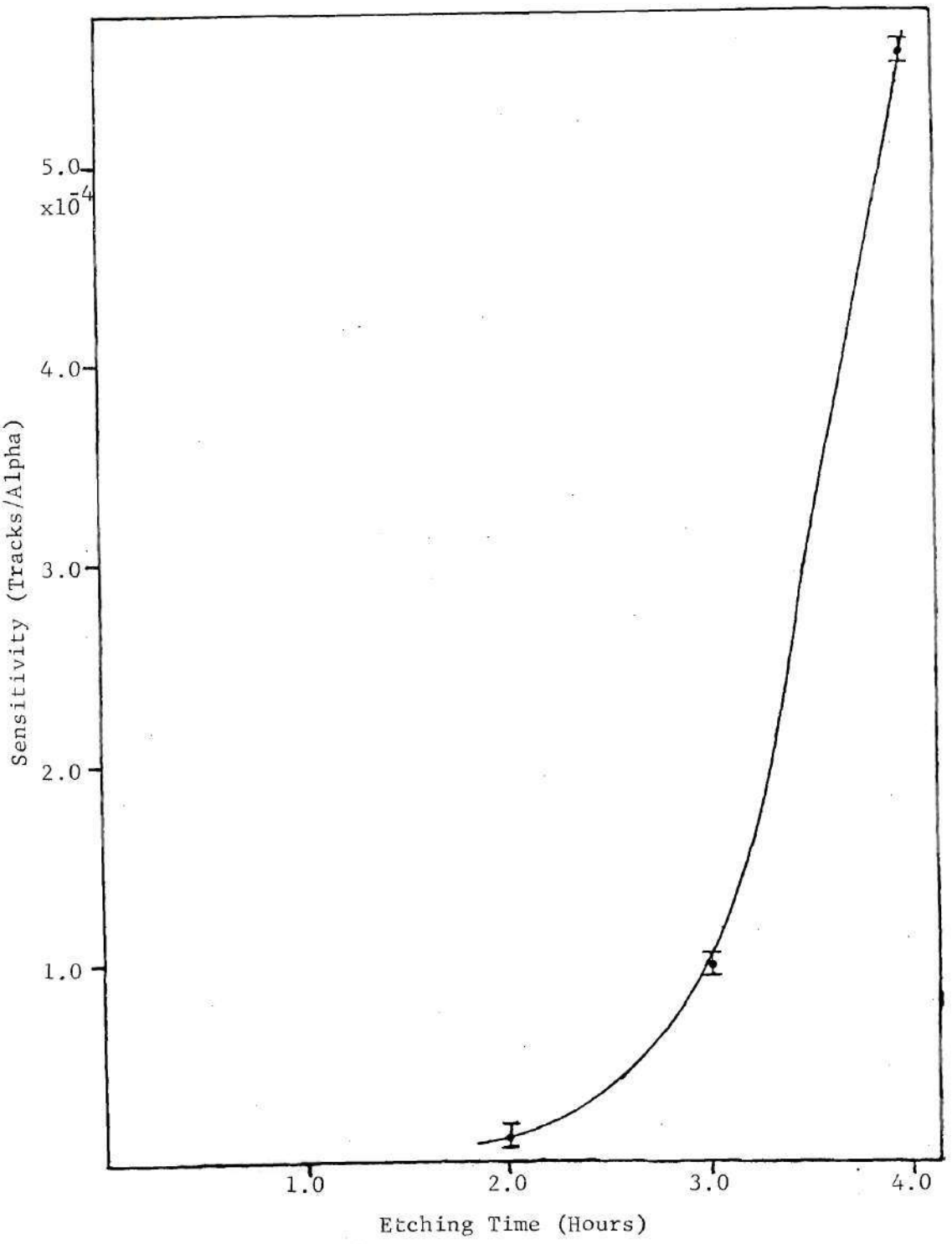

Figure 18. Graph Showing Sensitivity, Expressed as Tracks/Alpha, as a Function of Etching Time. Foils Were Etched in 45% KOH, at 800 V and 2 kHz for the Times Indicated

The foils remained in a closed lab desk drawer, masked side down, until removed prior to etching. The results are plotted on Figure 19. In each case 1.6516×10^7 alpha particles impinged upon the foil. Surprisingly enough this plot of sensitivity (tracks/alpha particle) versus waiting time showed a large increase in sensitivity as waiting time increased. One explanation of this result is as follows. When an alpha particle passes into the foil creating a track the volume around the track is left in a state of mechanical stress. This stress could then be relieved by the formation of tiny microcracks. The locations of these microcracks would be more susceptible to attack by the etchant because access to the inner part of the foil is now available to the etchant. If this explanation is true, then it follows that the longer one waits after irradiation of the foils before etching, the more microcracks will have formed as the stressed areas around the tracks relieve themselves. It could even be hypothesized that the great amplification realized by electrochemical etching is the result of an increase in microcrack formation caused by the 2 kHz oscillations employed in the electrochemical etching process. Another explanation of the mechanism of operation of electrochemical etching is the 2 kHz oscillations cause the positive and negative etchant ions to act as tiny "hammers" acting on the track to remove sections of polycarbonate material resulting in amplification of the original track.

5.4 Reproducibility

During the course of any experiment one must examine the reproducibility of his data. Normally, reproducibility evaluated external to any one experiment, especially data obtained on different days, tends to

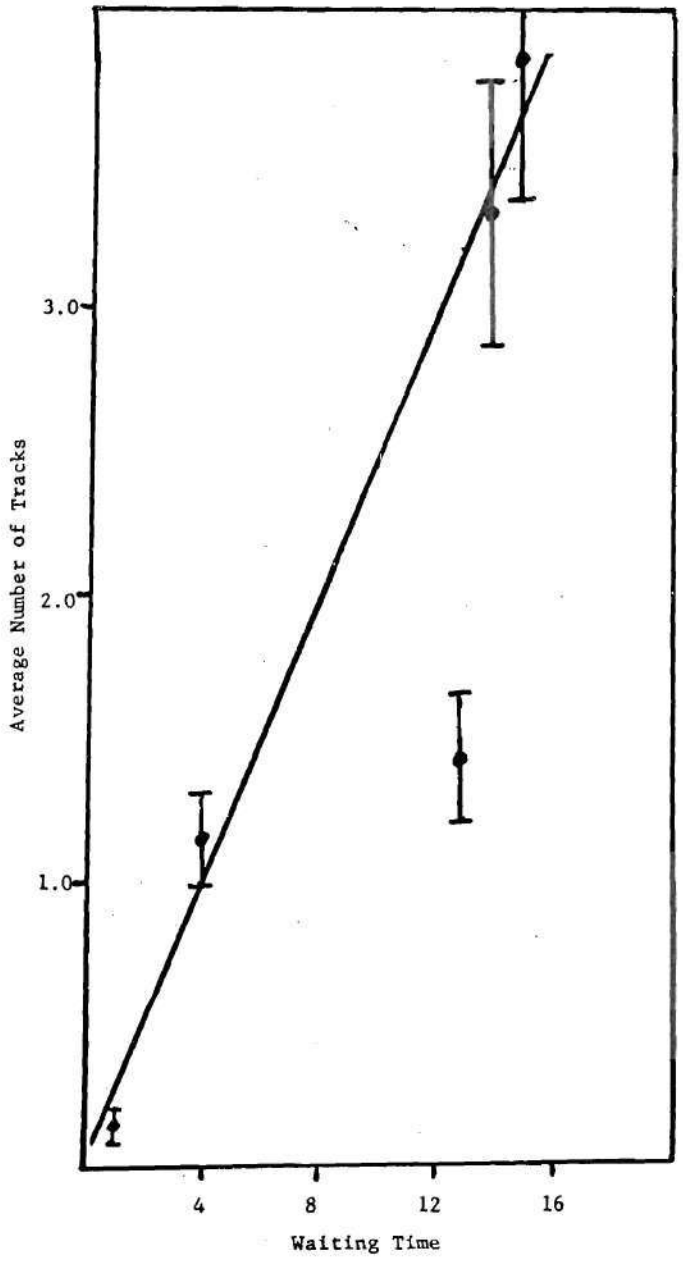

Figure 19. Sensitivity as a Function of Waiting Time Expressed as Average Number of Tracks Observed in a 120 μm Square. All Foils Were Irradiated by 1.65×10^7 ^{239}Pu Alpha Particles over 0.9 cm Diameter Circle. Error Bars Are ± 15%.

strengthen any conclusions drawn concerning reproducibility. Data examined from different experiments, obtained on different days, for the purpose of analysis of reproducibility tend to eliminate some of the biases that might be introduced during the performance of a particular experiment carried out on a particular day. These biases could include spurious electrical fluctuations of the line voltage, atmospheric variations and outside distractions affecting the experimenter, especially during tedious track counting.

To examine the reproducibility of this work, foils from two different experiments were selected, the sensitivity versus etching time and sensitivity versus waiting time experiments. These foils were irradiated and etched weeks apart, even within one experiment. Foils used for the reproducibility determination had been allowed to stand one week before etching. As previously mentioned, each foil was irradiated 24 hours in our vacuum-sealed alpha-calibrator by alpha particles traversing a 3.51 cm air gap (simulating 27 μm of polycarbonate) from our 2.0 μCi ^{239}Pu source. The absorber caused the alpha particles to lose enough energy before reaching the dosimeter to possess an LET at the maximum of the Bragg curve. Results of the reproducibility study are shown in Table 7. The collective average of the variation from the average for groups of comparable foils was 11 percent. Therefore 15 percent was selected as a conservative value to apply to the error in future measurements.

Table 7. Number of Counts Observed on Foils Used Throughout This Research

Foil	Absorber Thickness (μm)	Waiting Time (days)	$\bar{n}_o$	$\bar{n}_w$	Total Tracks
C15	27	1	0.01705	1.0	
C16	27	1	0.4091	1.756	
C18	27	1	0.04070	1.0	
C27	27	13	1.419	1.968	
C21	27	14	3.303	3.431	
C25	27	15	3.831	3.831	
Q1	28	--			174
Q2	28	--			157
V1	27	--			178
V2	27	--			170
U2	26	--			137
U1	26	--			106
T1	29	--			135
T2	29	--			115

NOTE: Several different absorber thicknesses and waiting times (time between irradiation and etching) are shown for these foils etched under standard conditions. The foils were etched over a nine month period.

5.5 Track Diameter Variation as a Function of Etching Time

To examine the track diameter as a function of etching time, the 250 μm thick polycarbonate foils were irradiated by one of three alpha particle sources, two 0.1 μCi ^{241}Am sources and one 0.2 μCi mixed nuclide source containing ^{239}Pu, ^{241}Am and ^{244}Cm. These foils were then etched for varying times between 15 minutes and 4 hours in 45% by weight

KOH using an applied voltage of 800 V at 2 kHz and 24°C, room temperature.

The results of the measurements of track diameter as a function of etching time are plotted in Figure 20, for times ranging from 15 minutes to 4 hours. Each point represents the average of the extremes in the measurements of track diameter performed using a Filar micrometer in place of our microscope eyepiece at a power of 430X. The error bars in this case are actually marking error ranges because they indicate the extreme values obtained for track diameter in each case. No tracks were observed for an etching time less than 30 minutes. The two curves reflect the presence of the two track sizes that were observed for the alpha particle irradiated foils. Figure 20 contains two curves for the following reason. After the polycarbonate foils were irradiated by alpha particles, etched by the standard technique and viewed, it appeared there were two distinct groups or categories of tracks on the foils (see also Figure 21). There were a few large tracks and many small tracks, but as shown in Figure 22, the number of large tracks decreased and the number of small tracks increased with increasing absorber thickness. To check if this phenomenon of the two categories of tracks was real, the diameters of the tracks on a foil were measured and the relative frequency of the various diameters plotted, Figure 23. Here the relative frequency, expressed in percent, of the track diameters appearing on the y-axis are plotted in steps of 0.5 μm in histogram fashion. One can plainly see two categories of tracks present on the foil represented graphically by the two large peaks of equal magnitude, one between 3.5 and 4.0 μm and the second between 10.0 and 10.5 μm. In general, no tracks were observed

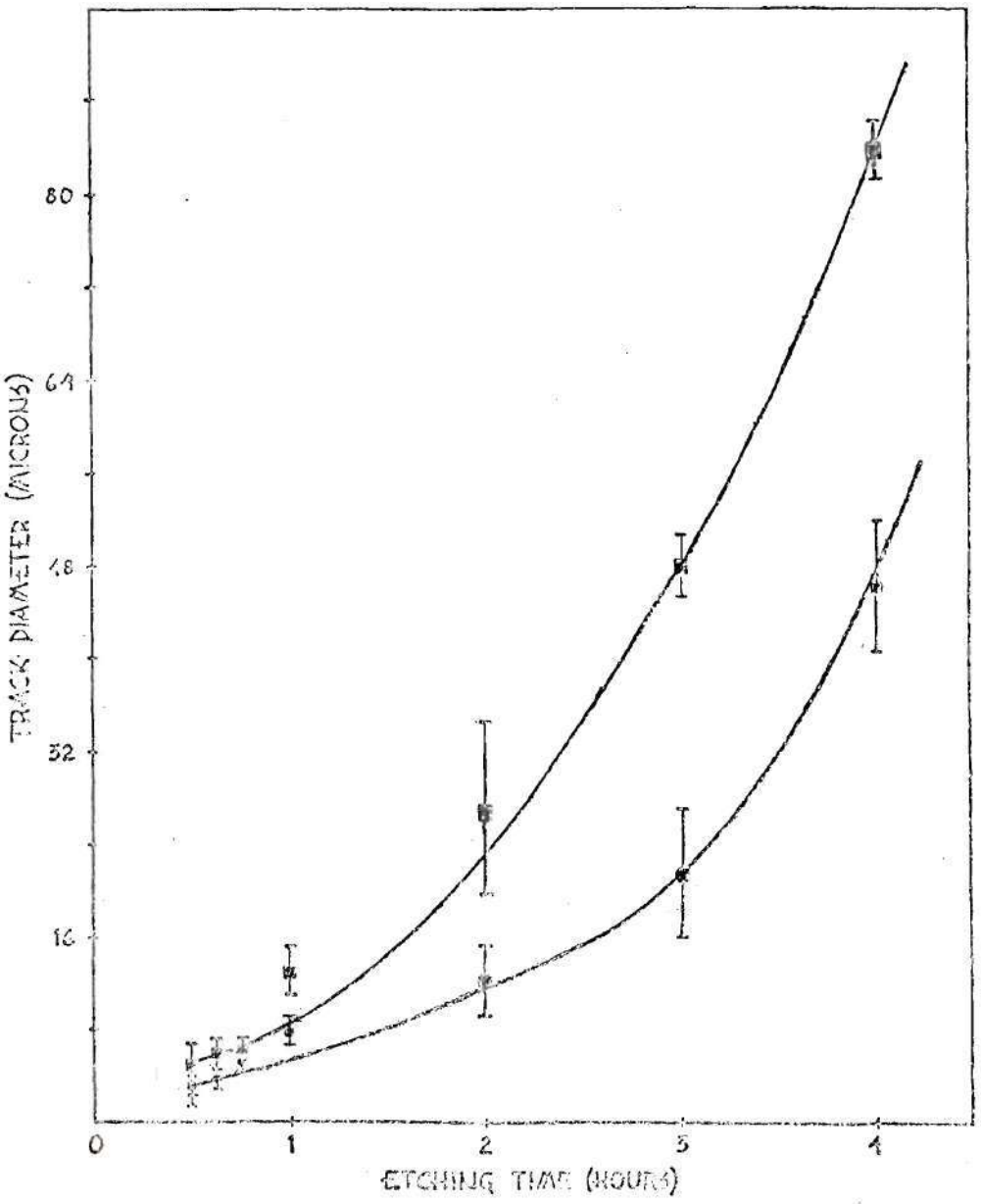

Figure 20. Variation of Track Diameter with Etching Time. Upper Curve Represents the Large Diameter Tracks, and the Lower Curve represents the Smaller Diameter Tracks

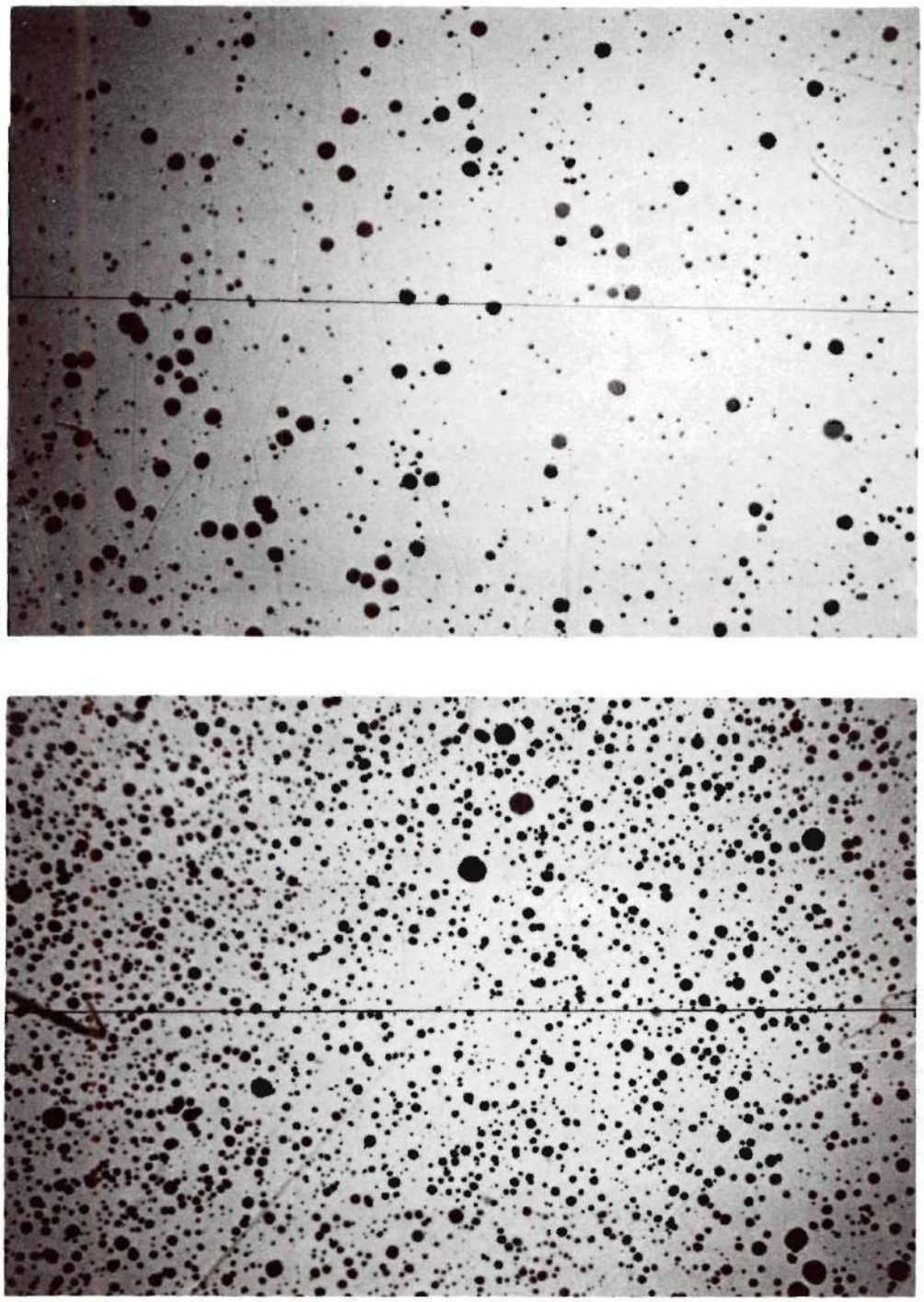

(a)

(b)

Figure 21. Tracks Created by the 5.44 MeV Alpha Particles of ^{241}Am at a Source to Dosimeter Distance of 2 mm in Air. Irradiation Time = 14 hours. A. Without Foil Masking. B. With Foil Masking. Etching Parameters--45% KOH, 800 Volts, 2 kHz and Etching Time 5 Hours

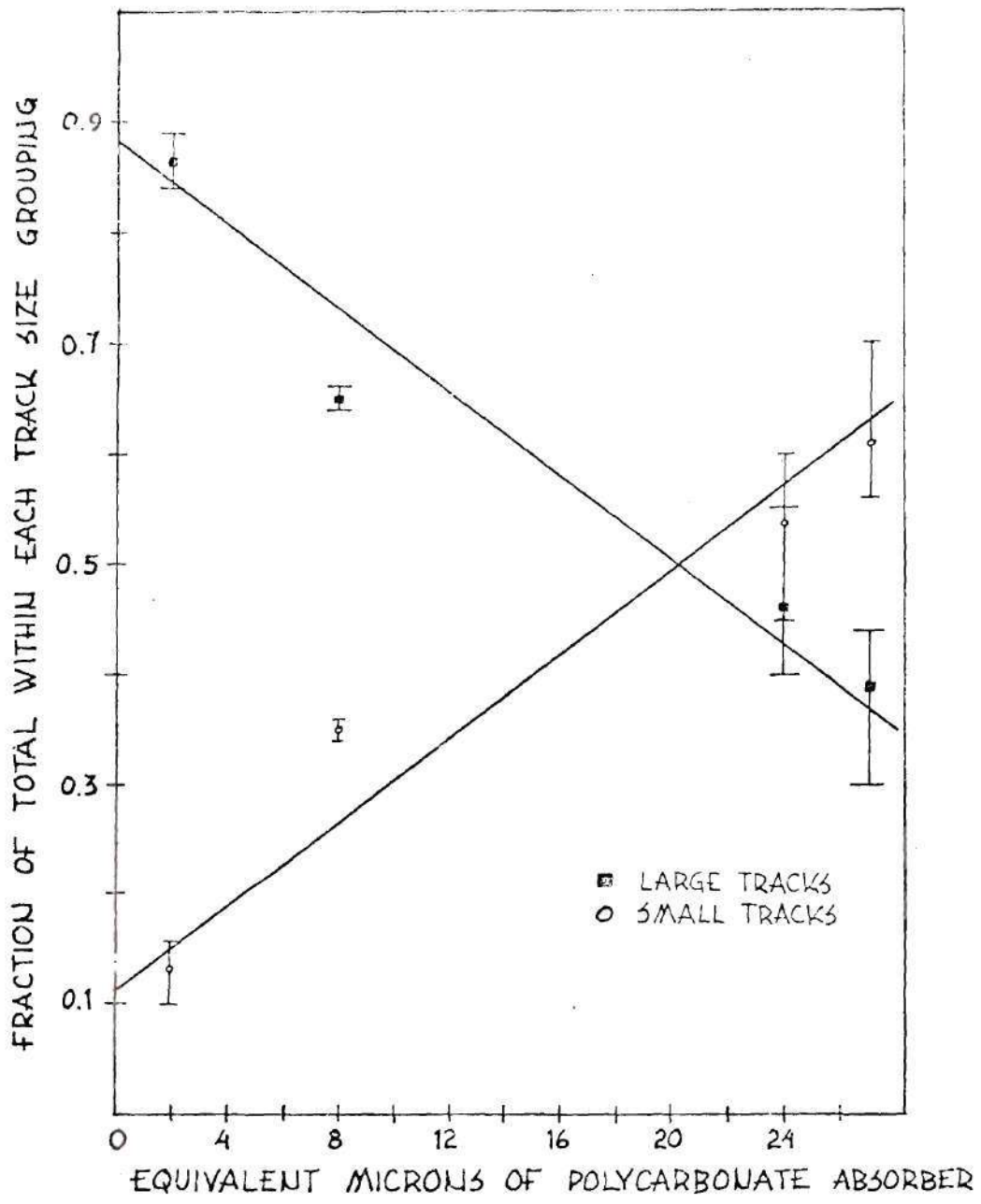

Figure 22. Change in the Fraction of the Total Number of Tracks on a Foil in Each Track Size Grouping as a Function of Alpha Particle Energy (Expressed as Microns of Absorber). Upper Curve is for Large Tracks and Lower Curve, Small Tracks

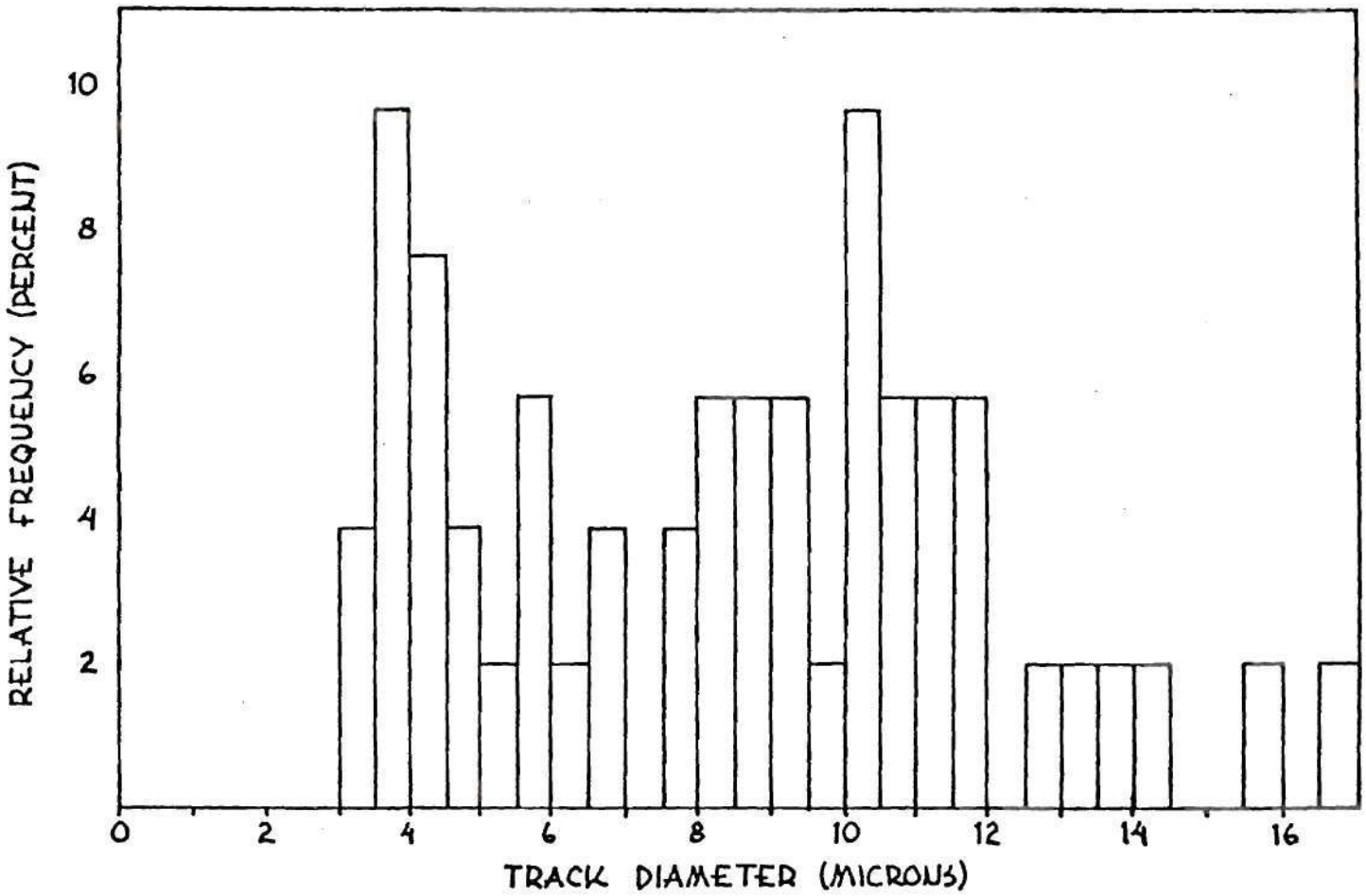

Figure 23. Relative Frequency of Track Diameters after Alpha Particle Exposure for a Foil Etched One Hour at 800 V, 2 kHz, 24°C in 45% KOH

smaller than 3.0 μm and none were observed greater than 115.5 μm throughout these measurements. Histograms similar to Figure 21 can be drawn also for each of the fouls used to generate Figure 20. These are presented in Figures 24 through 27 for absorber thicknesses 27 μm, 24 μm, 8 μm and 2 μm of polycarbonate respectively. By viewing Figure 24 for 27 μm and Figure 27 for 2 μm, the dramatic shift from the small to the large track diameters can be seen easily. The absorber varies alpha particle energy. Thicker absorber results in a smaller energy of the alpha particles incident on the dosimeter.

The data contained on these foils were used to generate Figure 22 in the following manner. According to Crawford[157] ". . .physical processes forming particulate distributions tend to produce a log-normal distribution." Distributions such as the Poisson distribution would not be expected to apply to the case here, namely single measurements of many different tracks, because the normal and Poisson distributions give the probability of a value n falling between n and n + dn. In other words one is removing samples from one pool of data. It would be expected, however, that many diameter measurements of <u>one</u> track would describe a Poisson distribution. The log-normal distribution is used to describe particle distributions where one has many different particles of varying diameters, each of which is measured once and then particle diameter measurements are fitted to the log-normal distribution. This is essentially the situation we have with our track diameter measurements. From this point the formulation of Crawford was used. A range of diameters, d, was selected equal to 10 μm. The number of tracks falling into each

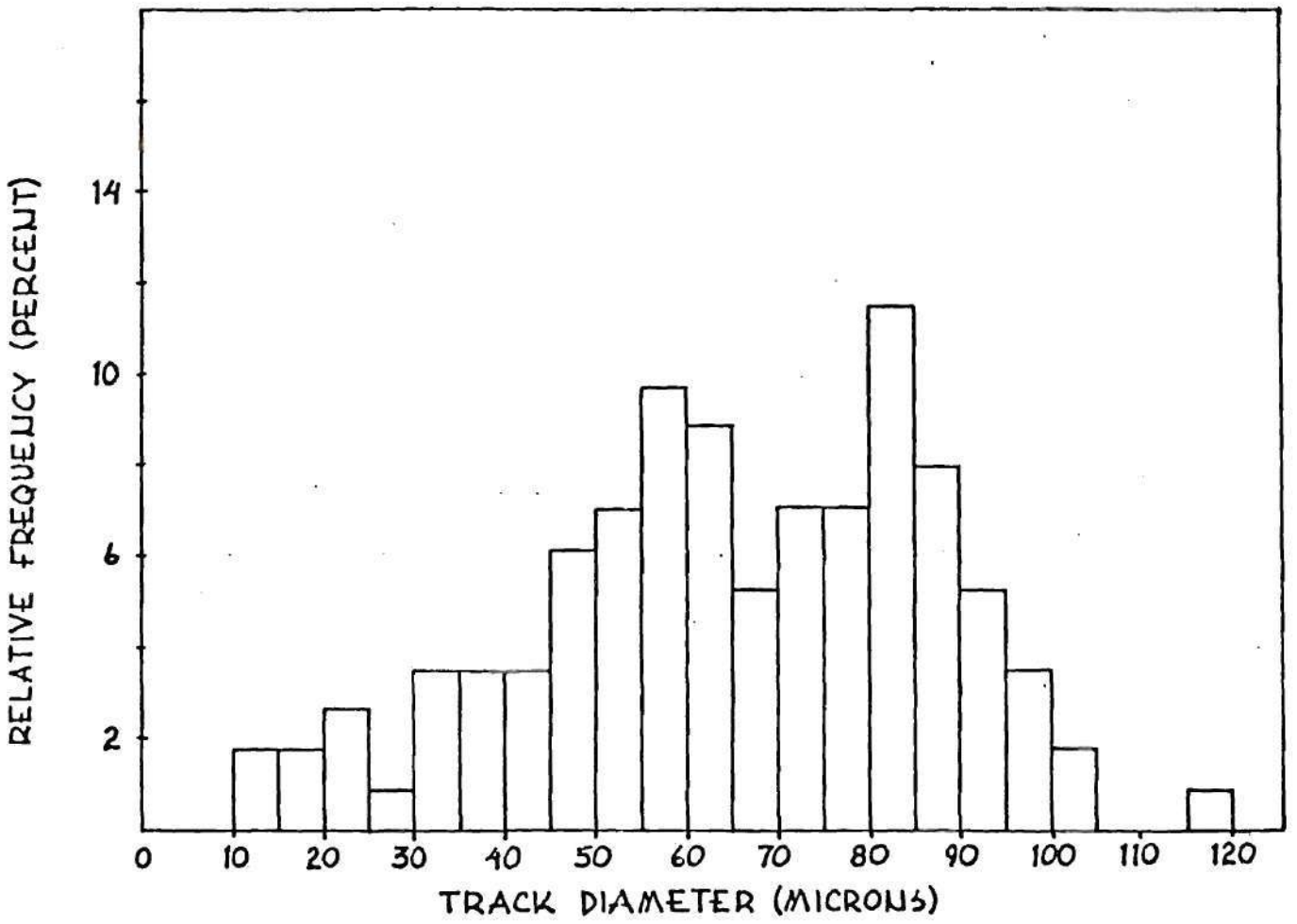

Figure 24. Relative Frequency of the Various Track Diameters for a Foil Using a 27 μm Absorber Between the Source and Foil. Ratio of Small Tracks to Large Tracks is 69:44. Etching Conditions Were 800 V, 2 kHz, 28% KOH, 24°C, and 4 Hours Etching Time

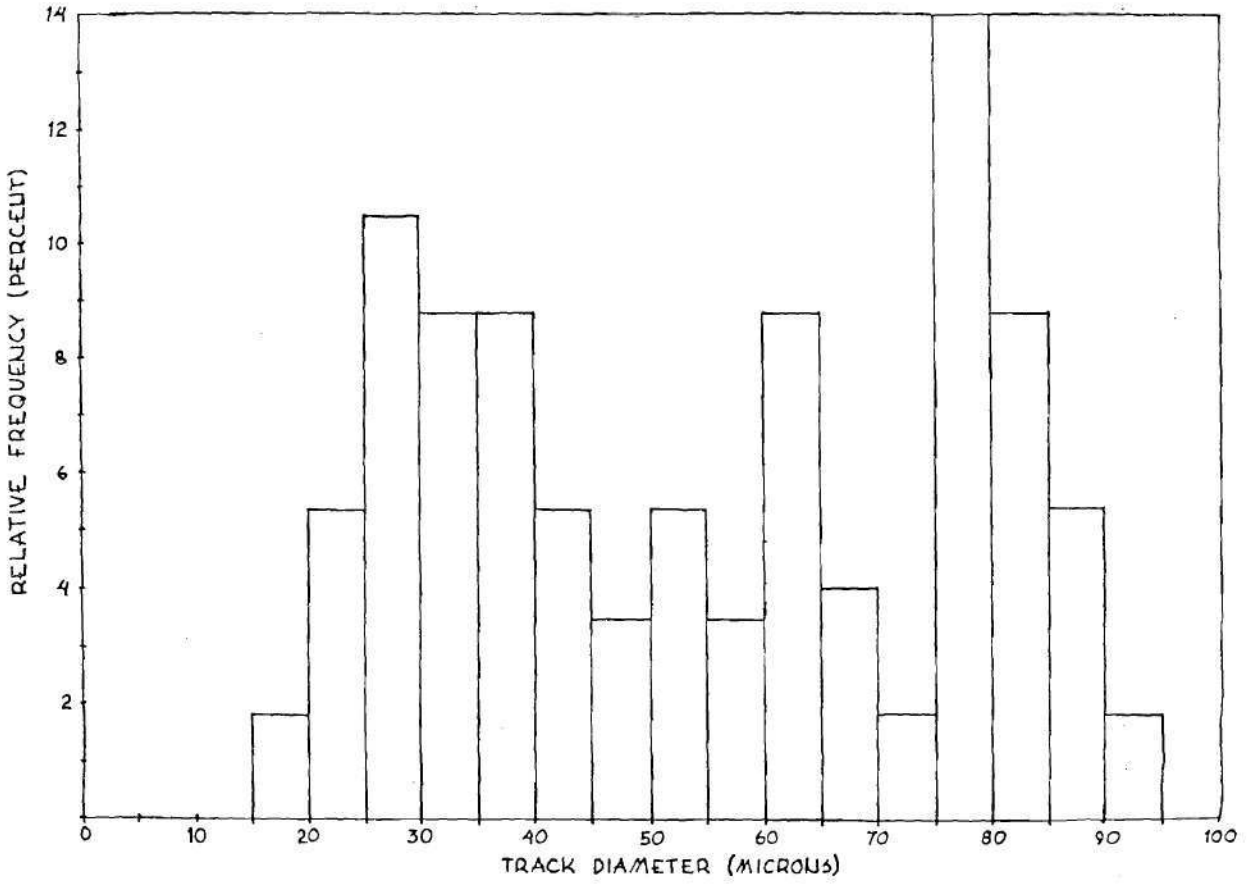

Figure 25. Relative Frequency of the Various Track Diameters for a Foil Using a 24 μm Absorber Thickness Between the Source and Foil. Ratio of Small Tracks to Large Tracks is 31:26. Etching Conditions Were 800 V, 2 kHz, 28% KOH, 24°C, and 4 Hours Etching Time

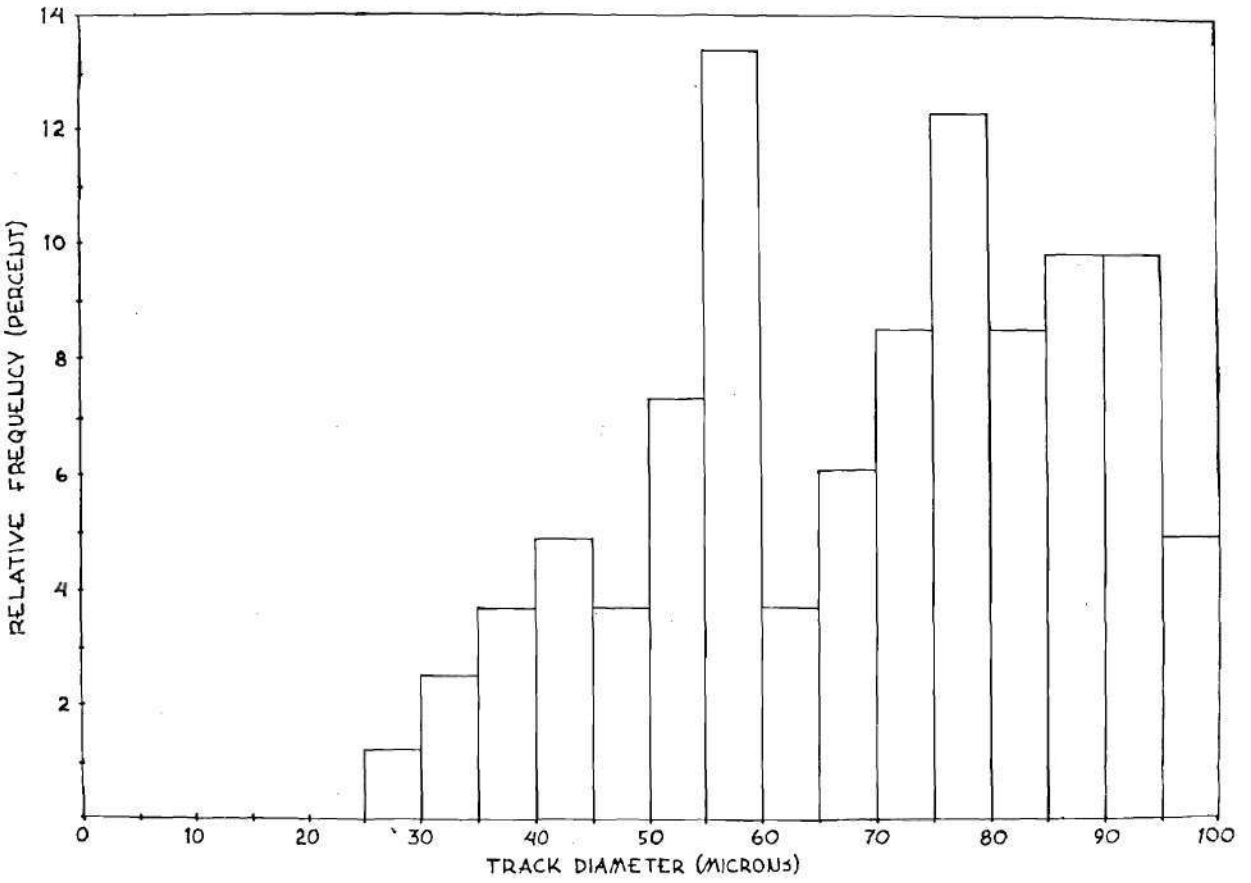

Figure 26. Relative Frequency of the Various Track Diameters for a Foil Using an 8 μm Absorber Between the Source and Foil. Ratio of Small Tracks to Large Tracks Is 29:53. Etching Conditions Were 800 V, 2 kHz, 28% KOH, 24°C, and 4 Hours Etching Time

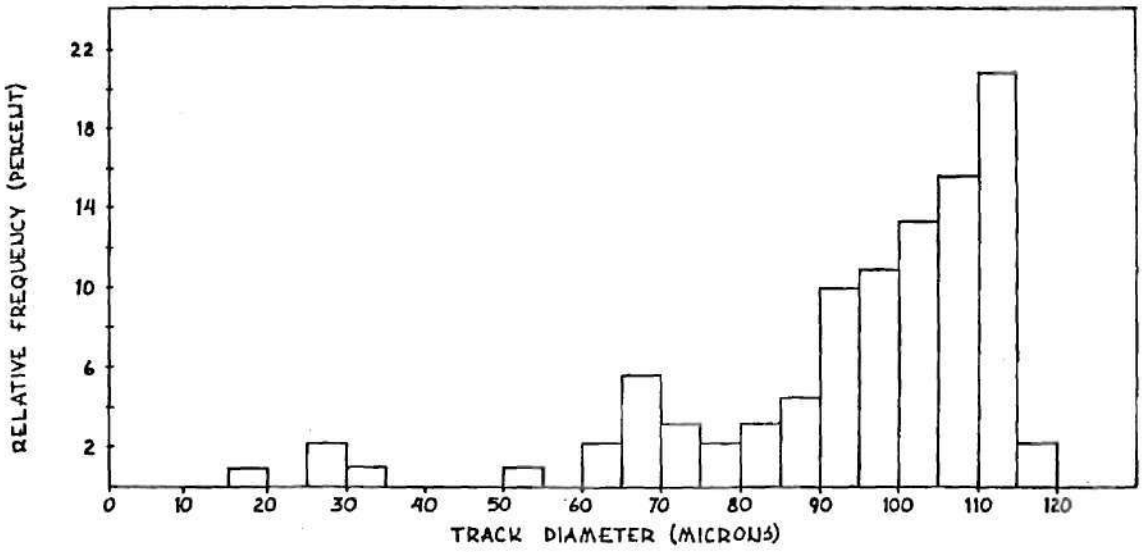

Figure 27. Relative Frequency of the Various Track Diameters for a Foil Using a 2 μm Absorber Between the Source and Foil. Ratio of Small Tracks to Large Tracks Is 12:78. Etching Conditions Were 800 V, 2 kHz, 28% KOH, 24°C, and 4 Hours Etching Time

range was determined as a fraction of the total number of tracks, $\Delta N_i/N$. Then each fraction was summed such that the last range of d gave a sum equal to 1.0. According to the method, if the values of each respective sum, $N(d_i)/N$ are plotted against the high end of the appropriate diameter range a straight line will result on probability-log paper if one log-normal distribution will describe the data. This provides not only a method of deciding how many tracks to assign to each track grouping, but it also allows a method to further prove the existence of two size groupings of tracks. These curves appear on Figure 28. Immediately apparent is the sharp break in the curve indicating the presence of two distributions. The point located at a track diameter of 20 μm seems to fall below the curve for the two transient cases, absorber thickness 8 μm and 24 μm. These fluctuations are not believed to be real, however, since the 20 μm point falls nicely on the curve for the extreme cases, 2 μm and 27 μm, that show the shift in track diameter best (*see histo*grams). Now, it is quite simple to determine the fraction of the total number of tracks in the small group of tracks. The line drawn through the lower end of the curve, corresponding to the small tracks, and extending until it crosses the largest tract diameter encountered will be indicating the contribution of this distribution as a fraction of the total, 100%. This is the fraction of tracks which fall into the small track log-normal distribution. It will be noted that this procedure is not unlike the procedure used to separate the contribution of counts from a mixture of two nuclides of differing halflives, one short and the other long. The log-probability curves were plotted six times for each

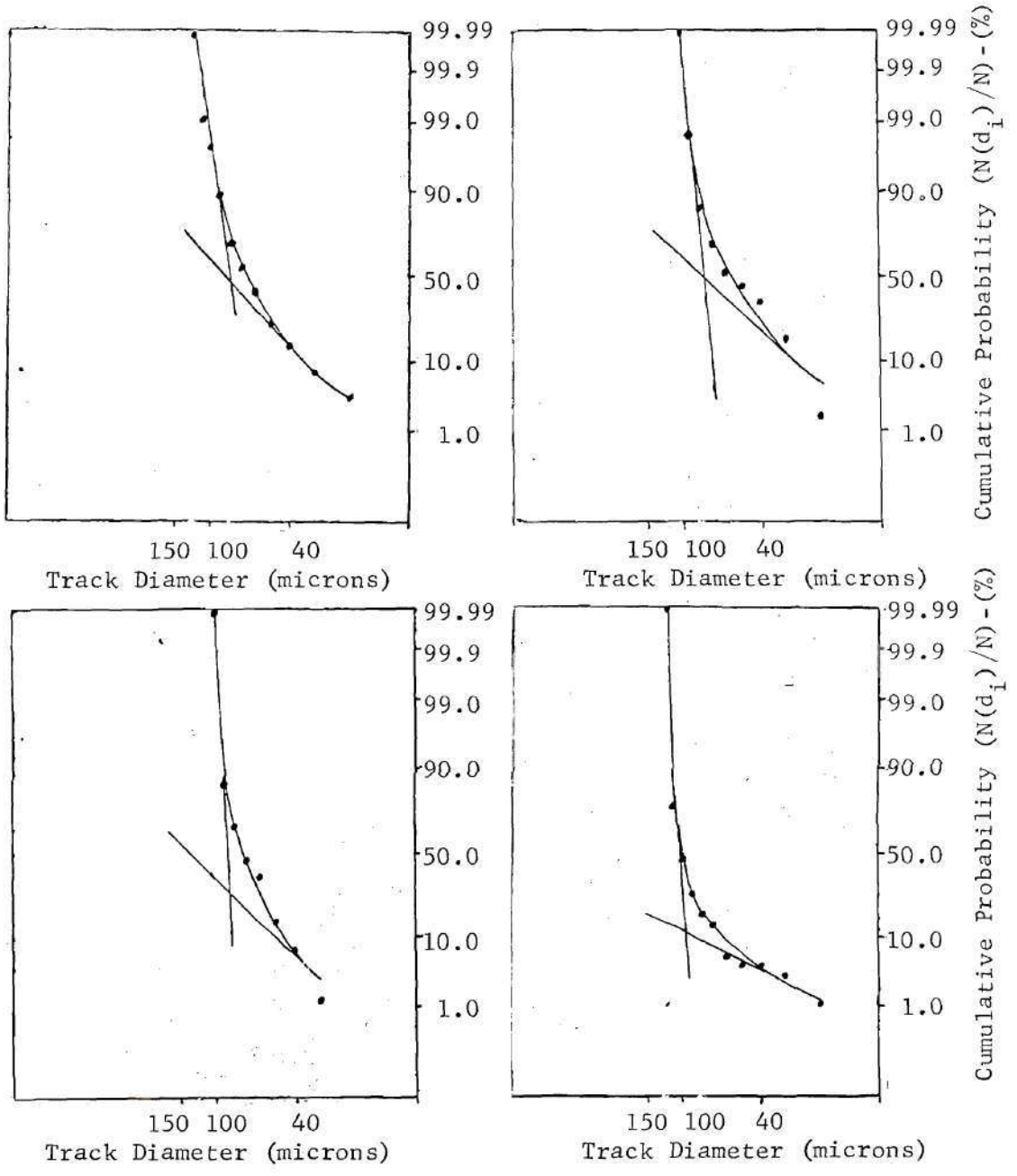

Figure 28. Plot of Cumulative Probability, $N(d_i)/N$ versus Track Diameter (Increasing to the Left) for Alpha Particle Irradiated Foils Electrochemically Etched Four Hours, at 800 V, 2 kHz, 28% KOH and 24°C. Probability Refers to the Occurrence of a Particular Track Diameter. Curve I Represents an Exposure with a 27 μm Absorber, Curve II a 24 μm Absorber, Curve III an 8 μm Absorber and Curve IV a 2 μm Absorber.

foil and the straight line representing the small track distribution plotted six times each, i.e. each one of the curves on Figure 28 represents one of the six curves used to obtain the values plotted on Figure 22. The average of these six values is plotted in Figure 22 and the maximum and minimum values are indicated by the error bars (or error ranges). Therefore when plotting Figure 20 one curve represents the large track diameter as a function of etching time and the lower curve the small track diameter as a function of etching time.

A reasonable explanation for the appearance of two categories of tracks on the polycarbonate foils after alpha particle irradiation is as follows. It is possible the smaller tracks could have been created by the alpha particles themselves and the larger tracks by the recoil of carbon and oxygen nuclei present in the polymer molecules composing polycarbonate. Of course, these latter interactions would not be of the elastic collision type found in fast neutron work due to the + 2 charge of the alpha particle. Instead, we could envision a Coulombic repulsion event during which the target nucleus does not remain stationary, like classical Rutherford scattering, but instead is "pushed" out of its lattice site by this repulsive force. This event would be possible especially for high energy alpha particles and large angles of alpha-particle deflection since more energy would be imparted to the recoil nucleus than in the opposite situation. This type of interaction was introduced by Rutherfore many years ago (Rutherford),[158] (Rutherford et al.).[159] Except for the work using protons and helium nuclei, much of this early work was concerned with heavier nuclei such as argon, gold

and copper in which this effect would be considerably reduced in importance due to the difference in mass between an alpha particle and, say, a gold nucleus. In polycarbonate and tissue the main target nuclei are carbon, oxygen and protons. Two pieces of experimental evidence suggest this explanation for the appearance of large tracks. First, the track diameters for the large group of tracks are approximately the same as we have observed for recoil particle tracks after fast neutron irradiation (Su and Morgan).[160] Second, the number of large tracks increased and the smaller tracks decreased with decreasing absorber thickness, Figure 22. The increase in large tracks would then be caused by the greater number of alpha particles possessing high energy. Thus, with less absorber more alpha particles have sufficient energy to "push" the polymer nuclei out of their lattice sites because as energy increases smaller and smaller angles of alpha particle deflection will give sufficient energy to the target nucleus to push it out of its lattice site, i.e. the larger the number of angles that can cause the event the higher the probability of the event. The decrease in smaller tracks would be caused by getting farther away from the Bragg peak where the highest LET was found for alpha particles. Energies near this Bragg peak may be the only region where alpha particles possess large enough -dE/dx to have a large probability of producing tracks of small diameter. With a larger absorber present many more alpha particles could be expected to be found within the high LET portion of the Bragg curve and fewer possessing high energy or low -dE/dx. A decrease in the large diameter tracks, but an increase in the number of small diameter tracks as the Bragg peak is approached

could be anticipated, with this explanation. The data of Rutherford also support this explanation of the increase in numbers of large tracks with decreasing absorber thickness. His curve for helium nuclei as targets clearly shows an increase in numbers of counts with increasing alpha particle energy, Figure 29. The increase as v_o is approached is caused by helium target nuclei recoiling into the ZnS screen along with scattered alpha particles and as Rutherford[159] indicates in the text accompanying the Figure, this effect increases with increasing alpha particle energy. Here the ratio v_o/v is the velocity of the alpha particle used in the study to the various velocities considered. The alpha sources used were "radium active deposit" which was ^{218}Po, ^{214}Pb and ^{214}Bi in equilibrium and "thorium active deposit" which was ^{228}Th. It is believed this effect could have ramifications in the field of internal dosimetry. To illustrate we could examine the energy expected to be possessed by these light recoiling nuclei. A vector diagram for the interaction is shown in Figure 30 where OA is the momentum vector for the incident alpha particle (mv_1), OB for the scattered alpha particle (mv_2), ϕ the angle of deflection and BA is the momentum vector for the recoiling nucleus (MV). By the law of cosines

$$(MV)^2 = (mv_1)^2 + (mv_2)^2 - 2(mv_1)(mv_2)\cos\phi$$

and by conservation of energy

$$MV^2 = mv_1^2 - mv_2^2.$$

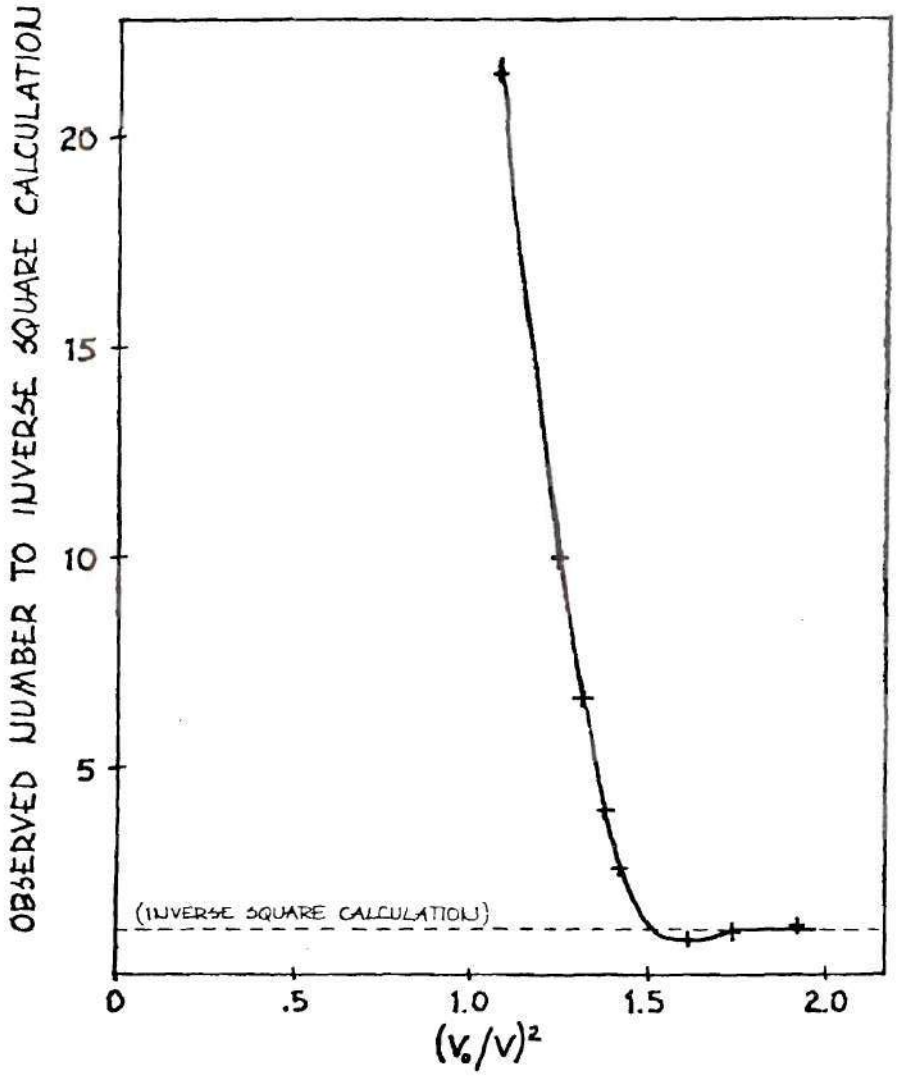

Figure 29. Graph Showing the Number of Counts Received on a ZnS Screen as a Function of Alpha Particle Velocity. Y-Axis is the Number of Counts Observed Divided by that Expected from an Inverse Square Calculation and the X-Axis is the Velocity Squared of the Alpha Particle Used Divided by the Square of the Alpha Particle Velocity Considered (Rutherford et al.)[159]

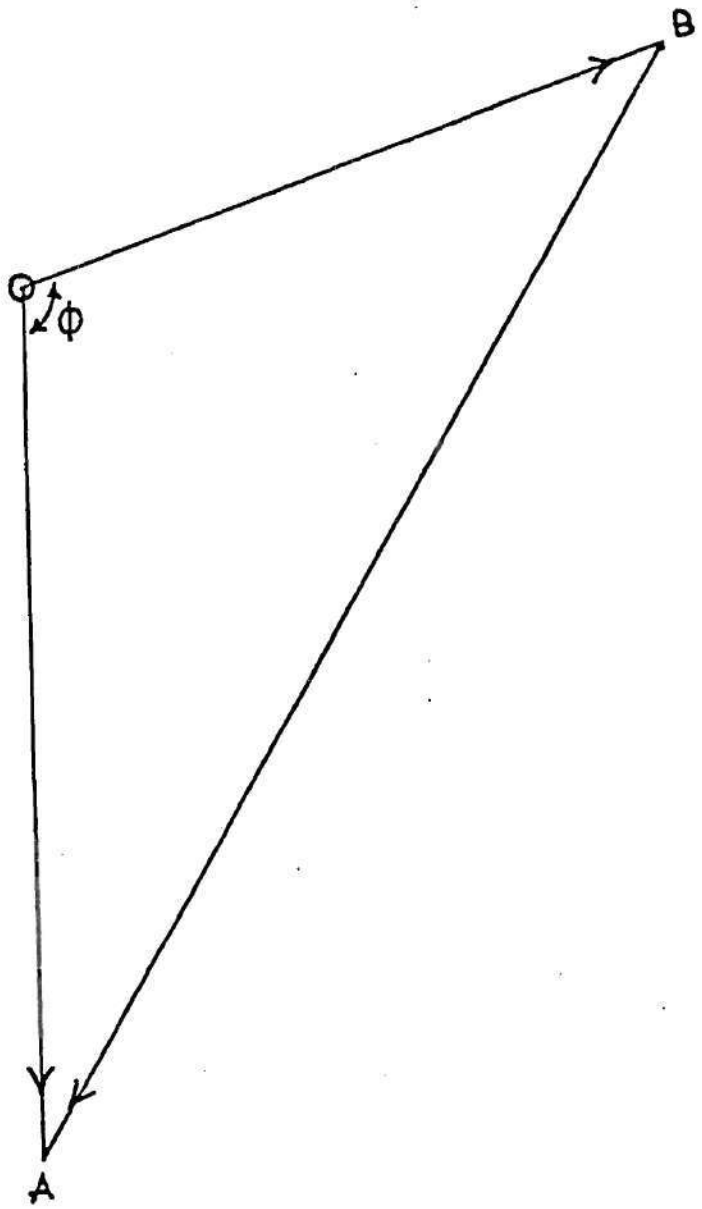

Figure 30. Vector Diagram Describing the Collision of an Alpha Particle and a Nucleus. The Momentum Vectors Are OA for the Incoming Alpha Particle, OB for Scattered Alpha Particle, and BA for the Recoil Nucleus

If we define $K = \frac{M}{m}$ and $v_2 = \rho v_1$ where $\rho < 1$ then from these two equations we quickly find

$$K - 1 = \rho^2(K + 1) - 2\rho\cos\phi$$

or

$$\rho = \frac{\cos\phi}{K+1} + \frac{1}{K+1}\sqrt{K^2 - \sin^2\phi}$$

If we now assume an initial alpha particle energy of 5.1 MeV, approximately equal to a ^{239}Pu alpha particle, we can calculate the energy expected to be given to the recoil nucleus. These values appear in Table 8 for various angles, ϕ. ΔE_2 is the scattered alpha particle energy and ΔE is given to the recoiling nucleus. For gold at 90^o $\Delta E = 0.21$ MeV and aluminum $\Delta E = 1.33$ MeV so we can see how much more important this type of scattering becomes for light nuclei (i.e., C and O) in these studies than was the case for heavy nucleii studied by Rutherford. For a head-on collision with a carbon nucleus almost 4 MeV is imparted to this nucleus. The implications in internal dosimetry are now becoming clearer. Instead of this 4 MeV being imparted to tissue by an alpha particle as we would assume in calculations of dose equivalent, this 4 MeV has been converted to a more efficient energy imparting means, i.e. a carbon nucleus. This could cause more severe damage to cells, especially in the close vicinity of the alpha emitter, than we would expect when considering only alpha particle energy deposition. Also, we have a direct mechanism now present to cause chromosome breakage. With this interaction, atoms simply could be removed or knocked out of a DNA chain, causing irreparable damage to

Table 8. The Energy of the Recoil Nucleus, ΔE, the Scattered Alpha Particle Energy, E_2, and the Ratio of Final to Initial Alpha Particle Velocity, ρ, Are Shown for Various Angles of Deflection of the Scattered Alpha Particle. $E_1 = 5.1$ MeV (initial alpha energy), $v_1 = 1.567 \times 10^9$ cm/sec and $m_\alpha = 6.647 \times 10^{-24}$ g

K	30°			60°			90°			150°			180°		
	ρ	E_2(MeV)	ΔE(MeV)	ρ	E_2	ΔE	ρ	E_2	ΔE	ρ	E_2	ΔE	ρ	E_2	ΔE
Carbon 3	0.956	4.66	0.44	0.843	3.63	1.48	0.707	2.55	2.55	0.523	1.40	3.71	0.500	1.28	3.83
Oxygen 4	0.967	4.77	0.33	0.881	3.96	1.44	0.775	3.06	2.04	0.621	1.97	3.13	0.600	1.84	3.26

this chain and possibly other chains due to the higher LET of the removed carbon or oxygen nucleus. The interaction indicated here would be occurring in addition to those effects described by Katz.[161] This is a direct mechanism for permanent change in a cell nucleus that should be considered during discussion of carcinogenicity and other cellular effects. One interesting side note is the possibility that the effect described above may never have been observed if the foils had not been composed of light nuclei as in tissue. This effect could actually be occurring in tissue as well as polycarbonate since the main components of tissue are nuclei whose mass is not greatly different from the alpha particle. Therefore large energy transfer can result from the alpha particle to the target nucleus in tissue as we observed in polycarbonate. Photographic emulsions, on the other hand, are not tissue equivalent. As Table 9 indicates, almost 17% of the atomic composition of NTA emulsion are the heavy nuclei silver and bromide. In polycarbonate foils we are observing the actual track created by the incident particle, amplified many times but in the emulsion we are only observing silver ions reduced by the passage of the ionizing particle close by. Discovery of the two track size effect on polycarbonate foils was made by measuring track diameters easily distinguishable with a light microscope. The corresponding effect on the emulsion would appear as a narrow track of reduced silver ions up to the point of collision, then a wide track of reduced silver ions would be present corresponding to the recoil nucleus for a 180^{o} collision. Of course no tracks would be seen from recoils of silver or bromide since they are too heavy to receive enough energy from the

Table 9. Elemental Composition of Kodak NTA Film

Element (g/mole)	Average Concentration (g/ml)	Atoms/ml	Atom % in 1 ml
Ag (107.870)	1.285	7.174×10^{21}	8.41
Br (79.909)	0.954	7.189×10^{21}	8.42
C (12.011)	0.354	1.775×10^{22}	20.8
H (1.00797)	0.063	3.764×10^{22}	44.1
O (15.9994)	0.307	1.156×10^{22}	13.5
N (14.007)	0.094	4.041×10^{21}	4.73
I	---*	---	---

*---indicates trace amount

alpha particle to move far enough to produce a recognizable track on the photographic emulsion (Rutherford et al.).[158,159] Due to the inherent difficulties in reading particle tracks (angular dependence causes some tracks to be unrecognizable if the angle of incidence is close to normal, high magnification required to read emulsions and background or artifacts, etc.) and non-tissue equivalence the two track sizes would not be expected to be observable in large enough numbers to reproduce the histograms describing this effect found in this section. The observance of effects such as these is one argument in favor of using a tissue equivalent material whenever possible to detect the interactions of radiation with tissue. If this suggestion is not followed, important interactions may be overlooked simply because the dosimeter selected does not interact with the radiation in the same manner as tissue. We can not pretend to know before hand when tissue equivalence is not necessary. If this interaction is occurring in tissue to the degree indicated by the data presented here, the recoil reaction may be more important than first seemed to be the case even though researchers such as Haque[163] state -dE/dx is the only quantity which is of prime importance for the purpose of alpha particle dosimetry.

CHAPTER VI

BONE DOSIMETRY

6.1 Description of Bones Utilized in These Studies

The bones used during the course of this research were removed from beagle dogs injected with known quantities of ^{239}Pu(IV) citrate and human bone samples of interest to attempt to obtain human data directly. The dog bone samples were generously given to us by Dr. W. S. S. Jee at the University of Utah and the human bone samples were donated through the courtesy of Dr. B. D. Breitenstein associated with the U.S. Transuranium Registry, Richland, Wash. The method of preparing the bone samples was as follows.

The beagle dog bones had been extracted by the Radiobiology Laboratory during autopsy of dogs injected at Level 5 (2.9 μCi/kg) and Level 3 (0.3 μCi/kg). As mentioned above, ^{239}Pu(IV) citrate solutions were used throughout all injections. The plutonium injected was part of four shipments received by the Radiobiology Laboratory. The first two batches came from the same source and had the following isotopic percent composition by weight (Jee)[164]:

^{239}Pu	99.696%
^{240}Pu	0.320%
^{241}Pu	0.00112%
^{241}Am	0.00046%
^{235}U	$\leq 1.55 \times 10^{-8}$ when Pu = 1

The values for the minor constituents are given as upper limits. The results of this study of the beagle dog bones are valid only for ^{239}Pu since all the other alpha emitters are present only in trace amounts. The third and fourth batches had an isotopic composition of ^{239}Pu of 99.89% ^{239}Pu but alpha-spectroscopy failed to indicate any other alpha emitters present in the sample. Therefore these results are applicable only for ^{239}Pu deposition in bone since other nuclides are present in such small amounts.

After injection of the plutonium citrate solution into the animal it is desirable to determine the skeletal burden of plutonium. The Utah workers have determined that the skeletal burden can be obtained from the following two equations (Stover et al.)[13]:

Level 5

$$B = 6.9 \exp(-0.0011\ T) + 42.8 \qquad (6.1)$$

Level 3

$$B = 15.2 \exp(-0.0011\ T) + 34.4 \qquad (6.2)$$

Here B is the percent of the injected dose retained uniformly in the skeleton after a post-injection time, T, in days. Table 10 lists the dogs used during the bone dosimetry portion of this work along with pertinent data such as post-injection time (time between injection and sacrifice of the animal), skeletal burden at death and type of bone obtained. The batches refer to the plutonium batches described above. Because severe cellular necrosis was noted at long post-injection times after injection at Level 5, only the shortest post-injection times were selected among the available samples (the longest selected was 92 days post-

Table 10. List of the Bones Used During This Research From Beagle Dogs Obtained from the University of Utah. Batch Refers to the Batch of Plutonium Used (Composition Described in Text). Terminal Body Burdens Were Determined Using the Equations of Stover.[13]

Dog	Type of Bone	Batch	Post Injection Time (days)	Terminal Skeletal Burden (μCi)
T10P5	Distal Femur	1 & 2	10	16.18
T50P3	Sternum	3 & 4	1175	0.606
T47P5	Lumbar Vertebra	3 & 4	69	18.43
T44P5	Lumbar Vertebra	3 & 4	35	16.14
T42P5	Lumbar Vertebra	3 & 4	13	13.57
T16P5	Lumbar Vertebra	1 & 2	92	14.96
T56P5.5	Distal Femur	3 & 4	7	20.74

injection) to avoid these problems and thus avoid ambiguities in interpreting the experimental results.

The bones were placed in acetone or 70% alcohol to serve as a mild fixative after extraction from the dogs. Then the bones were embedded in Bioplastic to provide a hard surface for cutting the delicate trabecular bone surfaces. A vacuum was created and released several times as the Bioplastic hardened to remove as much air as possible from the undecalcified bones. This process was the end result of many trials by the Utah group to find a process to retain living tissue conditions as closely as possible for the finished bone section. In biological experiments it is always necessary to make some statement as to the degree the completed section compares with the original living material. The best bone-dosimetry technique conceivable could not provide useful data unless the bone sample was able to represent closely the original living bone. The procedure described here allows fixing of the bone with no detectable loss of plutonium, no movement of macrophages or other cells along the osseous surfaces but can result in a 30% shrinkage of some cells. Therefore it is felt that this technique can represent the living bone quite well since the plutonium, cells and osseous structures remain in place at the cost of some cell shrinkage (Jee).[164]

Each bone, now sealed in Bioplastic, is ready to be sawed on the bone saw. This saw features a water-cooled blade that also serves to control the release of plutonium laden sawdust. Sections of bone 300 μm thick were removed until the bone was sectioned through the cortical bone layers. Each swath of the saw blade resulted in the cutting loss of about 400 μm of bone material in addition to the section removed. Therefore the

distance between the front portion of each bone section was 700 μm.

The human bones were removed from Case #01AT-0555. This man received some exposure to plutonium during his employment at Hanford but the level was below the level detectable by whole-body detectors and urine analyses. We used a rib during our dosimetry studies. The preparation procedure was as follows. The rib was first placed in the fixative formalin for 24 hours. Next the sample was placed in HNO_3 for acid decalcification. The HNO_3 solution was prepared by placing 200 ml of a 70 weight percent solution of HNO_3 solution in 2600 ml of water. The bone was checked every eight hours until it was soft. Then the sample was washed in water and neutralized with a drop of NH_3. Finally the rib was returned to the formalin until needed for sectioning. Sections were removed as follows. The bone was placed in a paraffin cassette containing bees wax and mounted on a microtome. Sections of 8 μm were removed until the endosteal face of the bone was exposed. The entire remaining bone (infinitely thick to alpha particles) was used during the dosimetry application described below. It was learned later that acid decalcification will cause the plutonium present in the bone to shift around but not be lost from the bone. Therefore, the original amount of plutonium should still be present but somewhat displaced from its original location. For this reason we were not able to use the human bone samples as extensively as first hoped. The final bone preparation procedure involved sawing the whole bone longitudinally through the center of the marrow cavity with a small hack saw. The halves were sanded down to expose the endosteal surface with fine-grain emery paper.

6.2 Osseous Microdosimetry

6.2.1 The Bone Dosimetry Technique

The technique we designed to determine the dose rate to the layer of tissue 10 μm thick on the endosteal surfaces of bone containing various amounts of ^{239}Pu was as follows. First the bone samples were allowed to expose our 250 μm thick polycarbonate foils for various times under various conditions. Some bones were exposed to polycarbonate foils with a 27 μm thick polycarbonate absorber between the foil and bone sample. This technique caused the incident alpha particles to have maximum probability of creating a track, see Figure 17, and maximum spatial resolution; however, sensitivity is lost due to the large number of alpha particles attenuated before reaching the polycarbonate dosimeter. The majority of foils was exposed by placing a large number of bone sections side-by-side on the bare face of a polycarbonate sheet, placing a second sheet on top of the bone sections (sandwiching them) and finally laying the setup between two pieces of wood and compressing the arrangement with C-clamps. Given the malleability of polycarbonate, the flat surface created by our bone preparation procedure and the great amount of pressure C-clamps can provide, it is difficult to imagine the air gap could be greater than a micron and was probably less.

The polycarbonate dosimetry foils were exposed to the trabecular bone surfaces for various times. We elected to observe only the trabecular bone surfaces (also called the endosteum of bone) since the radiosensitive osteogenic cells are located here as well as the highest concentration of plutonium (Jee et al.).[3] Other nuclides, such as ^{241}Am do not concentrate as much on the trabecular surfaces as plutonium (Polig).[165]

After removal from the exposure apparatus, the polycarbonate foils were electrochemically etched by our usual procedure. Etching time was four hours to minimize the large decrease in dosimeter sensitivity as etching time decreases, Figure 18. Next the foils were mounted on microscope slides for viewing on our microscope. Figure 31 shows results obtained by this technique for foils exposed 30 and 64 days and electrochemically etched.

We were interested in observing small fields during microscopic counting of the foils to approach a true average dose for alpha particle irradiation (Rossi).[166] A Whipple disk was utilized to aid in the counting. A 120 μm square at 430X was used throughout the foil counting procedure. Many randomly selected fields were counted for each foil, usually about 250 separate fields. The same counting procedure was used to count the calibration sources described below. From the data thus generated, two averages were calculated one including "zero" counts and the other not including these "zero" counts. Reasons for this will be presented below. Efficiency of detection of alpha particles from these infinitely thick bone samples would be expected to differ considerably from the efficienty for irradiation by monoenergetic alpha particles determined in Chapter V; for this reason the infinitely thick calibration foils were used to derive the efficiency factors.

Upon completion of foil counting we have the number of alpha particles incident upon the average 120 μm square. In order to determine dose rate to the 10 μm thick layer of tissue along the endosteal surface, the average energy absorbed in this layer, the mass of tissue involved and the exposure time will be required. These values were found as follows.

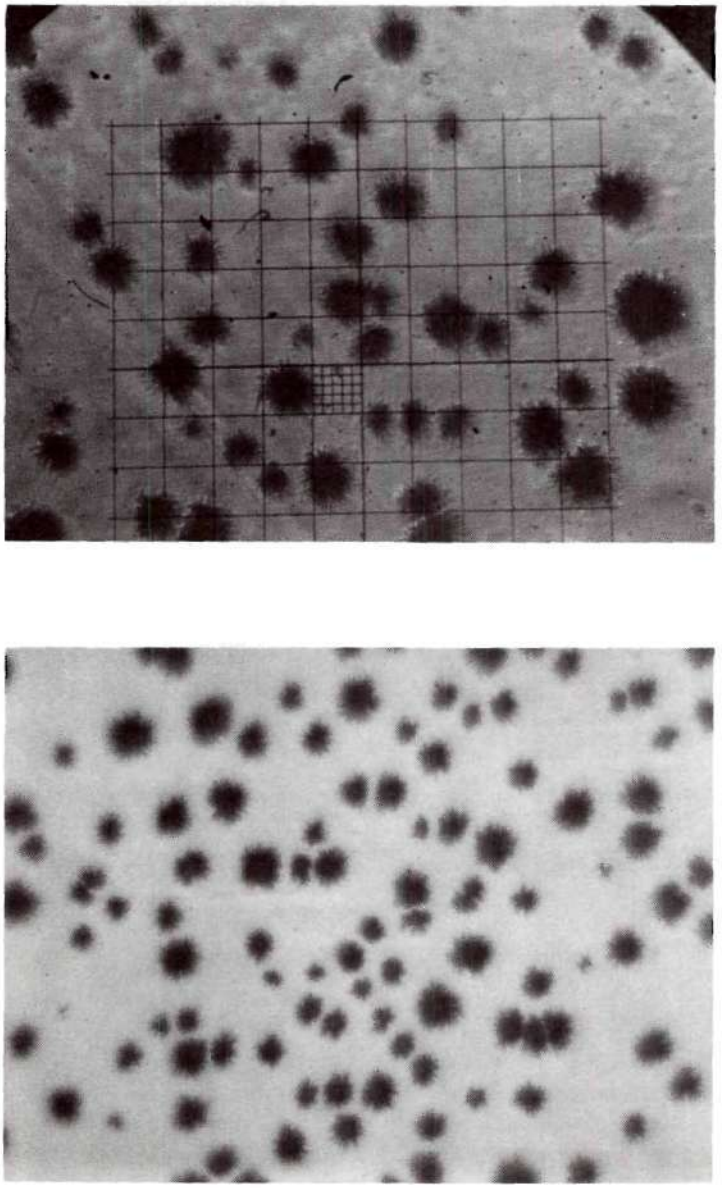

(a)

(b)

Figure 31. A. Dog T44P5 Section #3A, Exposed 30 Days and Shows one View of Tracks Obtained with Whipple Disk in Place, 430X. B. Dog T42P5 Section #1, Exposed 64 Days, 400X. Both Foils Were Electrochemically Etched by Our Standard Technique.

Since we wished to keep this dosimetry technique entirely experimental in nature, the experimental alpha absorption measurements of Harley and Pasternack[111,167-170] were selected to supply the energy absorbed. They determined the average energy transmitted through successive layers of polycarbonate absorbers. Then the energy channel number of a multi-channel analyzer was weighted by the number of counts and the average of the resulting distribution calculated. It is felt this is a better estimate of transmitted energy than merely selecting the peak of the spectrum, especially for dosimetry purposes. In Figure 32 (Harley)[170] we can see the curve is nearly linear over much of the range of absorber thicknesses. Linearity of this curve means that, if a ^{239}Pu alpha is emitted toward the 10 μm thick layer of tissue along the endosteal surface from depths in bone ranging from 0 to about 20 μm, approximately the same amount of energy will always be deposited in this 10 μm thick layer. Again, this refers to the average energy lost by the ^{239}Pu alpha particle in traversing the 10 μm layer only and gives no information as to the total energy lost by alpha particles emitted from various depths in bone. For this 10 μm thick layer we graphically determined the average energy absorbed to be 1.39 MeV. For a 20 μm thick layer the average energy absorbed would be 3.09 MeV. These values were obtained by reading several measurements directly from Figure 32 and calculating the numerical average. The value for the average energy absorbed per alpha particle multiplied by the average number of alpha particles incident upon the 120 μm square yields the average energy absorbed in the 10 μm (or 20 μm) thick layer of endosteal tissue. It will be noted, a 10 μm absorber was never used, the dosimeter was placed flush against the bone samples and gave the number of alphas

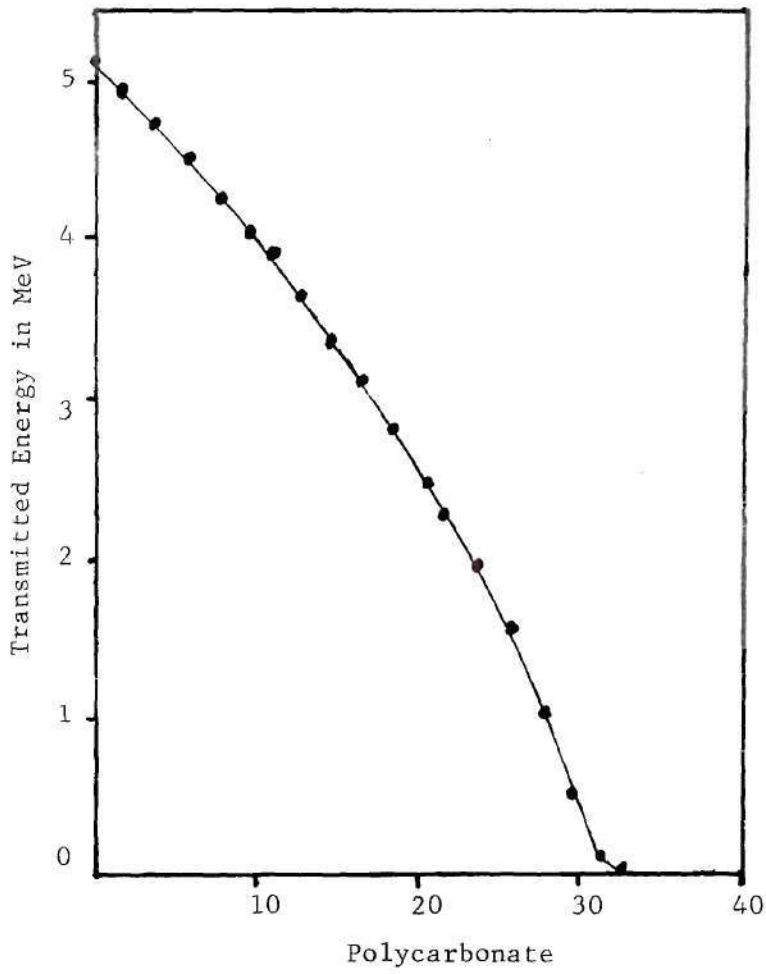

Figure 32. Curve Showing the Average Energy Transmitted by ^{239}Pu Alpha Particles Versus Absorber Thickness Expressed as Microns of Polycarbonate (Harley)[171]

traversing the 10 μm thick layer. Harley and Pasternack's data converted this value to absorbed energy, thereby avoiding a correction factor that would have been required to correct for alpha particles totally stopped in a 10 μm absorber placed between the bone and dosimeter and consequently not recorded.

Since exposure time is known, the mass of tissue considered is the only requirement still needed to obtain dose rate in rads per year. For a 10 μm thick layer of tissue on the endosteal surface outlined by the 120 μm square view port, see Figure 33, the mass $m = (120 \times 120 \times 10)\ \mu m \times 1.0\ (g/cm^3) \times 1\ cm^3/1 \times 10^{12}\ \mu m^3 = 1.44 \times 10^{-7}$ g, where the density of the 10 μm thick soft tissue layer is taken to be 1.0 g/cm^3 (Spiers),[82,103] (James and Kember).[7] Similarly, for a 20 μm thick layer, $m = 2.88 \times 10^{-7}$ g.

Using all of these values above, the equation for the dose rate in rads/year could be written

$$DR = \frac{NE}{\epsilon m T} C \qquad (6.3)$$

where

N = average number of tracks observed in the 120 μm square

E = the average energy deposited by the ^{239}Pu alpha particle in traversing the soft tissue layer, for 10 μm thick layers, E = 1.39 MeV and 20 μm thick layers, E = 3.09 MeV

ε = efficiency of track registration, tracks/α (see next section)

m = mass of the small tissue layer, for 10 μm thick layers, $m = 1.44 \times 10^{-7}$ g, and 20 μm thick layers, $m = 2.88 \times 10^{-7}$ g

T = exposure time in days

C = constant = $\frac{1.6 \times 10^{-6}}{100} \times 365.25$

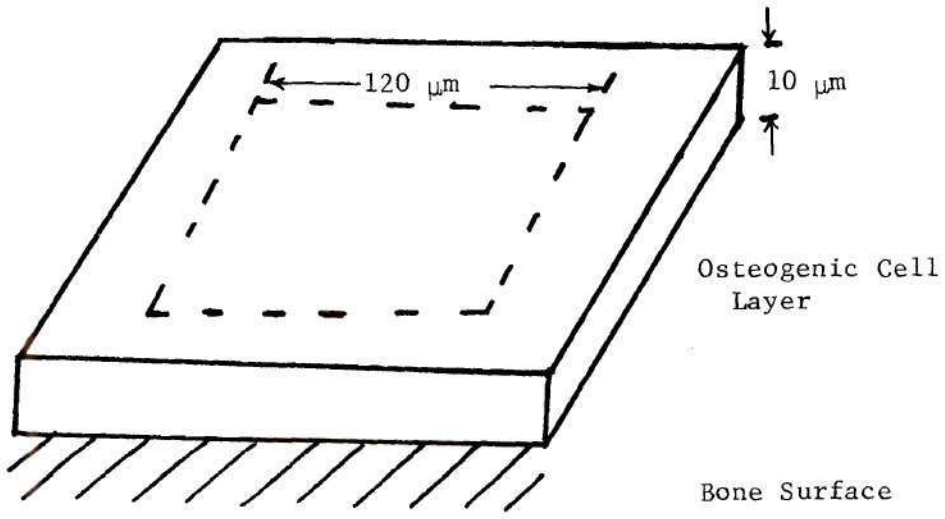

Figure 33. Sketch Showing the 120 x 120 x 10 μm Volume of Interest in the Endosteal Tissue Dose Rate Determination

The results of the bone dosimetry study are shown on Table 11. Columns 7 and 8 give the dose rate in rads per year including all the random scans where no tracks were observed in the 120 μm square, D_o, and Columns 9 and 10 give the dose rate excluding these zero track scans, D_w. The table indicates the highest dose rate observed relative to the skeletal burden of ^{239}Pu causing this dose rate was D_w = 317900 rads/yr for dog T47P5 and the lowest was D_o = 16.7 rads/yr for dog T56P5.5. The wide spread in dose rates recorded indicates the inhomogeneous distribution of plutonium known to exist on bone surfaces. Therefore the wide variation in dose rate noted as one proceeds down the column of increasing bone section numbers for one dog bone may not be unrealistic. The method of obtaining the efficiencies will be shown in the next section. The dose rates were calculated from eqn. (6.3) where the experimental measurements were the N values in the equation. There is some possibility the efficiency is too high for bone T56P5.5 yielding a low dose. This is suspected since the efficiency differs so much from all of the others. The procedure of presenting the dose including and not including zero scans offers an interesting possibility, the ability to calculate dose only to the volumes of tissue actually receiving alpha particle irradiation. In the past, dose was averaged over the entire skeleton, endosteal surface or endosteal surface with range of an alpha particle (Twente and Jee),[6] (Rowland and Marshall).[2] As is known, if the track of an alpha particle does not pass through a region of the foil scanned, there is no absorbed dose received by trabecular tissue <u>in vivo</u> at that point.

Therefore inclusion of the unirradiated region in an average dose

Table 11. Bone Dosimetry Results Indicating Dose in Rads per Year

Bone	Bone Section Number	Exposure Time (days)	Waiting Time (days)	Efficiency (tracks/α)	Skeletal Burden (μCi)	D_O (rads/yr)		D_W (rads/yr)		Experimental $MPOB_O$		Experimental $MPOB_W$	
						10 μm	20 μm	10 μm	20 μm	10 μm	20 μm	10 μm	20 μm
T42P5	1	64	0	2.22×10^{-5}	13.57	39580 ± 5937	44000 ± 6599	193800 ± 29080	215300 ± 32330	1.0×10^{-3}	9.2×10^{-4}	2.1×10^{-4}	1.9×10^{-4}
	2					1169 ± 175	1210 ± 195	45420 ± 6814	50480 ± 75730	3.5×10^{-2}	3.1×10^{-2}	8.9×10^{-4}	8.6×10^{-4}
	3					14330 ± 2150	15930 ± 2390	174800 ± 26230	194300 ± 29150	2.8×10^{-3}	2.5×10^{-3}	2.3×10^{-4}	2.1×10^{-4}
	4					523 ± 78	582 ± 87	39740 ± 5962	44170 ± 6627	7.8×10^{-2}	7.0×10^{-2}	1.0×10^{-3}	9.2×10^{-4}
	8					8168 ± 1225	9078 ± 1362	129200 ± 19380	143600 ± 21540	5.8×10^{-3}	4.8×10^{-3}	3.1×10^{-4}	2.7×10^{-4}
	9					15050 ± 2259	16730 ± 2511	192800 ± 28920	214300 ± 32140	3.1×10^{-4}	2.4×10^{-3}	2.1×10^{-4}	1.9×10^{-4}
	10					10680 ± 1602	11870 ± 1781	98680 ± 14810	109700 ± 16460	3.8×10^{-3}	3.4×10^{-3}	4.0×10^{-4}	3.6×10^{-4}
	11					14250 ± 2137	15840 ± 2376	130200 ± 19530	144700 ± 21710	2.8×10^{-3}	2.6×10^{-3}	3.1×10^{-4}	2.7×10^{-4}
	12					3806 ± 570	42230 ± 634	44710 ± 6707	49700 ± 7455	3.4×10^{-2}	3.0×10^{-2}	9.1×10^{-4}	8.1×10^{-4}
	13					1204 ± 181	1338 ± 201	53000 ± 7948	58910 ± 8835	3.3×10^{-2}	3.0×10^{-2}	7.7×10^{-4}	6.9×10^{-4}
T16P5	8	64	1	2.22×10^{-5}	14.96	1104 ± 167	1226 ± 186	39740 ± 5962	44170 ± 6627	4.1×10^{-2}	3.7×10^{-2}	1.0×10^{-3}	1.0×10^{-3}
	10					8136 ± 1220	9043 ± 1357	108800 ± 16320	120900 ± 18140	5.5×10^{-3}	5.0×10^{-3}	4.1×10^{-4}	3.6×10^{-4}
T56P5.5	1	34	0	3.77×10^{-3}	20.74	50 ± 7.6	55.9 ± 8.4	849 ± 128	944 ± 143	1.2	1.1	7.3×10^{-2}	6.6×10^{-2}
	2					151 ± 22.7	168.6 ± 25.2	1479 ± 222	1644 ± 247	4.1×10^{-1}	3.7×10^{-1}	4.2×10^{-2}	3.8×10^{-2}
	3					16.7 ± 2.5	18.6 ± 2.7	440 ± 66	490 ± 73	3.7	3.3	1.4×10^{-1}	1.3×10^{-1}
	4					28.2 ± 4.2	31.3 ± 4.7	680 ± 102	755 ± 113	2.2	2.0	9.2×10^{-2}	8.2×10^{-2}
	5					136 ± 20.5	151 ± 22.7	1579 ± 237	1755 ± 263	4.5×10^{-1}	4.1×10^{-1}	4.0×10^{-2}	3.5×10^{-2}
	8					44.8 ± 6.7	49.7 ± 7.4	484 ± 725	538 ± 81	1.2	1.3	1.3×10^{-1}	1.1×10^{-1}
	9					91.5 ± 13.8	102 ± 15.3	1011 ± 151	1123 ± 167	6.8×10^{-1}	6.1×10^{-1}	6.2×10^{-2}	5.5×10^{-2}
	10					56.5 ± 8.4	62.8 ± 9.4	565 ± 84	629 ± 94	1.1	.99	1.1×10^{-1}	9.9×10^{-2}

Table 11. Concluded

Bone	Bone Section Number	Exposure Time (days)	Waiting Time (days)	Efficiency (tracks/α)	Skeletal Burden (μCi)	D_o (rads/yr)		D_w (rads/yr)		Experimental			
						10 μm	20 μm	10 μm	20 μm	$MPOB_o$ (μCi)		$MPOB_w$ (μCi)	
										10 μm	20 μm	10 μm	10 μm
T10P5	2	64	6	2.76×10^{-3}	16.18	104 ± 15.6	115.7 ± 17.4	795 ± 119	884 ± 124	4.7×10^{-1}	4.2×10^{-1}	6.1×10^{-2}	5.5×10^{-2}
T50P3	-	200	0	1.00×10^{-5}	0.606	7274 ± 1090	8085 ± 1212	37430 ± 5614	41600 ± 6240	2.5×10^{-4}	2.3×10^{-4}	4.9×10^{-5}	4.4×10^{-5}
T47P5	2	64	1	2.22×10^{-5}	18.43	16470 ± 2468	18300 ± 2743	12980 ± 19840	144300 ± 22047	3.4×10^{-3}	3.0×10^{-3}	4.3×10^{-4}	3.8×10^{-4}
	3					2448 ± 367	2721 ± 408	84460 ± 12670	93970 ± 14090	2.6×10^{-2}	2.0×10^{-2}	6.5×10^{-4}	5.9×10^{-4}
	6					3416 ± 512	37970 ± 569	218600 ± 32790	243000 ± 36440	1.6×10^{-2}	1.5×10^{-2}	2.5×10^{-4}	2.3×10^{-4}
	7					2445 ± 367	2718 ± 408	317900 ± 47690	353400 ± 53010	2.3×10^{-2}	2.0×10^{-2}	1.7×10^{-4}	1.6×10^{-4}
	13					17210 ± 2582	19130 ± 2869	150200 ± 22570	166900 ± 25090	3.2×10^{-3}	2.9×10^{-3}	3.7×10^{-4}	3.3×10^{-4}
	14					3312 ± 496	3682 ± 552	145700 ± 21860	161900 ± 24300	1.7×10^{-2}	2.3×10^{-2}	3.8×10^{-4}	3.4×10^{-4}
T44P5	1A	30	0	7.75×10^{-4}	16.14	2358 ± 354	2621 ± 394	6189 ± 929	6879 ± 1033	2.1×10^{-2}	1.8×10^{-2}	7.8×10^{-3}	7.0×10^{-3}
	2A					2554 ± 384	2840 ± 426	4984 ± 748	5540 ± 832	1.9×10^{-2}	1.7×10^{-2}	9.7×10^{-3}	8.7×10^{-3}
	3A					3345 ± 506	3718 ± 557	6642 ± 996	7383 ± 1107	1.5×10^{-2}	1.3×10^{-2}	7.3×10^{-3}	6.6×10^{-3}
	1B	64	1	2.22×10^{-5}		977 ± 146	1085 ± 162	47690 ± 7155	53010 ± 7952	5.0×10^{-2}	4.5×10^{-2}	1.0×10^{-3}	9.1×10^{-4}
	2B					1807 ± 272	2009 ± 301	53000 ± 7948	58910 ± 8835	2.7×10^{-2}	2.4×10^{-2}	9.1×10^{-4}	8.2×10^{-4}
	3B					451 ± 68	502 ± 76	39740 ± 5964	44170 ± 6629	1.1×10^{-1}	9.7×10^{-2}	1.2×10^{-3}	1.1×10^{-3}
	4B					1954 ± 294	2173 ± 326	53000 ± 7948	58910 ± 8835	2.5×10^{-2}	2.2×10^{-2}	9.1×10^{-4}	8.2×10^{-4}
	7B					904 ± 135	1004 ± 150	59620 ± 8943	66270 ± 9940	5.4×10^{-2}	4.8×10^{-2}	8.1×10^{-4}	7.3×10^{-4}
Human Rib-3	--	159	0	1.00×10^{-5}		493 ± 74	548 ± 82	35480 ± 5322	39440 ± 5915	6.1×10^{-4}*	5.5×10^{-4}*	8.4×10^{-6}*	7.6×10^{-6}*
Human Rib-2	--	159	0	1.00×10^{-5}		73.9 ± 111	82.1 ± 123	44350 ± 6652	49290 ± 7394	4.1×10^{-4}	3.7×10^{-4}	6.8×10^{-6}	6.1×10^{-6}

* These values for the human rib are simply the factors needed to reduce the experimental dose to 0.3 rad/yr since the skeletal burden was below the detection limits of the Hanford facility.

NOTE: D_o is the dose including all zero values and D_w the dose excluding the zero values. The experimental MPOB is the given skeletal burden multiplied by the factor required to reduce the D_o or D_w value to 0.3 rad/yr and a factor of 10 to account for the skeletal mass difference between the dog and man. The 10 and 20 μm refer to endosteal tissue thicknesses. Error is ± 15%, obtained from our reproducibility studies.

calculation tends to lower the calculated dose much the same as if we included unirradiated populations in a calculation of man-rem to an irradiated population. We could argue, then, the second, higher dose most closely simulates reality but both data sets are presented for illustration. To use these data to determine the experimental maximum permissible skeletal burden, the MPOB, Columns 11-13, Table 11, look at bone T47P5 section #13. The dose rate is 17210 rads/yr and the skeletal burden is 18.43 μCi. We could determine a factor to multiply by this dose rate to lower it to the recommended limit for the endosteal tissues, 15 rem/yr or 0.3 rad/yr (ICRP).[81] This factor is 1.74×10^{-5}. Now if this factor is multiplied by the skeletal burden, 18.43 μCi, the experimental maximum permissible skeletal burden for dogs is obtained, 0.00032 μCi from these data. Now to convert from dog burden to man we multiply by 10, the difference in skeletal mass between dog and man and find 0.0032 μCi as the experimental maximum permissible skeletal burden for ^{239}Pu man (given on Table 11 as "Experimental MPOB"). Therefore, the present maximum permissible skeletal burden, 0.036 μCi (ICRP),[120] would be considered high by over a factor of 10 according to these data. The other values in Columns 11-13 in Table 11 follow in a similar manner. From these data it appears the present maximum permissible organ burden (MPOB) of 0.036 μCi is high by at least a factor of 700, if the minimum values are considered, by a factor of 2 if the weighted mean is calculated and about 4 times low if the maximum value is used.

Therefore the bone dosimetry technique used here could be summarized as follows: (1) prepare undecalcified bone sections, (2) press unmasked side of the polycarbonate foil against the section tightly, (3)

remove the foil, etch and mount on a microscope slide for viewing, (4) count random 120 μm squares (1.44×10^4 μm^2 areas), (5) take the average of these values and obtain dose rate from eqn. (6.3). If an experimental MPOB is desired to be calculated from the results of the dosimetry technique, use the following procedure: (1) divide 0.3 rad/yr by the experimentally determined dose rate, (2) multiply by 10 to convert from dog burden to man maximum permissible skeletal burden.

6.2.2 Calibration Procedure

We were not able to use the efficiency found in the previous chapter since monoenergetic alphas were used. Instead, for the bone sections, alpha energies will range from zero to the maximum energy since the sections were infinitely thick to alpha particles. Therefore calibration sources needed to be used to meet this latter condition. These sources are described on Table 12. They were obtained from Dr. J. M. Smith at the University of Utah and made by the Chemistry Group of the Radiobiology Laboratory. The values in column 2 of Table 12 were given with the sources and measured by liquid scintillation techniques before the sources were constructed. Each source was made infinitely thick for alpha particles and considered tissue equivalent. Foils C24 and WBA are constructed with Bioplastic (density 1.24 g/cm^3) and P.20 with methyl methacrylate (density 1.18 g/cm^3). Source strength (column 3) was calculated in the usual manner for an infinitely thick planar source, $S_v \times R/2$ where S_v is the volumetric source strength (concentration x density) and R is the range of the ^{239}Pu alpha particle, 34 μm. Exposure time, waiting time and average number of tracks have the same meaning as before and column 7 is column 3 multiplied by 1.44×10^4 μm^2 with the units conversion of μCi and cm to

Table 12. The Three Calibration Sources Are Shown, Source C24 Was Exposed Under Two Conditions. Concentration Was Given with the Source and Determined by Liquid Scintillation Before Each Source Was Constructed

Source	Concentration ($\mu Ci/g$)	Source Strength ($\mu Ci/cm^2$)	Exposure Time (days)	Waiting Time (days)	Average No. Tracks in 120 μm Square	Number Alphas in 120 μm Square	Efficiency (tracks/α)
C24 (^{239}Pu)	1.09×10^{-4}	2.30×10^{-7}	64	5	0.0187	6.77	2.76×10^{-3}
C24 (^{239}Pu)	1.09×10^{-4}	2.30×10^{-7}	34	-	0.0136	3.60	3.77×10^{-3}
P.20 (^{239}Pu)	2.50×10^{-2}	5.02×10^{-5}	30	-	0.537	693	7.75×10^{-4}
WBA (^{241}Am)	0.352	7.42×10^{-4}	64	1	0.485	2.19×10^{4}	2.22×10^{-5}

alphas and μm and the exposure time. As an example, take row 1, source C24. Here 2.30×10^{-7} μCi/cm^2 x 3.7×10^4 dis/(sec-μCi) x 8.64×10^4 sec/d x 1 cm^2/10^8 μm^2 x 64 d x 1.44×10^4 μm^2 = 6.77. The efficiency is column 6 divided by column 7 and these values appear in Table 11. The values in column 6 were less than one because not every random scan yielded one observable track. Some scans contained more than one track but the average was less than one. The same counting system was used for the bones and sources. These sources were placed in position between the bone samples as the bone samples and sources lay flat beside each other with the same polycarbonate sheet pressed tightly against samples and sources. This method assured similar irradiation conditions. Also, the sources were etched along with the bone samples at the end of the exposure period.

6.2.3 Reproducibility of Bone Results

The values of reproducibility indicated on Table 11 were obtained as follows. Table 7 shows a number of foils, giving energy of the incident alpha particles (expressed as μm of polycarbonate), waiting time and tracks recorded on each foil. These foils were etched many weeks, even months apart. The average of the percent variations from the mean of the number of tracks for each comparable foil is 11%. Therefore a 15% error was selected as a conservative number to use throughout the measurements to follow.

There are few experimental techniques available for determining similar dose rates for direct comparison with our results. To compare the bone dosimetry results here with results of others we will first compare

our data with the calculational techniques of Thorne,[109] Marshall et al.[172] and Spiers and Vaughan.[173] They calculated 7880 rads/yr, 4510 rads/yr and 2356 rads/yr for an 18.43 μCi skeletal burden delivering a dose rate to the 10 μm thick layer of tissue along the endosteal surface, respectively. Many of the experimental values shown in Table 11 fall within the range of these measurements, such as T47P5 section #3, 6, 7 and 14 and T42P5 section #8 and 12. Many other values, however, are much higher in Table 11 especially when the zero scans are excluded. This is to be expected since such allowance for the regions of zero dose is not made in the calculations as it is in this work.

The one technique involving experimental determination of the endosteal dose rate uses photographic emulsion. It is possible to draw a direct comparison between the proposed technique here and the one used by the Utah workers (Twente and Jee).[6] In the paper mentioned they determined the endosteal dose rate to one of the same bones used in this work, the lumbar vertebra of dog T16P5. Twente and Jee used Ilford C-2 nuclear track emulsions clamped to the bone sample. After developing, tracks were counted along short lengths of the endosteum and disintegration rate per unit area of the alpha emitting source calculated. This latter value was used to calculate average dose rate delivered throughout a specified distance (they used the ^{239}Pu alpha range) from an alpha emitting plane source by the equation

$$\text{average dose rate} = \frac{D'E}{2R\rho}\left(1 + \ln\frac{R}{X}\right) \qquad (6.4)$$

where D' = disintegration rate per unit area of source

E = energy of the emitted alpha particle

R = range of the alpha in the medium considered

ρ = density of the medium

X = any specified distance from the source

Using this formulation Twente and Jee found the endosteal dose rate to be 22630 rads/yr for the lumbar centrum of dog T16P5. Looking at Table 11 we found D_o = 1104 rads/yr and D_w = 39740 rads/yr for section #8 of dog T16P5 and D_o = 8136 rads/yr and D_w = 108,800 rads/yr for section 10. The D_w value would not be expected to compare favorably with the Twente and Jee result since no effort was made to exclude any *tissue not* irradiated by alpha particles. The D_o value might be expected to compare, however. If we examine their technique, they used the full 5.15 MeV ^{239}Pu alpha energy, whereas this work used only the average energy absorbed in the 10 μm layer, 1.39 MeV. If we increase our value of D_o for section #10 by 5.15/1.39 we obtain 29,900 rads/yr, a difference of 24%. Considering the vast differences inherent in the techniques, even the basic detection system was different, these two values are about equal.

6.2.4 NTA Emulsion Exposure

We were also interested in noting the locations of the tracks appearing on our polycarbonate foils with respect to the special structures of bone. Therefore a set of Kodak NTA emulsion plates were exposed to the bone samples and developed to obtain autoradiograms. To make the comparison of the two methods, polycarbonate foils and emulsions possible, a procedure allowing the simultaneous exposure of the two was required.

The following technique was developed. First a rectangular section of corrugated cardboard was cut the same size as the standard microscope slides. Next a plain microscope slide was placed over one section of cardboard. A rectangular section of polycarbonate foil was positioned on the slide with the foil masking removed on the side of the foil facing upward. Then one of the bone sections was fixed to the foil and outlined on the foil with a dissecting needle. This completes the portion that can be accomplished outside the darkroom. It is a good policy to give prior consideration to the procedure to be followed during the handling of these emulsions so that as many portions as possible of the technique can be carried out in room light. In the darkroom, one NTA, 25 μm thick emulsion slide was placed, emulsion side down, over the sample. Then a second piece of corrugated cardboard was positioned over the emulsion slide completing the "sandwich," as shown on Figure 34. Lastly two hosecock clamps were tightened around the cardboard sections to hold the slide and foil snugly against the bone section. Several assemblies of this kind were placed in a gallon paint can with appropriate cushioning materials. The can was sealed tightly with duct tape upon filling and placed in a refrigerator during the exposure period since it is best to keep NTA emulsion plates cool at all times. After the desired exposure time, the can was opened in the darkroom. The polycarbonate foils were developed by the electrochemical etching procedure. The photographic plates were developed in Kodak D-19 Developer for seven minutes, then placed in Kodak Fixer for 10 minutes, Kodak Photo-Flo-200 solution for two minutes and hung to dry. During each phase of the developing procedure gentle agitation of the

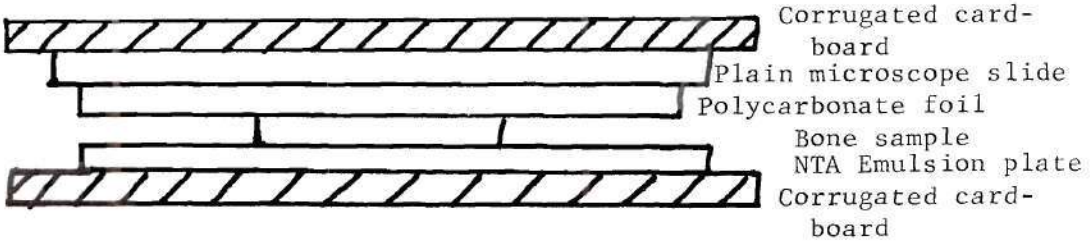

Figure 34. Sketch of the Relative Position of the Two Pieces of Corrugated Cardboard, NTA Emulsion Plate, Bone Sample, Polycarbonate Foil and Plain Microscope Slide

solutions over the plates was maintained. The darkroom lights are not needed after 2 or 3 minutes have elapsed in the "fixing" portion of the developing procedure. The foil and plates were superimposed to observe any relation between the tracks appearing on the two. Results are shown in Figures 35-37. Figure 35 shows the characteristic trabecular deposition of ^{239}Pu on the NTA emulsion plate. The bone used was a distal femur from dog T56P5.5 and section #4. Magnification was 100X and exposure time 49 days. The image on the emulsion was formed by the ionization of the medium by alpha particles since no thermal neutron irradiation was used. Figure 36 shows the same bone sample only here the bone sample exposed a polycarbonate foil for 49 days. We again discovered the trabecular bone surface outline after electrochemically etching the foil (magnification was 100X). As far as we know this is the first report of a bone image on a polycarbonate foil, after electrochemical etching, formed by exposure to alpha particles alone. Figure 37 is a photograph of the image of a portion of trabecular surface formed by superposition of polycarbonate foil image and NTA emulsion image. The hazy image is the NTA image and the small black dots, the etched tracks view at 100X. It is possible more quantitative information could be obtained concerning the dose delivered by ^{239}Pu to endosteal tissues since the outline of the surfaces is so well defined and each track easy to count.

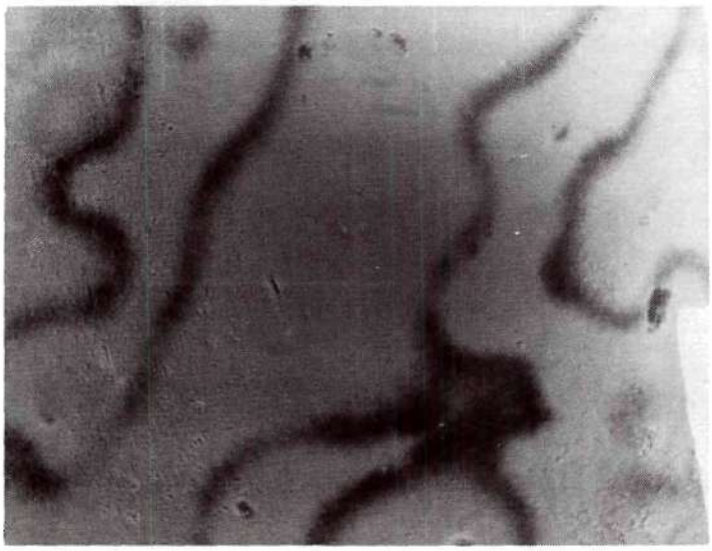

Figure 35. Photograph of NTA Image of the Trabecular Tissues of Bone T56P5.5 Section #4 Formed by 49 Days Exposure and Viewed at 100X

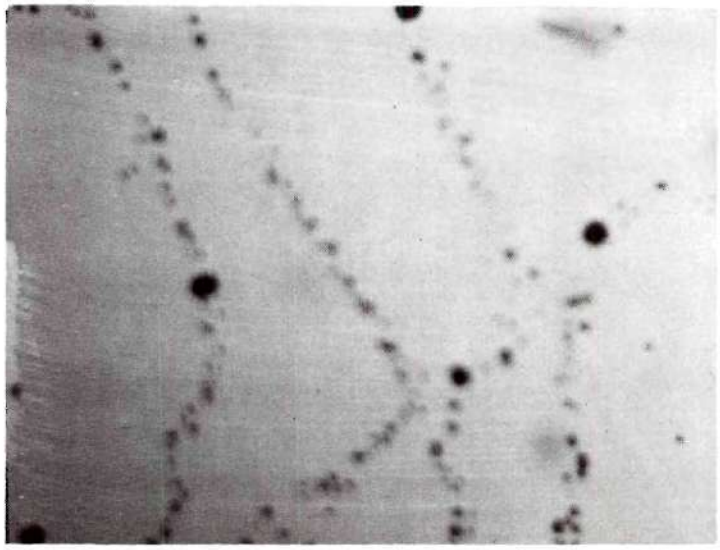

Figure 36. Photograph of Polycarbonate Foil Showing Trabecular Surface Image After Exposure for 49 Days and Etched Electrochemically. Bone T56P5.5 Section #4 Was Used; Magnification Was 100X

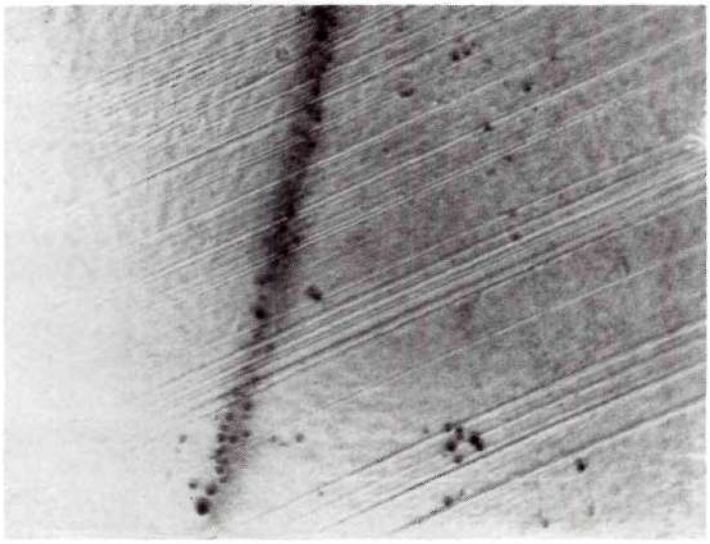

Figure 37. Photograph of Superimposed Image of Trabecular Surface Using Images Shown on Figures 35 and 36. Hazy Image Is NTA Emulsion Image and Black Dots Are the Etched Pits.

CHAPTER VII

CONCLUSIONS AND RECOMMENDATIONS

7.1 Conclusions

The first objective of this research project after selecting the electrochemical etching system as the dosimetry system of choice was demonstrating the feasibility of polycarbonate foils as an alpha particle detector. The ability of polycarbonate foils to register alpha particle tracks when amplified by electrochemical etching was indicated on the photographs on Figures 21 and 31. The sensitivities found for this system were between 1×10^{-5} tracks per alpha (approximately equal to the efficiency of fast neutron detection) and 3.77×10^{-3} tracks per alpha. Sensitivity was dependent upon the alpha source (whether it was very thin or infinitely thick for alpha particles), etching time and waiting period between irradiation and etching. If the source was a thin alpha particle source, the sensitivity depended on whether or not the LET was at the maximum of the Bragg peak as a result of the use of absorbers to decrease the energy of the alpha particle. The sensitivity for the electrochemical etching system was considerably less than the sensitivity of photographic emulsions but the electrochemical etching system offers simplicity, no fading, smaller size, lower cost and tissue equivalence not found with emulsions.

Increasing the time between irradiation and etching, termed the waiting period, was found to increase the apparent efficiency of etchable

track production dramatically but the effect is still not clearly understood. This result was surprising and was examined closely and quantified, as shown on Figure 22. By choice of waiting time the sensitivity of the method can be improved. Track diameter as a function of etching time was also studied and one of the results was the discovery of two categories of tracks on etched foils after exposure to alpha particle radiations. A proposed explanation for this important effect was offered. The two track size discovery could become important because it provides a mechanism to obtain information on LET. The background routinely achievable was found to be 2.0 tracks/cm^2, for the selected foil material, and bulk etching rate was 0.16 μm/hr.

As the next major objective, it was found possible to use the electrochemical etching system for the purpose of the dosimetry of ^{239}Pu in bone. Actual dose measurements were made. Briefly the procedure developed was (1) to prepare undecalcified, 300 μm thick bone sections, (2) press polycarbonate sheet, masking side up, tightly against the bone sections interspaced with calibration sources (see Table 12), (3) after the exposure time, remove polycarbonate and etch the portion of foil above bone sections and calibration sources simultaneously, (4) count foils using randomly scanned 120 μm square areas to obtain the average number of tracks in that foil volume, (5) calculate the dose rate. The calibration procedure accounted for waiting time effects and any effects possibly inherent in any particular portion of foil since calibration sources were always developed and counted the same way as the foils exposed to the bone sections. By compiling data on different foils used in this research it was determined that measurements were accurate within ± 15%. Factors

affecting accuracy were observational errors, statistical errors, low efficiency, positional errors and inhomogeniety of the samples. The results showed a wide point-to-point variation in dose measured. This variation was believed to be caused by inhomogeneities in the three dimensional deposition of plutonium in bone. Results were presented for a dose rate, D_o, that included all scans of the 120 μm square resulting in no counts and D_w, that did not include these zero scans. Thus an attempt was made to determine dose only for tissue masses actually receiving the alpha particle dose. As deposition of plutonium varies so does the dose from ^{239}Pu. Therefore quoting average concentrations or bone burdens may not be very meaningful in giving information as to these highly localized doses because low skeletal burden can result in high doses in localized areas. These effects could explain the differences between Thorne's, Spier's and Marshall's normalized calculations and this work. Agreement was found between the experimental measurements of Twente and Jee using photographic emulsions and this work, when comparing our D_o values with Twente and Jee experimental values. D_o for the dog bones ranged from 16.7 rads/yr to 39580 rads/yr for dog T56P5.5 section #3 (skeletal burden 20.74 μCi) and dog T42P5 section #1 (skeletal burden 13.57 μCi), respectively. D_w ranged from 440 rads/yr to 317900 rads/yr for dog T56P5.5 section #3 (skeletal burden 20.74 μCi) and dog T47P5 section #7 (skeletal burden 18.43 μCi), respectively, considering 10 μm thick osteogenic cell layers only and plutonium in the citrate.

The dose rate per microcurie (observed dose rate ÷ skeletal burden) for these bones was as follows. For D_o, dose rate per microcurie was 0.81 rad/yr/μCi for bone T56P5.5 section #3 and 2917 rads/yr/μCi for bone T42P5

section #1. For D_w we found 21.2 rads/yr/μCi for bone T56P5.5 section #3 and 17250 rads/yr/μCi for bone T47P5 section #7. Again this is not a completely accurate way to state these results since the procedure of calculating dose/μCi in effect averages the dose to a 120 μm square over the entire skeleton producing an unrealistic value and does not take into consideration the inhomogeneities in the ^{239}Pu distribution we found.

ICRP has set a limit of 30 rem/yr to the bone as a whole and 15 rem/yr (0.3 rad/yr) to the endosteum of bone. If one wishes to use the results of the present investigation to relate to such a limit, one has to extrapolate these results to the skeleton as a whole. The results show there is an enormous variation in dose rate from point to point even in close proximity on the same bone so different values of maximum permissible skeletal burden can be obtained by this extrapolation procedure depending on the dose rate considered. We scaled the recorded dose rates down to the ICRP value of 0.3 rad/yr and scaled the Utah total skeletal burden by the same factor to arrive at the maximum permissible skeletal burden extrapolated from the bone section considered. It is found that the average value of all the experimental maximum permissible skeletal burdens calculated from the D_w values for a 10 μm osteogenic layer is half the present ICRP value of 0.036 μCi and the maximum and minimum values are four times greater than and 700 times less than the ICRP values, respectively.

We also examined the possible effects of body burden on bone turnover. It is known high skeletal burdens of ^{239}Pu cause necroses of tissues and turnover essentially ceases. There is some possibility the large dose observed for dog T50P3 was partly due to these turnover effects since a skeletal burden of only 0.606 μCi existed whereas other burdens were a

factor of 20 higher. We cannot be conclusive on this point, however, because not enough data exist for small skeletal burdens here and none for intermediate skeletal burdens, i.e. 3, 4, 5, 6 μCi, etc. When such data are obtained some of the scatter in the dose rates observed due to the inhomogeneity in the osseous distribution of plutonium might be minimized.

7.2 Recommendations

While conducting this research related to the dosimetry of ^{239}Pu in bone a number of new and interesting areas that could be explored were realized. Now that this new technique for bone dosimetry has been developed, namely (1) expose infinitely thick bones to polycarbonate foils, tightly pressed against the bone sections, (2) remove foils and etch, (3) count using the small squares on a Whipple disk, (4) calculate an average number of tracks, (5) insert these values in the equation $D = \frac{N}{\epsilon T}$ 56.41 for dose rate 0-10 μm or $D = \frac{N}{\epsilon T}$ 62.701 for the dose rate 0-20 μm removed from the endosteal surfaces, it is important to use this technique as much as possible to add to the collective body of data. This would include not only bones of differing plutonium content but also other bone-seeking alpha emitters such as ^{241}Am.

We have shown the existence of the two track sizes on alpha particla irradiated polycarbonate foils and quantified this effect as a function of alpha particle energy. Other experiments need to be performed to examine this effect. One could irradiate one group of foils with accelerator-produced alpha particles of various energies and a second group with accelerator produced carbon and oxygen nuclei and compare track diameter frequency histograms. Additionally, one could polarize

the incident alpha particles to maximize the probability of interaction with carbon and oxygen nuclei to see if the effect is enhanced. The nature of the interaction could be confirmed by such an experiment.

Another interesting effect observed was an increase in sensitivity of the system as waiting time increased. Waiting time was defined as the time between irradiation and etching. This new and somewhat surprising result needs to be examined further to determine if it is only observed after alpha particle irradiation, what conditions enhance or reduce the effect and the precise mechanism that yields the increase in sensitivity. It is possible the sensitivity of the electrochemical etching system can be greatly improved by waiting time variation.

During this work we have used planar bone sections and placed our dosimeter flat against one face. We know the distribution of ^{239}Pu in osseous tissue is highly inhomogeneous in three dimensions as well as two, as the present work clearly indicates. Therefore, knowledge concerning the three dimensional dose distribution could be obtained by using cubes of trabecular tissue, rather than flat sections, and pressing foils against each face of the cube.

The dosimetry technique described herein is quite general and not difficult to perform. In fact there is really no technical problem insurmountable in nature that would prevent the identical technique, including data reduction, to be used to determine the dosimetry of other tissues. Therefore we would like to see this technique applied to tissues such as lung, liver, etc. or any organ where internally deposited alpha emitters are found. This technique has the advantage of detecting the actual particle irradiating tissue in vivo and not using fission fragments

to calculate activity and then dose. Here, dose was obtained directly.

Some of the recommendations mentioned above are proposed to be carried out under current contracts with the Department of Energy and other recommendations are as yet untried. These are only a few of the possibilities one could imagine to use this general technique.

BIBLIOGRAPHY

1. Vaughan, J., B. Bleancy and D. M. Taylor, "Distribution, Excretion and Effects of Plutonium as a Bone Seeker," in Uranium-Plutonium-Transplutonic Elements, H. C. Hodge, J. N. Stannard and J. B. Hursh, Eds., Springer-Verlag, New York, 1973.

2. Rowland, R. E. and J. H. Marshall, "Radium in Human Bone: the Dose in Microscopic Volumes of Bone," Rad. Res., 11, 299 (1959).

3. Jee, W. S. S., J. S. Arnold, T. H. Cochran, J. A. Twente and R. S. Michal, 'Relationship of Microdistribution of Alpha Particles to Damage," in Some Aspects of Internal Radiation, T. F. Dougherty, W. S. S. Jee, C. W. Mays and B. J. Stover, Eds., Pergamon Press, Oxford, 27 (1962).

4. Wronski, T. J., J. M. Smith and W. S. S. Jee, "A Preliminary Report on the Correlation of the Rate of Trabecular Bone Turnover and ^{239}Pu Concentration on Trabecular Surfaces with the Incidence of Osteosarcoma at Selected Skeletal Sites," COO-119-253, March, 1977, 172.

5. Smith, J. M., D. R. Atherton, T. J. Wronski and W. S. S. Jee, "^{239}Pu Standards for Quantitative Neutron-Induced Autoradiography," COO-119-252, March, 1977, 162.

6. Twente, J. A. and W. S. S. Jee, "The Determination of Localized Concentration of ^{239}Pu in Bone," Health Physics, 5, 142 (1961).

7 James, A C. and Kember, N. F., "Alpha Particle Incidence in Small Targets," Phys. Med. Biol., 15, 39 (1970).

8. Mays, C. W. and R. D. Lloyd, "Bone Sarcoma Incidence vs. Alpha Particle Dose," in Radiobiology of Plutonium, B. J. Stover and W. S. S. Jee, Eds., The J. W. Press, 1972.

9. Spiess, H. and C. W. Mays, "Bone Cancers Induced by ^{224}Ra (ThX) in Children and Adults," Health Physics, 19, 713 (1970).

10. Evans, R. D., A. T. Keane and M. M. Shanahan, "Radiogenic Effects in Man of Long Term Skeletal Alpha Irradiation," in Radiobiology of Plutonium, B. J. Stover and W. S. S. Jee, Eds., The J. W. Press, 1972.

11. Jee, W. S. S., 'Distribution and Toxicity of ^{239}Pu in Bone," Health Physics, 22, 583 (1972).

12. Stover, B. J. and W. S. S. Jee, Eds., Radiobiology of Plutonium, The J. W. Press, Salt Lake City, 1972.

13. Stover, B. J., D. R. Atherton, W. Stevens, D. S. Buster and F. W. Bruenger, "Effect of Dose Level on Skeletal Retention of ^{239}Pu(IV) in the Beagle," Rad. Res., 69, 442 (1977).

14. Mays, C. W., W. S. S. Jee and R. D. Lloyd, Delayed Effects of Bone-Seeking Radionuclides, The University of Utah Press, 1969.

15. Jee, W. S. S., The Health Effects of Plutonium and Radium, The J. W. Press, Salt Lake City, 1976.

16. Jee, W. S. S., Research in Radiobiology, The University of Utah, COO-119-253, March, 1977.

17. Arnold, J. S. and W. S. S. Jee, "Bone Growth and Osteoclastic Activity as Indicated by Radioautographic Distribution of Plutonium," Amer. Journ. of Anatomy, 101, 367 (1957).

18. Durbin, P. W., "Plutonium in Mammals--Influence of Plutonium Chemistry, Route of Administration and Physiological Status of the Animal on Initial Distribution and Long Term Metabolism," Health Physics, 29, 495 (1975).

19. Durbin, P. W., "Distribution of Transuranium Elements in Mammals," Health Physics, 8, 665 (1962).

20. Durbin, P. W., "Plutonium in Man: A Twenty Five Year Review," UCRL-20850 (1971).

21. Durbin, P. W., "Plutonium in Man: A New Look at the Old Data," in Radiobiology of Plutonium, B. J. Stover and W S. S. Jee, Eds., The J. W. Press, Salt Lake City, 1972.

22. Durbin, P. W., M. W. Horovitz and E. R. Close, "Plutonium Kinetics in the Rat," Health Physics, 22, 731 (1972).

23. Scott, K. G., D. Axelrod, J. Crowley and J. G. Hamilton, "Deposition and Fate of Plutonium, Uranium and Their Fission Products Inhaled as Aerosols by Rats and Man," Arch. Pathol., 48, 31 (1949).

24. Scott, K. G., D. Axelrod, H. Fisher, J. F. Crowley and J. G. Hamilton, "The Metabolism of Plutonium in Rats Following Intramuscular Injection," J. Biol. Chem., 176, 283 (1948).

25. Hamilton, J G., "Health Division," Metallurgical Lab Report CH-1459, February 29, 1944.

26. Lafuma, J., "Treatment of ^{239}Pu Contamination," CEA-CONF-1549, 1970.

27. Nenot, J. C., M. Morin and J. Lafuma, "Metabolic and Therapeutic Study of Respiratory Contamination by Certain Actinides in Solution," Health Physics, 20, 167 (1971).

28. Nenot, J. C., R. Masse, M. Morin and J. Lafuma, "Experimental Comparative Study of the Behavior of ^{237}Np, ^{238}Pu, ^{239}Pu, ^{241}Am and ^{242}Cm in Bone," Health Physics, 22, 657 (1972).

29. Nenot, J. C., M. Morin, W. Skupinski and J. Lafuma, "Experimental Removal of ^{144}Ce, ^{241}Am, ^{242}Cm and ^{238}Pu from the Rat Skeleton," Health Physics, 23, 635 (1972).

30. Nenot, J. C., M. Morin and J. Lafuma, "Experimental Contamination by Americum in Solutions and Their Treatment," Health Physics, 20, 383 (1971).

31. Bair, W. J., J. F. Park and W. J. Clarke, "Long-Term Study of Inhaled Plutonium in Dogs," AFWL-TR-214, 1966, 58.

32. Bair, W J., "Inhalation of Radionuclides and Carcinogenesis," CONF-691001, 1970.

33. Bair, W. J., D. H. Willard and L. A. Temple, "Plutonium Inhalation Studies I: Retention and Translocation of Inhaled $^{239}PuO_2$ Particles in Mice," Health Physics, 7, 54 (1961).

34. Bair, W. J. and D. H. Willard, "Plutonium Inhalation Studies IV: Mortality in Dogs After Inhalation of $^{239}PuO_2$," USAEC Doc. Hw-68803, 1966, 24.

35. Bair, W. J., D. H. Willard, J. P. Herring and L. A. George, II, "Retention, Translocation and Excretion of Inhaled $^{239}PuO_2$," Health Physics, 8, 639 (1962).

36. Bair, W. J., "Toxicology of Inhaled Plutonium," CONF-700816, 2, 697 (1970).

37. Bair, W. J., "Plutonium Inhalation Studies," BNWL-1221, 1970.

38. Thompson, R. C., W. J. Bair, S. Marks and M. F. Sullivan, "Evaluation of Internal Exposure Hazards for Several Radioisotopes Encountered in Reactor Operation," in Proceedings of the Second U. N. International Conference on the Peaceful Uses of Atomic Energy, 23 (U.N. Geneva), 1958, 283.

39. Thompson, R. C., "Proceedings of the Hanford Symposium on the Biology of Transuranic Elements," Health Physics, 8, 561 (1962) (Selected Papers).

40. Thompson, R. C., "Animal Data on Plutonium Toxicity," Health Physics, 29, 519 (1975).

41. Thompson, R. C., "Biological Factors," Plutonium Handbook: A Guide to the Technology, 2, Wick, O. J., Ed., Gordon and Breach, New York, 1967, 785.

42. Thompson, R. C., "Properties of Radionuclides in Tissues: A New Look at Some Old Problems," in Diagnosis and Treatment of Deposited Radionuclides, H. A. Kornberg and W. D. Norwood, Eds., Excerpts Medica Foundation, Amsterdam, 1968, 39.

43. Thompson, R. C. and W. J. Bair, Eds., "Proceedings of the Hanford Symposium on the Biological Implications of the Transuranium Elements," Health Physics, 22, 533 (1972) (Selected Papers).

44. Thompson, R. C., J. F. Park and W. J. Bair, "Some Speculative Extensions to Man of Animal Risk Data on Plutonium," in Radiobiology of Plutonium, B. J. Stover and W. S. S. Jee, Eds., The J. W. Press, 1972.

45. Clarke, W. J., "Comparative Histopathology of ^{239}Pu, ^{235}Ra and ^{90}Sr in Pig Bone," Health Physics, 8, 621 (1962).

46. Clarke, W. J., J. F. Park, J L. Palotay and W. J. Bair, "Plutonium Inhalation Studies," Health Physics, 12, 609 (1966).

47. Bustad, L. K., M. Goldman, L. S. Rosenblatt, C. W. Mays, N. W. Hetherington, W. J. Bair, R. O. McClellan, C. R. Richmond and R. E. Rowland, "Evaluation of Long-Term Effects of Exposure to Internally Deposited Radionuclides," Peaceful Uses of Atomic Energy, 11, 1972, 125.

48. Taylor, D. M., "Chemical and Physical Properties of Plutonium," in Uranium-Plutonium-Transplutonic Elements, H. C. Hodge, J. N. Stannard and J. B. Hursh, Eds., Springer-Verlag, New York, 1973.

49. Sohrabi, M., "Electrochemical Etching Amplification of Low-LET Recoil Particle Tracks in Polymers for Fast Neutron Dosimetry," Ph.D. Dissertation, Georgia Institute of Technology, Rept. ORO-4814-5, 1975.

50. Rutherford E. and F. Soddy, "The Cause and Nature of Radioactivity Part I," Phil. Mag., 4, 370 (1902).

51. Rutherford, E. and F. Soddy, "The Cause and Nature of Radioactivity Part II," Phil. Mag., 4, 569 (1902).

52. Rutherford, E. and F. Soddy, "The Radioactivity of Uranium," Phil. Mag., 5, 441 (1903).

53. Rutherford, E. and F. Soddy, "Condensation of Radioactive Emanations," Phil. Mag., 5, 561 (1903).

54 Rutherford, E. and F. Soddy, "Radioactive Change," Phil. Mag., 5, 576 (1903).

55. Cember, H., Introduction to Health Physics, Pergamon Press, Oxford, 1969.

56. Price, W. J., Nuclear Radiation Detection, McGraw-Hill Book Company, New York, 1964, Chapters 1 and 7.

57. Morgan, K. Z. and J. E. Turner, Principles of Radiation Protection, 2nd Edition, Robert E. Krieger Publishing Company, New York, 1973.

58 Warren, S., "Effects of Low Levels of Radiation on Rodents and Potential Effects in Man," Health Physics, 29, 251 (1975).

59. Marshall, J. H. and P. G. Groer, "A Theory of the Induction of Bone Cancer by Alpha Radiation," Rad. Res., 71, 149 (1977).

60. Hasterlik, R. J., A. J. Finkel and C. E. Miller, "The Cancer Hazards of Industrial and Accidental Exposure to Radioactive Isotopes," Ann. N. Y. Acad. Sci., 114, 832 (1964).

61. Lea, D. E., Actions of Radiations on Living Cells, Cambridge at the University Press, 1946, Chapters 3, 6 and 7.

62. Casarett, A. P., Radiation Biology, Prentice-Hall, Inc., 1968, Chapters 4 and 5.

63. Marquart, K. H., "Early Ultrastructural Changes in Osteocytes from the Proximal Tibial Metaphysis of Mice after the Incorporation of ^{224}Ra," Rad. Res., 69, 40 (1977).

64. Evans, R. D., "The Effect of Skeletally Deposited Alpha Ray Emitters in Man," Br. J. Radiol., 39, 881 (1966).

65 Bergonie, J. and T. Tribondeau, "Interpretation of Some Results of Radiotherapy and an Attempt at Determining a Logical Technique of Treatment," Rad. Res., 11, 587 (1959) [tr. of 1906 original].

66. Vaughan, J., "Bone Surfaces: What Are They?" in Radiobiology of Plutonium, B. J. Stover and W. S. S. Jee, Eds., The J. W. Press, Salt Lake City, 1972.

67. Rubin, P., Clinical Oncology, American Cancer Society, New York, 1974.

68. Muller, H. J., "Artificial Transmutation of the Gene," Science, 66, 84 (1927).

69. Lyons, M. F., D. G. Papworth and R. J. S. Phillips, "Dose-Rate and Mutation Frequency after Irradiation of Mouse Spermatagonia," Nat. New Biol., 238, 101 (1972).

70. Bacq, Z. M. and P. Alexander, Fundamentals of Radiobiology, Pergamon Press, 1961, Chapter 9.

71. Elkind, M. M. and G. F. Whitmore, The Radiobiology of Cultured Mammalian Cells, Gordon and Breach, 1967, Chapters 1 and 5.

72. Okada, S., Radiation Biochemistry, Vol. I, Academic Press, 1970, Chapter 2.

73. Villee, C. A. and V. G. Dethier, Biological Principles and Processes, W. B. Sanders Company, 1971, Chapter 3.

74. Safe Handling of Radioactive Luminous Compounds, National Bureau of Standards (U.S.) Handbook, 27 (1941).

75. Gofman, J. W. and A. R. Tamplin, "The Question of Safe Radiation Thresholds for Alpha Emitting Bone Seekers in Man," Health Physics, 21, 47 (1971).

76. Aub, J. C., R. D. Evans, L. H. Hempelmann and H. S. Martland, "The Late Effects of Internally-Deposited Radioactive Materials in Man," Medicine, 31, 221 (1952).

77. Morgan, K. Z., "The Need for Radiation Protection," Rad. Tech., 44, 385 (1973).

78. Martell, E. A., "Tobacco Radioactivity and Cancer in Smokers," Amer. Scientist, 63, 404 (1975).

79. Looney, W. B., "Tumor Induction in Man Following Radium and Thorium (Thoratrast) Administration," TID-20008, Dept. of Comm., Washington, 1964.

80. Spiess, H. and C. W. Mays, "Bone Cancers Induced by ^{224}Ra (ThX) in Children and Adults," Erratum, Health Physics, 20, 543 (1971).

81. A Review of the Radiosensitivity of the Tissues in Bone, ICRP Publication 11, 1967.

82. Spiers, F. W., "A Review of the Theoretical and Experimental Methods of Determining Radiation Dose in Bone," Br. J. Radiol., 39, 216 (1966).

83. Thomas, C., Ed., Taber's Cyclopedic Medical Dictionary, Twelfth Edition, F. A. Davis Company, Philadelphia, 1975.

84. Kimmel, D. B. and W. S. S. Jee, "Quantitative Histology of Tabecular Bone Surfaces of Young Adult Beagles," COO-119-252, 1977, 152.

85. Spiers, F W., S. D. King and A. H. Beddoe, "Measurements of Endosteal Surface Areas in Human Long Bones: Relationship to Sites of Occurrence of Osteosarcoma," Brit. Journ. of Radiol., 50, 769 (1977).

86. Vaughan, J. and M. Williamson, "Variation in 'Turnover Rates' in Different Parts of the Skeleton in Relation to Tumour Incidence Due to Strontium-90 Deposition," in Strontium Metabolism, J. M. A. Lenihan, J. F. Loutit and J. H. Martin, Eds., Academic Press, New York, 1967.

87. Momeni, M M., L. S. Rosenblatt and N. Jow, "Retention and Distribution of ^{226}Pu in Beagles," Health Physics, 30, 369 (1976).

88. Momeni, M. M., J. R. Williams, N. Jow and L. S. Rosenblatt, "Dose Rates, Dose and Time Effects of $^{90}Sr + ^{90}Y$ and ^{226}Ra on Beagle Skeleton," Health Physics, 30, 381 (1976).

89. Lloyd, R. D., C. W. Mays and D. R. Atherton, "Distribution of Injected ^{226}Ra and ^{90}Sr in the Beagle Skeleton," Health Physics, 30, 183 (1976).

90. Lloyd, E., "The Distribution of Radium in Human Bone," Br. J. Radiol., 34, 521 (1961).

91. Jee, W. S. S., R. B. Dell and L. G. Miller, "High Resolution Neutron Induced Autoradiography of Bone Containing ^{239}Pu," Health Physics, 22, 761 (1972).

92. Taylor, D. M., "Some Aspects of Comparative Metabolism of Plutonium and Americium in Rats," Health Physics, 8, 673 (1962).

93. Kiefer, H. and R. Maushart, Radiation Protection Measurement, Pergamon Press, Oxford, 1972, Chapters 3 and 4.

94. Becker, K. and D. R. Johnson, "Nonphotographic Alpha Autoradiography and Neutron Induced Autoradiography," Science, 167, 1370 (1970).

95. Hamilton, E. I., "The Registration of Charged Particles in Solids: An Alternative to Autoradiography in the Life Sciences," Int. J. Appl. Rad. and Isotopes, 19, 159 (1968).

96. Cole, A., D. J. Simmons, H. Cummins, F. J. Congel and J. Kastner, "Application of Cellulose Nitrate Films for Alpha Autoradiography of Bone," Health Physics, 19, 55 (1970).

97. Schlenker, R. A. and B. G. Itman, "Fission Track Autoradiographies," ANL-8060-11, 1973, 163.

98. Simmons, D. J. and K. T. Fitzgerald, "Application of Cellulose Nitrate Films for Alpha Autoradiography of Bone II. Resolution and Sensitivity of Cellulose Nitrate Films, ANL-8060-11, 1973, 208.

99. Rogers, A. W., Techniques of Autoradiography, Elsevier Publishing Company, 1967, Chapters 3, 11 and 16.

100. Barkas, W. H., Nuclear Research Emulsions Vols. I & II, Academic Press, New York, 1973.

101. Yagoda, H., Radioactive Measurements with Nuclear Emulsions, John Wiley and Sons, 1949, Chapter 4.

102. Till, J. E., "The Toxicity of Uranium and Plutonium to the Developing Embryos of Fish," Ph.D. Dissertation, Georgia Institute of Technology, 1976, Chapters 3 and 4.

103. Spiers, F. W., "Alpha Ray Dosage in Bone Containing Radium," Br. J. Radiol., 26, 296 (1953).

104. Kononenko, A. M., "Calculation of the Intensity of the Alpha Radiation Dose Arising from a Radioactive Substance Distributed Inside the Organism," Biofizika Academy (U.S.S.R.), 11(i), 98 (1957).

105. Stover, B. J., "Skeletal Dosimetry in the Beagle," in The Health Effects of Plutonium and Radium, W. S. S. Jee, Ed., The J. W. Press, Salt Lake City, 1976.

106. Kimmel, D B., W. S. S. Jee, T. J. Wronski, D. R. Atherton, R. A. Schlenker and B. J. Stover, "A Morphometric and Autoradiographic Study of the Ulna and Second Lumbar Vertebral Body of Young Adult Beagles," in The Health Effects of Plutonium and Radium, W. S. S. Jee, Ed., The J. W. Press, Salt Lake City, 1976.

107. McDowell, W. J. and J. F. Weiss, "Liquid Scintillation Alpha Counting and Spectrometry and Its Application to Bone and Tissue Samples," Health Physics, 32, 73 (1977).

108. Charlton, D. E. and D. V. Cormack, "A Method for Calculating the Alpha Ray Dosage to Soft Tissue-Filled Cavities in Bone," Br. J. Radiol., 35, 473 (1962).

109. Thorne, M. C., "Aspects of the Dosimetry of Alpha Emitting Radionuclides in Bone with Particular Emphasis on ^{226}Ra and ^{239}Pu," Phys. Med. Biol., 22, 36 (1977).

110. Green, D., G. Howells and M. C. Thorne, "A New Method for the Accurate Localization of ^{239}Pu in Bone," Phys. Med. Biol., 22, 284 (1977).

111. Harley, N. H. and B. S. Pasternak, "Alpha Absorption Measurements Applied to Lung Dose from Radon Daughters," Health Physics, 23, 771 (1972).

112. Mole, R. H., "Endosteal Sensitivity to Tumor Induction by Radiation in Different Species, A Partial Answer to an Unsolved Question?," in Delayed Effects of Bone-Seeking Radionuclides, C. W. Mays, W.S.S. Jee, and R. D. Lloyd, Eds., The University of Utah Press, 1969.

113. Natural Science Group, International Peace Bureau, Geneva, "The Physical and Medical Effects of the Hiroshima and Nagasaki Bombs," Bull. of the Atomic Scientists, 54 (December, 1977).

114. Recommendations of the International Commission on Radiological Protection, Publication 26, 1977.

115. Cross, F. T., Personal communication, June, 1978.

116. Stannard, J. N., "Biomedical Aspects of Plutonium (Discovery, Development, Projections)," in Uranium Plutonium Transplutonic Elements, H. C. Hodge, J. N. Stannard and J. B. Hursh, Eds., Springer-Verlag, New York, 1973.

117. Seaborg, G. T., "Plutonium Revisited," in Radiobiology of Plutonium, B. J. Stover and W. S. S. Jee, Eds., The J. W. Press, Salt Lake City, 1972.

118. Eisenbud, M., Environmental Radioactivity, Academic Press, New York, 1973, Chapter 14.

119. Radiological Health Handbook, Bureau of Radiological Health, U. S. Department of Health, Education and Welfare, 1970.

120. Recommendations of the International Commission on Radiological Protection, Report of Committee II on Permissible Dose for Internal Radiation, ICRP Publication 2, 1959.

121. Lindenbaum, A., M. W. Rosenthal and M. Smoler, "An Autoradiographic Study of the Changes in Distribution of Polymeric Plutonium in Mouse Tissues," in Diagnosis and Treatment of Deposited Radionuclides, H. A. Kornberg and W. D. Norwood, Eds., Exerpta Medica Foundation, Amsterdam, 1968.

122. Rosenthal, M. W., J. H. Marshall and A. Lindenbaum, "Autoradiographic and Radiochemical Studies of the Effect of Colloidal State of Intravenously Injected Plutonium on Its Distribution in Bone and Marrow," in Diagnosis and Treatment of Deposited Radionuclides, H. A. Kornberg and W. D. Norwood, Eds., Excerpta Medica Foundation, Amsterdam, 1968.

123. Markley, J. F., M. W. Rosenthal and A. Lindenbaum, "Distribution and Removal of Monomeric and Polymeric Plutonium in Rats and Mice," Int. J. Rad. Biol., 8, 271 (1964).

124. Stover, B. J., W. Stevens and F. W. Bruenger, "Chemical Associations of ^{239}Pu(IV) and ^{241}Am(III) in Blood, Liver and Thyroid," in Radiobiology of Plutonium, B. J. Stover and W. S. S. Jee, Eds., The J. W. Press, Salt Lake City, 1972.

125. Stover, B. J. and C. N. Stover, "The Laboratory for Radiobiology at the University of Utah," in Radiobiology of Plutonium, B. J. Stover and W. S. S. Jee, Eds., The J. W. Press, Salt Lake City, 1972.

126. Taylor, G. N., W. R. Christensen, L. Shabestari and W. S. S. Jee, "The General Syndrome Induced by ^{239}Pu in the Beagle," in Radiobiology of Plutonium, B. J. Stover and W. S. S. Jee, Eds., The J. W. Press, Salt Lake City, 1972.

127. Task Group on Lung Dynamics, Health Physics, 12, 173 (1966).

128. Tamplin, A. P. and T. B. Cochran, "The Hot Particle Issue: A Critique of WASH-1320," Wash., D.C., Nat. Resources Defense Council, Nov. 1974.

129. Edsal, J. T., "Toxicity of Plutonium and Some Other Actinides," Bull. Atomic Scien., 27 (Sept. 1976).

130. Morgan, K. Z., "Suggested Reduction of Permissible Exposure to Plutonium and Other Transuranic Elements," Am. Ind. Hygiene Assn. J., 567 (August, 1975).

131. Price, P. B. and R. M. Walker, "Chemical Etching of Charged Particles," J. Appl. Phys., 33, 3407 (1962).

132. Fleischer, R. L., P. B. Price and R. M. Walker, Nuclear Tracks in Solids, University of California Press, 1975.

133. Iyer, R. H. and V. V. Rao, "Solid State Detectors Help Search for Uranium," Nuclear India, 15, 1 (1976).

134. Boyett, R. H., D. R. Johnson and K. Becker, "Some Studies on the Chemical Damage Mechanism Along Charged-Particle Tracks in Polymers," Rad. Res., 42, 1 (1970).

135. Fleischer, R. M., P. B. Price and R. M. Walker, "Ion Explosion Spike Mechanism for Formation of Charged-Particle Tracks in Solids," J. Appl. Phys., 36, 3645 (1965).

136. Tommasino, L. and C. Armellini, "A New Technique for Damage Track Detectors," Rad. Effects, 20, 253 (1973).

137. Sohrabi, M. and K. Z. Morgan, "Effect of Polycarbonate Foil Thickness on Electrochemical Etching Amplification of Recoil Particle Tracks for Fast Neutron Dosimetry," Proc. 9th Midyear Symp. Health Phys. Soc., Denver, Colorado (1976).

138. Sohrabi, M. and K. Z. Morgan, "Recent Developments in Fast Neutron Personnel Dosimetry Using Track Etch Methods," Proc. 3rd Eur. Cong. of IRPA, Paper 14, Amsterdam, Netherlands (1975).

139. Sohrabi, M. and K. Z. Morgan, "Some New Characteristics of a Polycarbonate Fast Neutron Personnel Dosimeter," Paper 186, American Industrial Hygiene Conference, Atlanta, Georgia (May, 1976).

140. Morgan, K. Z. and M. Sohrabi, "Development and Application with Some Fast Neutron Dosimetry Techniques Utilizing Plastic Track Detectors for Radiotherapy and Health Physics," Prog. Rept. ORO-4814-1, USERDA Cont. No. AT-(40-1)-4818 (1975).

141. Sohrabi, M. and K. Z. Morgan, "Some Studies on the Development and Applications of Recoil Particle Track Amplification by Electrochemical Etching for Fast Neutron Dosimetry," ORO-4814-9, May, 1976.

142. Beach, J L. and K. Becker, "Improvement in Spatial Resolution of Track-Etching Microradiography," Nuc. Inst. and Methods, 130, 499 (1975).

143. Somogyi, G. and D. S. Srivastava, "Alpha Radiography with Plastic Track Detectors," Int. J. Appl. Rad. Isotopes, 22, 289 (1971).

144. Somogyi, G., "Processing of Plastic Track Detectors," Nuclear Track Detection, 1, 3 (1977).

145. Stillwagon, G. B., S. J. Su and K. Z. Morgan, "Adapting the Polycarbonate Dosimeter and Electrochemical Etching to the Microdosimetry of ^{239}Pu in Bone," Trans. Health Physics Society Conference, Atlanta, Georgia, 1977.

146. Stillwagon, G. B. and K. Z. Morgan, "Calibration of the Polycarbonate Dosimeter for the Microdosimetry of ^{239}Pu Alpha Particles in Bone, Trans. Health Physics Society Conference, Atlanta, Georgia, Student Session, 1977.

147. Su, Shian-Jang, "Neutron Dosimetry Using Electrochemical Etching," Trans. Am. Nu. Soc. Stud. Conf., Raleigh, N.C., II-29 (1977).

148. Stillwagon, G. B., S. J. Su and K. Z. Morgan, Letter to the Editor concerning our determination of the bulk etching rate of polycarbonate foils, to be published, Health Phys. Journ., 1978.

149. Stillwagon, G. B. and K. Z. Morgan, "Alpha Particle Track Production in Polycarbonate Foils Amplified by Electrochemical Etching," Trans. Health Physics Society Conf., Minneapolis Minnesota, 1978. See also Trans. Southeast Regional Nuclear Science and Engineering Student Conf., Gainesville, Florida, 1978. This paper has also been submitted to the journal Nuclear Track Detection for publication.

150. Stillwagon, G. B. and K. Z. Morgan, Note to the Editor concerning our discovery and quantification of the two track sizes observed on alpha particle irradiated polycarbonate foils electrochemically etched, to be published, Health Physice Journal, 1978.

151. J. Tripier, R. Oppel, G. Remy and M. Debeauvais, "Fast Neutron Dosimetry by Means of a Cellulose Nitrate Detector," Nucl. Inst. Methods, 125, 487 (1975).

152. D. R. Johnson and K. Becker, "Mechanisms and Applications of Nuclear Track Etching in Polymers," ORNL-TM-2826, Oak Ridge National Laboratory (1970).

153. Sohrabi, M. and K. Becker, "Some Studies on the Application of Track Etching in Fast Neutron Personnel Dosimetry," ORNL-TM-3605, ORNL (1971).

154. Sohrabi, M., "The Amplification of Recoil Particle Tracks in Polymers and Its Application in Fast Neutron Personnel Dosimetry," Health Phys., 27;598 (1974)

155. Stillwagon, G. B., S. J. Su and K. Z. Morgan, "Some Studies on the Development and Application of Particle Track Amplification by the Electrochemical Etching Method for the Purpose of Dosimetry," Prog. Rept., Aug., 1977.

156. Stillwagon, G. B., S. J. Su and K. Z. Morgan," Some Studies on the Development and Application of the Electrochemical Etching Technique," Prog. Rept., Aug., 1978.

157. Crawford, M., Air Pollution Control Theory, McGraw-Hill Book Company, New York, 1976, Chapter 4.

158. Rutherford, E., "The Scattering of α and β Particles by Matter and the Structure of the Atom," Phil. Mag., 21, 669 (1911).

159. Rutherford, E., J. Chadwick and C. D. Ellis, Radiations from Radioactive Substances, Cambridge University Press, London, 1930, Chapter 9.

160. Su, S. J. and K. Z. Morgan, "Energy Dependence of Fast Neutron Dosimetry Using Electrochemical Etching," Trans. Amer. Nucl. Soc. Stud. Conf., Gainesville, Florida (1978).

161. Katz, R., "Track Structure Theory in Radiobiology and in Radiation Detection," Nuclear Track Detection, 2, 1 (1978).

162. Kodak Corporation, Data Release, Kodak Materials for Nuclear Physics and Radiography.

163. Hague, A. K. M. M., "Energy Expended by Alpha Particles in Lung Tissue," Brit. J. Appl. Phys., 17, 905 (1966).

164. Norwood, W. D. and C. W. Newton, Jr., "U.S. Transuranium Registry *Study of Thirty Autopsies*," *Health Physics*, 28, 669 (1975).

165. Jee, W. S. S., Personal Communication, August, 1978.

166. Polig, E., "Effect of ^{241}Am on Bone Structure According to Its Microdistribution," in Biological and Environmental Effects of Low-Level Radiation, Vol. II, International Atomic Energy Agency, Vienna, 1976.

167. Rossi, H. H., "Experimental Limitations of Microdosimetry," Symposium on Microdosimetry, 2D, Stresa (1969) Proc.

168. Harley, N. H. and B. S. Pasternack, "Experimental Absorption Applied to Lung Dose from Thoron Daughters," Health Physics, 24, 379 (1973).

169. Harley, N. H., B. S. Pasternack and J. H. Harley, "Alpha Absorption Measurements Applied to Lung Dose from Plutonium-239," Health Physics, 28, 61 (1975).

170. Harley, N. H. and B. S. Pasternack, "A Comparison of the Dose to Dells on Trabecular Bone Surfaces from Plutonium-239 and Radium-226 Based on Experimental Alpha Absorption Measurements," Health Physics, 30, 35 (1976).

171. Harley, N. H., Personal Communication, June, 1978.

172. Marshall, J. H., P. G. Groer and R. A. Schlenker, "Dose to Endosteal Cells and Relative Distribution Factors for Radium-224 and Plutonium-239 Compared to Radium-226," in Radiological and Environmental Research Division Annual Report, July 73--June 74, ANL-75-3 pt 2, 71, 1975.

173. Spiers, F. W. and J. Vaughan, "Hazards of Plutonium with Special Reference to the Skeleton," Nature, 259, 531 (1976).

VITA

Gary Bouldin Stillwagon was born in Memphis, Tennessee on December 30, 1951. He received a Bachelor of Science degree in physics from the Georgia Institute of Technology in 1974. After graduation he worked in the Methodist Hospital in Memphis, Tennessee as a medical physicist. He calibrated therapy, diagnostic and nuclear medicine machines as well as wrote procedures for the on-line calibration of the latter machines and taught a course in X-ray and Radium Physics.

In August 1975, Mr. Stillwagon received a Master of Science degree in nuclear engineering from the Georgia Institute of Technology. After graduation he worked toward the Doctor of Philosophy degree in nuclear engineering with a specialty in health physics under the direction of Dr. Karl Z. Morgan.

During the time he was pursuing the doctoral degree, Mr. Stillwagon was awarded research assistantships funded by the U.S. Energy Research and Development Administration and the Department of Energy. He served as co-principal investigator on projects funded by ERDA and DOE. Mr. Stillwagon was awarded the best paper in his session during the 1978 American Nuclear Society Regional Conference in Gainesville, Florida, and one of the 1978 Health Physics Society STUDENT AWARDS. Additionally, he taught a portion of the Health Physics Certification Exam Short Course offered at the Georgia Institute of Technology. In June 1978, he worked at the Radiobiology Laboratory, University of Utah, under the direction

of Dr. W. S. S. Jee, and studied the deposition of actinide elements in bone.

Mr. Stillwagon is the author or co-author of the following papers, publications and reports:

1. "Void Fractions in Cruciform-like Flow Channels," Trans. Am. Nuc. Soc. Stud. Conf., Atlanta, Georgia (1975).
2. "The Importance of Void Geometry Representation for Plutonium Recycle Analysis in Boiling Water Reactors," Trans. Am. Nuc. Soc. Stud. Conf., University of Virginia, Charlottesville, Virginia (1976).
3. "The Gas Core Actinide Transmutation Reactor," Trans. Am. Nuc. Soc. Stud. Conf., University of Virginia, Charlottesville, Virginia (1976).
4. "The Importance of Void Geometry Representation for Plutonium Recycle Analysis in Boiling Water Reactors," Trans. Am. Nuc. Soc. Conf., Toronto, Canada (1976), with R. W. Carlson.
5. "Adapting the Polycarbonate Detector and Electrochemical Etching to the Microdosimetry of ^{239}Pu in Bone," Trans. Am. Nuc. Soc. Stud. Conf., Raleigh, N. C. (1977).
6. Proposed research for the Ph.D. degree, "The Microdosimetry of ^{239}Pu in Bone Utilizing the Polycarbonate Dosimeter and Electrochemical Etching," in partial fulfillment of the Ph.D. degree, Georgia Institute of Technology (1977).
7. "Adapting the Polycarbonate Detector and Electrochemical Etching to the Microdosimetry of ^{239}Pu in Bone," Trans. Health Physics Soc. Conf., Atlanta, Georgia (1977), with S. J. Su and K. Z. Morgan.
8. "Neutron Dosimetry Using Electrochemical Etching," Health Physics Soc. Conf., Atlanta, Georgia (1977), with S. J. Su and K. Z. Morgan.
9. "Calibration of the Polycarbonate Detector for the Microdosimetry of ^{239}Pu Alpha Particles in Bone," Trans. Health Physics Soc. Conf., Atlanta, Georgia (1977), with K. Z. Morgan.
10. Letter to the Editor concerning the determination of the bulk etching rate of polycarbonate foils, Health Physics Journal, June 1978, with S. J. Su and K. Z. Morgan.
11. "Alpha Particle Track Production in Polycarbonate Foils Amplified by Electrochemical Etching," Trans. Health Physics Soc. Conf., Minneapolis, Minnesota, 1978. See also Trans. Southeast Regional Nuclear Science and Engineering Student Conference, Gainesville, Florida, 1978. (This paper won the 1978 Health Physics Society STUDENT AWARD, the BEST PAPER IN SESSION award in the Health and Medical Radiation Physics session, Trans. Southeast Regional Nuclear Science and Engineering Student Conference, Gainesville, Florida (1978), and has been submitted to the journal, Nuclear Track Detection for publication.), with K. Z. Morgan.
12. Letter to the Editor concerning the discovery of the two categories of tracks discovered on polycarbonate foils after alpha particle irradiation and electrochemical etching; to be published, Health Physics Journal, 1978 with K. Z. Morgan.

Mr. Stillwagon has several years of teaching and research experience and some clinical, medical physics experience in the institutions with which he has been associated. He has been active in social and scientific groups and he is a member of the Health Physics Society, the American Association of Physicists in Medicine and the American Nuclear Society.